Physics – Uspekhi **44** (7) 681 – 724 (2001)

REVIEWS OF TOPICAL PROBLEMS PACS numbers: **61.41.+e**, **61.43.–j**, 61.43.Bn, 61.43.Hv, **61.46.+w**

A cluster model for the polymer amorphous state

G V Kozlov, V U Novikov

DOI: 10.1070/PU2001v044n07ABEH000832

Contents

Abstract. Some aspects of local order in the amorphous state of a glassy polymer are discussed. The physical principles behind a cluster model involving the new concept of a structural defect are presented. A comparative analysis of three major approaches to describing the amorphous state of a polymer is given. It is shown that the cluster model is in reality a unified model which presents a new explanation for many qualitative results produced in the past on polymer structure and processes involved and which, unlike previous approaches, has the advantage of being quantitative. Possible future directions in polymer structure studies are outlined.

1. Introduction

The structure of the amorphous state of glassy polymers is one of the most important and conflicting problems in polymer physics. Until 1957, it was generally believed that in the amorphous phase the chain macromolecules making a polymer are randomly distributed and the 'spaghetti' (random-coil chain) model provides a correct description of its structure (or lack of it, to be precise) in this phase. It was suggested in Ref. [1] for the first time that there is a short-range (or local) order in polymers, based on the comparison of the amorphous phase segmental volume and density, solid-phase crystallization effect, etc.

In a later period, this hypothesis was extensively discussed by the advocates of the two conflicting concepts. There are at least two reasons for the local order problem to be at the center of attention as far as amorphous polymers are concerned. One is of fundamental importance because local order, if any, must influence polymer properties in the same way as the crystalline state influences the properties of amorphous – crystalline polymers. The other reason is of methodological character, there being no direct experimental approaches leading to an unambiguous solution of the problem in question.

A most forcible argument in favor of the random-coil chain concept is provided by the results of experiments on small-angle neutron scattering, which suggest that the radius of inertia $\langle R_g^2 \rangle$ of a macromolecule in a θ-solvent and in bulk polymer is approximately the same [2]. However, certain authors are of a different opinion. Boyer [3] presented a speculative scheme (Fig. 1a) in which the presence of local order does not necessarily affect the length of the radius of inertia of a macromolecule. Moreover, studies of small-angle neutron scattering demonstrated a marked discrepancy between conformations of chains for mesophase-forming polyethyl siloxane in a solution and in the condensed state [4]. This difference for a crystallizable high-molecular polyethylene terephthalate is less delineated and does not exceed 15%. [5]. It is natural to suggest that conformational changes of the chains in the course of local order formation should be even weaker than during the formation of a mesophase or crystalline regions. For this reason, the change of $\langle R_g^2 \rangle$ in the first case is on the order of a few percent, i.e. within experimental error ($\sim 8\%$) [6], which makes it rather difficult to identify. It will be shown below that the poor variability of $\langle R_g^2 \rangle$ upon transition from the solution to the condensed state does not interfere with the formation of regions of local order.

There are two principal models of regions of local order in the amorphous state of glassy polymers. In the beginning, it was thought that such a region is analogous to a folded-chain crystallite (FCC) [7]. This view had undoubtedly formed under the influence of the discovery by Fischer [8], Keller [9], and Till [10] of a crystallite structure composed of single-crystal folded-chain lamellae. Close to this model is the so-called 'meandering' model of Pechhold [11]. Another class of models for regions of local order is exhibited by the so-called micellar domain structure [12] which represents a sort of prolate-chain crystallite (PCC) analogue (Fig. 1b).

X-ray diffraction techniques appear to yield the most weighty data in support of local ordering in amorphous

G V Kozlov Kabardino-Balkariya State University
ul. Chernyshevskogo 173, 360004 Nal'chik, Russian Federation
Tel. (7-866) 225 44 75
V U Novikov Moscow State Open University
ul. P. Korchagina 22, 129805 Moscow, Russian Federation
Tel. (7-095) 909 39 15
E-mail: vknovik@cityline.ru

Received 6 July 2000, revised 21 November 2000
Uspekhi Fizicheskikh Nauk **171** (7) 717 – 764 (2001)
Translated by Yu V Morozov; edited by A Radzig

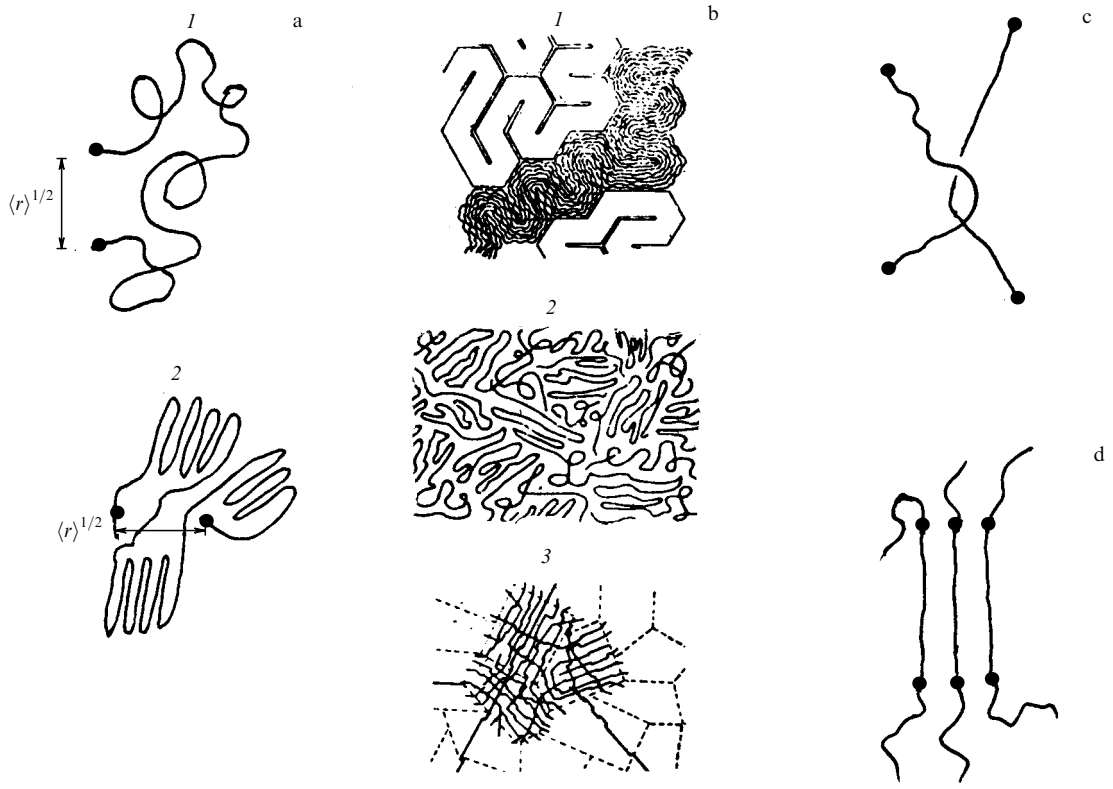

Figure 1. Schematic (model) representation of the coiled molecule (a) (*1* — statistical ball, *2* — the same with locally ordered regions) [3]; amorphous state (b) (*1* — meandering model, *2* — folded-chain micellar model, *3* — micellar domain structure) [12]; 'macromolecular interlacing' (c), and cluster (d).

polymers [13 – 16]. It was shown in Ref. [14] that the shape of the amorphous halo on large-angle X-ray diffractograms provides a qualitative characteristic of one or another local order constant which becomes the interplanar spacing for polymer crystals — that is, a long-range order parameter. It is important that the number of these constants, i.e. the sum of reflexes producing the amorphous halo, can be both a property of the material and an individual characteristic of the sample, indicative of the nature and degree of amorphous phase ordering. In the following pages, it will be shown how this general principle can be applied to confirm in experiment the validity of the cluster model of the polymer amorphous state structure. Indirect evidence of local ordering in the amorphous state of glassy polymers was also obtained with the aid of other up-to-date experimental techniques such as nuclear magnetic resonance [17 – 19], IR spectroscopy [20], thermal analysis [21, 22], electron diffraction [23], small-angle neutron scattering [24], and thermal expansion analysis [25]. Simulation of polymer structure by the Monte Carlo method confirmed the feasibility of local ordering even if only the packing density is considered [26]. A number of theoretical studies demonstrated the possibility of local order realization in the amorphous state of glassy polymers despite the aforementioned invariability of the quantity $\langle R_g^2 \rangle$ [3] (at least to within the experimental error). Also, they explained the constancy of glass transition to melting temperature ratio in polymers [27].

As far as the size of the regions of local order is concerned, it should be noted that in earlier works they were considered to be rather lengthy (up to several thousands of angstroms [28 – 30]). In the course of time, however, this view changed, and Boyer (following Robertson) suggested that regions of local order should actually be smaller than 5.0 nm, while regions of long-range order are bigger than 10.0 nm [3]. Certainly, the size is not the sole property responsible for the difference between the regions of local and long-range orders. The latter are characterized with necessity by spatial ordering [31].

A review published by Fischer and Dettenmaier [32] marked an important stage in the development of views on the nature of local ordering in glassy polymers. In the first place, these authors showed that the extent of locally ordered regions can hardly exceed 1.0 nm (or 2.0 nm as later estimated by Wendorff [33]). Secondly, the local order in the glassy state was shown to be sensitive to thermal fluctuations. In other words, its degree is a function of temperature. For this reason, it should be borne in mind that the phrase 'the order frozen to below the glass transition temperature T_g' does not suggest a constancy of order parameter (e.g., a free volume [32]) at $T < T_g$. 'Freezing' of local order in the glassy state is due to its high viscosity in contrast with low-molecular-weight liquids in which the local order is of dynamic nature [3]. It will be shown below that the cluster model is fully consistent with these conditions.

Today, practically all researchers recognize the occurrence of local order in the amorphous phase of glassy polymers. In the end, even Flory [2], a most staunch opponent of this concept, eventually came to share this view even though with some reservation to the effect that the degree of ordering in polymers is not higher than in low-molecular liquids. Therefore, a major concern at present is the accurate structural identification of locally ordered regions and the development on this basis of a quantitative concept which the cluster model actually represents.

Another important aspect of the approach being considered is the definition of a structural defect for the

amorphous state of glassy polymers. The influence of the dislocation theory on the development of the metals science is well known [34], hence the numerous attempts to use disclination–dislocation analogies for the description of amorphous polymer properties [35–40]. However, the lack of a quantitative structure concept resulted in the structural defects being treated as essentially molecular ones [35, 36, 39] or totally unrelated to the polymer structure [37, 38, 40]. An altogether new interpretation of a structural defect for polymers will be presented below.

There are numerous interpretations of local order and experimental findings allowing for its particular quantitative evaluation. We shall consider in this paper a few examples illustrating both the qualitative and quantitative consistency of the cluster model with the results of earlier studies. They confirm that the cluster model not only agrees with the data accumulated in this branch of polymer physics but also provides a basis for their integration.

Being dependent on a quantitative assessment, the cluster model is designed for the analytical description of structure–properties relationships in glassy polymers. For this purpose, the existing approaches to such phenomena as elasticity, flow, fracture, etc. had to be revised. The use of the cluster model for the description of different properties (mechanical and thermodynamic, transport, etc.) of various types of polymers will be illustrated in the forthcoming sections of this paper.

In addition, it is worthwhile to note that one of the promising lines of further research concerned with the local order in polymers is their consideration as dissipative structures [41–44]. This approach allows for the employment of the mathematical apparatus of synergetics [45, 46] to describe the structure of polymers. A major advantage of this approach to the elucidation of the amorphous polymer structure consists in the possibility of studying the relationship between the parameters of the initial glassy polymer structure and its modification by various (e.g., mechanical) factors. A similar principle of research was employed in Refs [47, 48] where the Grüneisen parameter characterizing the degree of interatomic bond anharmonicity served as a measure of polymer structural change. With this in mind, the objective of the present review is to analyze current views about the local order, structure, and properties of glassy polymers with recourse to the cluster model concept.

2. Model of the amorphous state of glassy polymers

Widely known experimental findings created a prerequisite for the development of the cluster model of the amorphous polymer structure. It was demonstrated by Haward and coworkers [49, 50] that the behavior of glassy polymers experiencing deformation beyond yield stress (in the plateau region of forced rubber-like elasticity) obeys the equations of the theory of rubber elasticity. In this case, large strains are described either by the Langevin equations [51, 52] or in the framework of the Gaussian interpretation [53] where a polymer chain does not approach a fully stretched condition and the relation between the true stress σ_{true} and the degree of stretch λ for uniaxial tension has the form [53]

$$\sigma_{true} = G_p\left(\lambda^2 - \frac{1}{\lambda}\right), \tag{1}$$

where G_p is the so-called modulus of strain hardening.

Formally, the knowledge of the quantity G_p permits one to determine the density V_e of the network of chain entanglements with the help of the well-known formulas for rubber-like elasticity:

$$G_p = \frac{\rho RT}{M_e}, \tag{2}$$

$$V_e = \frac{\rho N_A}{M_e}, \tag{3}$$

where ρ is the polymer density, R is the molar gas constant, T is the testing temperature, M_e is the molecular weight of a chain segment between entanglements, and N_A is the Avogadro constant.

However, attempts to estimate M_e (or V_e) using G_p values derived from Eqn (1) lead to an incredibly low M_e (or unrealistically high V_e) at variance with Gaussian statistics which implies the presence of at least 13 links in a chain segment enclosed between entanglements [54]. Possible causes of this discrepancy are discussed at some length in Ref. [53], where it is assigned to the interpretation of the entanglements as conventional interlacings ('loops') of macromolecular chains (Fig. 1c). In an attempt to solve this problem, the authors of Ref. [55] suggested that, besides the conventional network of such interlaced chains in glassy-state polymers, there is another type of macromolecular linkage structurally resembling prolate-chain crystallites (PCC) and schematically depicted in Fig. 1d. Such entanglement sites (which should rather be called binding sites) are characterized by a high degree of functionality F (the functionality of a site is understood as the number of chains that emanate from it) [56] and will be further referred to as clusters. A cluster comprises segments of different macromolecules. The length of each segment is assumed to be equal to the length l_{st} of the statistic segment ('stiffness-providing polymer segment' [57]). In this case, the effective (real) molecular weight of the chain segment between clusters M_e^{eff} can be estimated as follows [56]:

$$M_e^{eff} = M_e \frac{F}{2}. \tag{4}$$

Evidently, at a sufficiently large F, it is possible to obtain sensible M_e^{eff} values meeting the requirements of Gaussian statistics. In what follows, the subscripts 'cl' and 'e' will be used to designate parameters of a cluster network of entanglements and conventional network of macromolecular interlacings, respectively. Thus, the model described in Ref. [55] suggests that the structure of the amorphous polymer state can be simulated by regions of collinear close-packed segments (clusters) embedded in a loose-packed matrix. Simultaneously, clusters play the role of multifunctional sites in the network of physical couplings. The value of F can be found (again in the framework of the rubber-like elasticity concept) in the following way

$$F = \frac{2G_\infty}{kTV_{cl}} + 2, \tag{5}$$

where G_∞ is the equilibrium shear modulus, and k is the Boltzmann constant.

Figure 2a shows the temperature dependences of $V_{cl}(T)$ for polycarbonate (PC) and polyarylate (PAr), which indicate that V_{cl} decreases with rising T. Furthermore, these dependences exhibit two characteristic temperatures. One, the

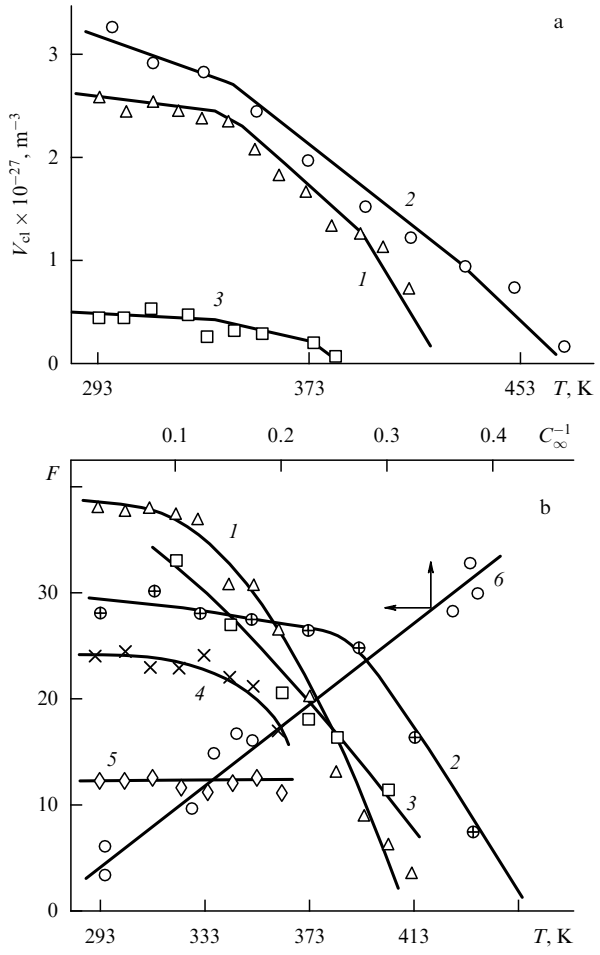

Figure 2. Plots of (a) density V_{cl} of cluster network of entanglements vs. temperature T for PC (*1*, *3*) and PAr (*2*) (*1*, *2* — stable, and *3* — unstable network) [55], and (b) cluster functionality F vs. temperature T [for PC (*1* – *3*), HDPE (*4*, *5*)] and inverse characteristic ratio C_∞^{-1} (*6*). Curve *1* is obtained from Eqn (5), curve *2* from Eqn (11), curve *3* from Eqn (6). Curves *4* and *5* are for HDPE and HDPE + 0.05 Z, respectively.

polymer glass transition temperature T_g, is responsible for the complete cluster decomposition corresponding to the transition of the polymer to the rubbery state. The other, T_g', corresponds to the inflection on $V_{cl}(T)$ curves and is approximately 50 K below T_g. It was shown in earlier studies [59, 60] in the framework of local order concepts that the temperature T_g' is associated with unfreezing of segmental mobility in loose-packed regions of the polymer. This means that in the cluster model T_g' can be associated with devitrification of a loose-packed matrix. The dependences $F(T)$ for these polymers have a similar form (Fig. 2b).

The two principal models of the regions of local order in polymers have one point in common — these regions play the role of nodes in the physical network of macromolecular interlacings [55, 61]. However, their response to mechanical deformation must be significantly different. 'Bundles' appear to be able to unfold and adopt a straightened conformation under large strains, whereas clusters are not, and deformation of the polymer occurs only via straightening of penetrating chains (orientation along the applied stress). Turning back to the analogy with crystalline morphology of polymers, it should be noted that large strains of amorphous – crystalline polymers (amounting to 1000 – 2000% for polyethylenes) are realized through crystallite unfolding [62]. This means that the measurement of limiting deformations may provide arguments in favor of one or another type of the regions of local order in the polymer amorphous state [63].

It has been suggested in Ref. [61] that 'bundles' may serve as sources of polymer segments entering 'interstitial sites' (i.e. interbundle regions) by virtue of their ability to unfold, which they share with folded-chain crystallites (FCC). In the light of this analogy, it is worth noting a significant difference between limiting degrees of stretch λ_{lim} of amorphous plastic polymers and such amorphous – crystalline polymers as high-density polyethylene (HDPE) and polypropylene (PP). For these polymers, crystallite unfolding under large strains has been confirmed by experiment ($\lambda_{lim} = 1.6$ for PC, $\lambda_{lim} = 6$ for PP, and $\lambda_{lim} = 13$ for HDPE at room temperature [64]). The explanation of this difference requires the quantitative assessments [63].

Gent and Madan [64] suggested that the stretch occurs via straightening of crystalline or amorphous sequences. In this case, λ_{lim} may be expressed as the number of times f which the molecule passes through one and the same crystallite (or 'bundle'):

$$\frac{1}{\lambda_{lim}} = \frac{K}{f} + \frac{(1-K)^{1/2}}{n_{st}^{1/2}}\,, \qquad (6)$$

where K is the degree of crystallinity, and n_{st} is the number of equivalent statistical links between entanglement sites in the melt. Usually, n_{st} varies from 100 to 300. Because this parameter has no significant effect on the final result, it is assumed to equal 225 for all polymers used in Ref. [63].

Evidently, the quantity f determines the number of folds formed by a molecule in FCC (or 'bundle'). For folding to be the case, the condition $f \geqslant 2$ must be fulfilled. The estimated f values for HDPE and PP presented in Table 1 are as expected indicating that a macromolecule of HDPE is folded more than 50 times, while that of PP only 5 times, in good agreement with the results reported in paper [64].

Table 1. Folding parameter f for amorphous and amorphous – crystalline polymers.

Polymer	T, K	λ_{lim}	K	φ_{cl}	f
Polyethylene	293	13	0.69		53
Polypropylene	293	6	0.50		4.7
Polycarbonate	333	1.91		0.33	0.70
	353	2.23		0.29	0.73
	373	2.15		0.24	0.57
	393	2.36		0.19	0.52
	413	2.75		0.11	0.35
Polyarylate	293	1.66		0.50	0.89
	313	1.67		0.38	0.68
	333	1.66		0.37	0.66
	353	1.76		0.31	0.59
	373	1.66		0.25	0.45
	393	1.70		0.19	0.35
	413	1.75		0.16	0.30
	433	1.80		0.13	0.25
	453	1.86		0.11	0.22
	473	1.97		0.01	0.02

An equivalent of the degree of crystallinity K for amorphous glassy polymers is the relative number of clusters φ_{cl}. The value of φ_{cl} can be estimated in the following way. The overall length L of macromolecules per unit volume of the polymer (on the assumption of their

close packing) is [65]

$$L = S^{-1}, \tag{7}$$

where S is the cross-section area of a macromolecule.

The length of the statistic segment l_{st} is estimated to be [66]

$$l_{st} = l_0 C_\infty, \tag{8}$$

where l_0 is the length of the skeletal bond in the main chain, and C_∞ is the characteristic ratio which describes the flexibility of the macromolecule [67].

The total length L_{cl} of segments in the clusters per unit volume of the polymer is estimated as [68]

$$L_{cl} = l_{st} V_{cl}, \tag{9}$$

and the quantity φ_{cl} is expressed as the ratio

$$\varphi_{cl} = \frac{L_{cl}}{L}. \tag{10}$$

Values of φ_{cl} obtained from Eqns (7)–(10) are presented in Table 1. Results of the calculations for PC and PAr using experimental values of λ_{lim} indicate that in all cases $f < 1$ (see Table 1). This suggests the absence of chain folding in the regions of local order (nodes in the physical network of macromolecular interlacings) of these polymers. Also, it should be noted that the crystallite unfolding in amorphous–crystalline polymers begins at strains of the order of 50–100% [69]. The use of $\lambda_{lim} \sim 2$ for amorphous segments of HDPE in Eqn (6) and $\varphi_{cl} \cong 0.2$ yields $f < 1$. This means that macromolecular folding in amorphous–crystalline polymers takes place only in crystalline regions.

Therefore, calculations in paper [63] indicate that a prolate-chain crystallite analogue (cluster) is the most likely type of supersegmental structures in the polymer amorphous state (see Fig. 1d).

It has been mentioned above that Flory's main argument [2, 56, 70] against local ordering in amorphous polymers was the identical shape of a macromolecular ball in a θ-solvent and in the condensed state as reflected in the similar root-mean-square distance between macromolecular ends. It was however shown in Ref. [71] that this does not interfere with the formation of clusters considered again as multifunctional nodes in the network of physical entanglements. Evidently, this condition must hold for the cluster model too. Forsman [72] derived the following equation to estimate the number of segments n_{seg} in a polymer cluster:

$$n_{seg}^{1/2} = \frac{B_2}{4A}\left\{1 - \left[1 - \frac{16A\left[1 - \ln(C\rho\varphi_{cl})\right]}{B_2^2}\right]^{1/2}\right\}, \tag{11}$$

where B_2 is a dimensionless quantity characterizing the intersegmental interaction energy, and C is the polymer concentration. Quantity A reflects a change of a macromolecular size prior to and after cluster formation and can be found from the ratio [72]

$$A = \frac{\alpha^4 - \alpha^2 + 1}{\alpha^2}, \tag{12}$$

where the parameter α is given as

$$\alpha = \frac{\langle h^2 \rangle}{\langle h_0^2 \rangle}. \tag{13}$$

In this equation, h_0 and h are the root-mean-square distances between macromolecular ends before and after clustering.

For the above reason, $\alpha \cong 1$. The comparison of F values for PC, calculated by Eqns (5) and (6) with the use of Eqn (11) ($F = 2n_{seg}$), is presented in Fig. 2b (curves *1* and *3*). It can be seen that a calculation using equation (6) allows for the correct quantitative estimation of F and the expected trend of a temperature dependence. However, an accurate assessment in the framework of Flory's concept [72] is hardly possible in the case of amorphous polymers, because Eqn (5) is an approximation.

Strictly speaking, the quantity F does not show the degree of local order. However, it may characterize the degree of interpenetration of macromolecular balls in the condensed state of polymers, because the clusters are formed by segments composed of different macromolecules. It has been demonstrated by Aharoni [73] that the characteristic ratio C_∞ can play a similar role. If this assumption is correct, F must correlate with C_∞. It has been confirmed in Ref. [71] that such a correlation does exist (see Fig. 2b, curve *6*).

It can be shown that the formation of a cluster structure is consistent with general concepts, for example, Gladyshev's evolution theory of hierarchical systems [74–79]. Experimental verification of the physicochemical theory of chemical system evolution [74] was undertaken based on the correlation between the melting temperature T_m and the Gibbs specific function of intermolecular interactions ΔG^{im} (the superscript 'im' points out the intermolecular or, as in our case, intersegmental nature of interactions) [76, 78, 79]. The choice of these parameters has been substantiated in Refs [76–79].

As is well known, the Gibbs–Helmholtz equation is true for the processes taking place in simple closed systems:

$$\left.\frac{\partial(\Delta G/T)}{\partial(1/T)}\right|_P = \Delta H, \tag{14}$$

where, ΔG and ΔH are changes of the Gibbs function and enthalpy, respectively, T is the temperature, and P the pressure.

If ΔH is assumed independent of T in a given temperature interval, the following equation holds for the nonequilibrium phase transition, i.e. self-assembly of an individual substance, at temperature T:

$$\Delta G^{im} = \frac{\Delta H_m^{im}}{T_m}(T_m - T) = \frac{\Delta H_m^{im}}{T_m}\Delta T = \Delta S_m^{im}\Delta T, \tag{15}$$

where ΔG^{im} is the change in the Gibbs function during crystallization (self-assembly) of the substance being studied from the overcooled state at $T = T_m - \Delta T$, ΔH_m^{im} is the change of enthalpy in the course of crystallization (solidification), and ΔS_m^{im} is the crystallization entropy (the entropy change during phase transition).

It was suggested in Refs [74, 76, 78] that Eqn (15) should also be used for open systems in which neither the composition nor T_m is subject to significant alteration. Later studies demonstrated the possibility of applying this equation to various chemical compounds having melting temperatures $T_m < 100\,^\circ$C and undergoing condensation at a constant temperature $T = T_0\,(25\,^\circ$C) [76–79]. With a stricter approach, for these cases Eqn (15) should be written in the

form

$$\Delta G_i^{\mathrm{im}} = \frac{\Delta H_{\mathrm{m}i}^{\mathrm{im}}}{T_{\mathrm{m}i}}(T_{\mathrm{m}i} - T_0) = \Delta S_{\mathrm{m}i}^{\mathrm{im}} \Delta T, \qquad (16)$$

where the subscripts $i = 1, 2, \ldots, n$ refer to different substances. Equation (16) is an analogue of Eqn (15) in terms of form. In other respects, these two equations are basically different in that the latter contains a variable ΔG^{im} characterizing the nonequilibrium transition of an individual substance in the system at any temperature $T < T_{\mathrm{m}}$. The values of $\Delta H_{\mathrm{m}}^{\mathrm{im}}$, $\Delta S_{\mathrm{m}}^{\mathrm{im}}$, T_{m} refer to this individual substance and are assumed to be constants. On the whole, however, Eqn (15) represents a functional dependence $\Delta G^{\mathrm{im}} = f(T)$. In Eqn (16), the variable ΔG^{im} is related to nonequilibrium transitions of various compounds with different melting temperatures $T_{\mathrm{m}i}$ at a constant (standard) temperature T_0. In this case, equation (16) represents the function $\Delta G_i^{\mathrm{im}} = f(T_{\mathrm{m}i})$ [78]. A method for the calculation of quantity ΔG^{im} for polymers is described in Ref. [80].

Figure 3 shows the dependence of ΔG^{im} on $\Delta T = T_{\mathrm{g}} - 293$ K for amorphous glassy, amorphous–crystalline, and cross-linked polymers [80]. As expected, ΔG^{im} decreases linearly with increasing ΔT (in fact, T_{g}). It is even more important that the straight line in Fig. 3, which fairly well approximates the results of the study, is consistent with the findings of Refs [76–79] presented as the plot of ΔG^{im} versus ΔT for quite different chemical compounds, but with the coefficient 10 : 1 along the axis ΔG^{im}. This is due to the difference between the molar volumes of the segments (i.e. kinetically independent fragments) and compounds used in Ref. [76], which amounts to approximately one order of magnitude. In principle, this allows one to compute the size of the segment, which is unlike in different polymers. A departure from the plot for polymers with high T_{g} reflects the peculiarities of the supersegmental structure of these substances [76]. The data of Fig. 3 indicate that the postulated cluster model based on the assumption of local order in the amorphous state of polymers is in good qualitative and quantitative agreement with a much more general macrothermodynamic hierarchic model [74–79] and occupies a relevant energy niche in the hierarchy of real world structures. The plot in Fig. 3 readily illustrates the tendency of structural evolution of a physically aging polymer. With the trend in the polymer structure to equilibrium, G^{im} tends to a minimum (i.e. ΔG^{im} shifts towards negative values). A concomitant enhancement of local order is accompanied by a rise in T_{g} [81]. Equally possible is polymer 'rejuvenation', i.e. a process thermodynamically opposite to that considered above. In practice, it is realized through 'pumping' mechanical or other energy into the polymer [82].

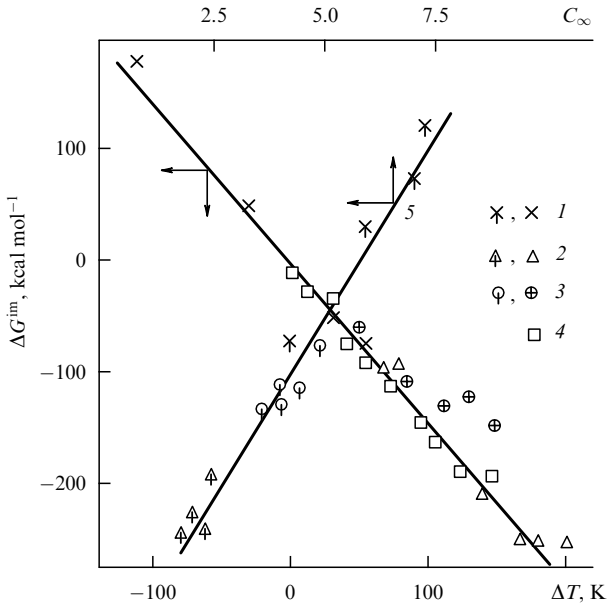

Figure 3. Plots of the Gibbs specific function ΔG^{im} of the nonequilibrium phase transition vs. $\Delta T = T_{\mathrm{g}} - 293$ K for amorphous–crystalline (*1*), amorphous glassy (*2*), cross-linked (*3*) polymers and PC (*4*) ($\Delta T = T_{\mathrm{g}} - T$) and characteristic C_∞ ratio (*5*) [80].

The dependences (following from Gibbs–Helmholtz–Gladyshev equations) presented in Fig. 3 hold true both for different polymers and for one polymer at varying T. Points *4* in Fig. 3 show the dependence $\Delta G^{\mathrm{im}}(\Delta T)$ for PC, which is in quantitative agreement with the general dependence for ΔG^{im}. Therefore, in the case of polymers, Eqns (15) and (16) are simultaneously fulfilled; in other words, the formation of supersegmental structures constitutes a nonequilibrium transition giving rise to nonequilibrium structures. Characteristically, the onset of their formation corresponds to the glass transition — that is, the transition from an equilibrium devitrified state to a weakly nonequilibrium glassy state.

Finally, it should be noted that the values of ΔG^{im} 'controlling' the formation of supersegmental structures in polymers are in a definite manner related to their molecular characteristics. Because polymers are solids composed of long-chain macromolecules, it should be expected that the most important (or at least one of the most important) parameter is the polymer chain flexibility described by the characteristic ratio C_∞ [83]. For this reason, Fig. 3 (curve *5*) shows the dependence $\Delta G^{\mathrm{im}}(C_\infty)$ exhibiting the well-apparent tendency of ΔG^{im} to increase (in parallel to a decrease of T_{g}) with increasing chain flexibility. The sole significant deviation from this rule, displayed by polystyrene, may be due to the well-known specificity of its chemical composition [84]. The correlation between G^{im} and C_∞ is in perfect agreement with the earlier postulated growth of T_{g} with increasing polymer chain stiffness [84].

It may be concluded that the dependences $\Delta G^{\mathrm{im}}(\Delta T)$ for the polymer supersegmental structure obtained in the framework of the macrothermodynamic hierarchic model are consistent, both qualitatively and quantitatively, with the analogous correlations for a wide variety of chemical compounds reported in earlier studies [76, 78, 79, 85]. This confirms the reality of these structures in the amorphous polymer state. Equations (15) and (16) are equally applicable to the description of thermodynamical behavior of these structures and can be used for their quantitative simulation. If stricter calculations are needed, corrections for variations of thermal capacity during phase transitions can be introduced [85].

An experimental evaluation [53] revealed the temperature (T) dependence of the modulus of strain hardening G_{p}. It follows from Fig. 2a (curves *1*, *2*), taking into account Eqns (1)–(3), that the cluster model directly leads to such a dependence, thus suggesting that the local order has thermofluctuation nature. This was taken into consideration in work [86] within the framework of the statistical theory of fluctuations. Fellers and Huang [87] used this theory for the

description of crazing in amorphous polymers. They derived an expression for the estimation of the polymer volume V_0 in which the probability of fluctuations is unity:

$$\frac{\sigma_c V_0^{1/2}}{(2kT_0B)^{1/2}} = 3.87, \quad (17)$$

where σ_c is the crazing stress, T_0 is the equilibrium temperature having a glass transition temperature T_g as the lower limit, and B is the bulk modulus. The methods for computation of σ_c and B are described in Ref. [86].

Table 2 compares the intercluster distances R_{cl} and linear size l_{fl} at which the probability of fluctuations is unity. The parameter l_{fl} is taken to equal $V_0^{1/3}$, and R_{cl} is found from the equation [88]

$$R_{cl} \cong 18\left(\frac{2V_{cl}}{F}\right)^{-1/3} \text{ Å}. \quad (18)$$

It follows from Table 2 that these parameters are very similar in terms of both absolute value and tendency to change. This means that on the scale of the characteristic size of a cluster structure, an amorphous polymer (or the amorphous phase of an amorphous–crystalline polymer) may be regarded as a microheterogeneous system of thermofluctuational origin [86].

Table 2. Comparison of intercluster distances R_{cl} and linear size l_{fl} at which the probability of fluctuations is unity [86].

Polymer	R_{cl}, nm	l_{fl}, nm
Polystyrene	3.61	7.64
Polymethyl methacrylate	3.16	3.17
Polyvinyl chloride	2.71	5.40
Polycarbonate	3.11	3.79
Polysulfone	2.50	3.64

Although the mechanism of fluidity in amorphous glassy polymers has for a long time been a focus of interest for many researchers, there is not yet a concerted opinion regarding its nature. One of the popular fluidity theories is based on the postulate of mechanical devitrification of polymers [89]. There are many arguments for and against this concept. A detailed discussion of them is beyond the scope of the present review. Suffice it to say that its validity is confirmed by the aforementioned 'rubber-like' behavior of amorphous glassy polymers at the plateau of forced rubber-like elasticity (cold flow). An argument against the concept is the overestimated (by at least one order of magnitude) plateau stress σ_{pl} for a devitrified polymer, which is not significantly different from the yield stress σ_y. This apparent discrepancy is easily resolved in the framework of the cluster model which implies that a loose-packed matrix is maintained in the glassy state (at $T < T_g'$) by a mesh of smaller (therefore, thermodynamically less stable) clusters [90]. Within the framework of such a structural model, fluidity (cold flow) of the amorphous glassy polymer is associated with mechanical devitrification of not all the polymer but only its loose-packed matrix [91]. In this case, large σ_{pl} values are due to the high density V_{cl} of the network of the conserved big (with large F) stable clusters, and the application of the rubber elasticity concept is justified by the rubbery state of the loose-packed matrix. Evidently, the well-known fall in the stress $\Delta\sigma$ beyond the yield stress in such an interpretation is related to the decomposition of unstable clusters in the loose-packed matrix, with their network density V_{cl}^{us} controlling $\Delta\sigma$. As mentioned above, V_{cl} can be found from the forced rubber-like elasticity plateau; hence, the approximate ratio [90]

$$\frac{\Delta\sigma}{\sigma_y} = \frac{V_{cl}^{us}}{V_{cl} + V_{cl}^{us}}, \quad (19)$$

which allows V_{cl}^{us} to be estimated.

It has been shown that $\Delta\sigma$ (hence, V_{cl}^{us}) decreases with rising temperature T [92]. This agrees with the proposed model where the cluster network density is a function of T (in contrast to the network of conventional interlacings [93]). Figure 2a (curves *2*, *3*) compares the temperature dependences of V_{cl} and V_{cl}^{us} for PC, calculated with the help of Eqns (1) and (19), respectively. As expected, the quantity V_{cl}^{us} at a temperature nearly 50 K below T_g (i.e. at T_g') relating to the polymer is practically zero due to the thermal devitrification of the loose-packed matrix [60].

An additional network of physical links can form in polymers as a result of strong interactions. A possible variant of such a structure was examined in Refs [94, 95] using an epoxy polymer (EP) modified by adamantane carboxylic acids. The authors studied parent EP with varied cross-link density ν_{cr} and modified systems differing in the type of adamantanoic acid used for the treatment and in the mode of its admission. The latter systems were hardened with diamine (EPD) or anhydride before (EPAh) and after ($EPAh_{ag}$) ageing in the air for 3 years [94, 95]. A linear growth of V_{cl} with increasing ν_{cr} was documented for EP [96], as shown in Fig. 4a. A similar dependence was found for epoxy polymers modified by carboxylic acids. In this case, however, extrapolation of dependences to $\nu_{cr} = 0$ did not always result in zero V_{cl}. This suggests that the systems considered had an additional network of physical entanglements formed by the interaction of adamantane fragments. The density ΔV_e of such a network is equivalent to the difference between V_{cl} for modified and unmodified epoxy polymers [95]. Comparison of ΔV_e and V_{cl}^{us} reveals the similarity of their absolute values. It is therefore suggested that the network of unstable clusters holding the loose-packed matrix in the glassy state is formed as a result of interactions between adamantane fragments [95]. It was shown later by large-angle X-ray diffractometry that, in terms of energy characteristics (hence, in terms of type), a network of physical links formed by strong interactions between adamantane fragments is intermediate between the cluster network and the network of conventional interlacings.

The application of the cluster model to such amorphous–crystalline polymers as polyethylenes deserves special consideration. It is well known that the polyethylene amorphous phase is in the devitrified state at room or similar temperatures. Bearing in mind the above results, this phase is at first sight missing a local order. However, a more detailed study did not confirm this inference [97–103]. We shall therefore show in the first place that the nodes of the network of physical links in high- and low-density polyethylenes (HDPE and LDPE, respectively) make up the regions of local order (clusters) and are of thermofluctuation nature. Thereafter, the possibility of artificial variation of V_{cl} and the effect of this factor on the structure of amorphous–crystalline HDPE will be demonstrated.

In the framework of Landau's phenomenological theory of second-order phase transitions [104], the order parameter

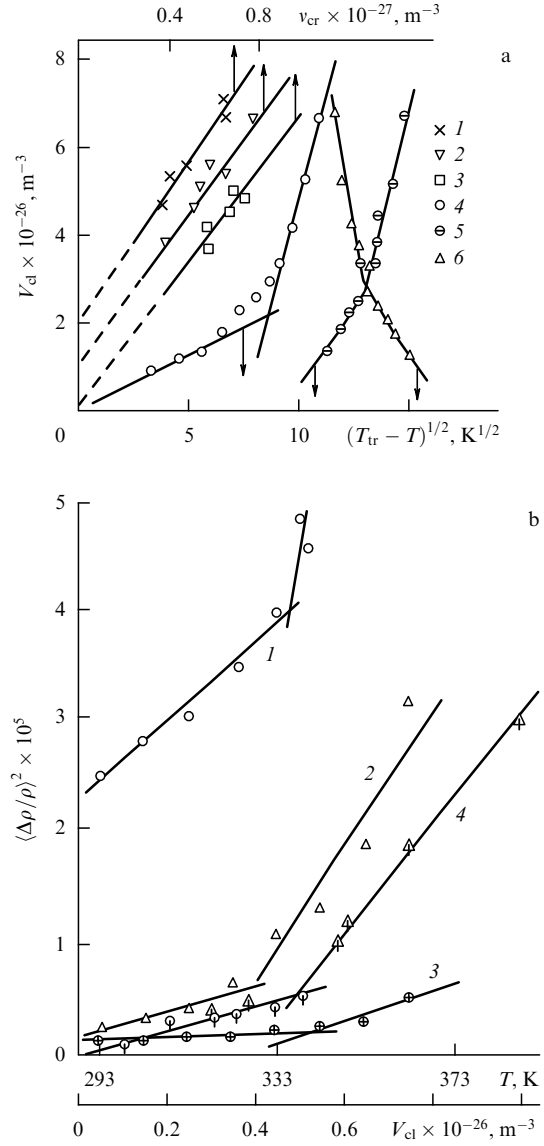

Figure 4. Plots of (a) density V_{cl} of a cluster network of entanglements vs. density v_{cr} of sites of a chemical bond network [for EPD (*1*), EPAh (*2*), $EPAh_{ag}$ (*3*)] [94] and the parameter $(T_{tr} - T)^{1/2}$ corresponding to the Landau equation for second-order phase transitions (the transition temperature T_{tr} is taken as T_g (*4*), T_m (*5*), and T_{ll} (*6*) [107]), and (b) density fluctuations $\langle \Delta\rho/\rho \rangle^2$ (calculated by Eqns (24) — curve *1*, and (23) — curves *2*, *3*) vs. temperature T and density V_{cl} of a cluster network of entanglements (curve *4*) for high-density (open circles) and low-density (triangles) polyethylenes [107].

ψ_{op} unambiguously related to one of the most important thermodynamic properties, namely, a change of entropy ΔS, is defined as

$$\psi_{op} = \left(\frac{a}{2C}\right)^{1/2} (T_{tr} - T)^{1/2}, \tag{20}$$

where a and C are parameters, and T_{tr} is the transition temperature.

That the application of the Landau theory in the case under consideration is correct has been confirmed by the experimentally found form $(T_{tr} - T)^{1/2}$ of the temperature dependence of ψ_{op} [104]. It follows from Fig. 4a that V_{cl} exhibits a similar form of temperature dependence. Here, T_{tr} was represented by the glass transition temperature T_g (as is usual in the Landau theory [104]), melting temperature T_m, and 'liquid 1 – liquid 2' transition temperature T_{ll} approximately expressed as [57]

$$T_{ll} \cong (1.2 \pm 0.05) T_m . \tag{21}$$

The data presented in Fig. 4a (curves *4* – *6*) suggest that the density V_{cl} of a cluster network of entanglements is an analogue of the order parameter ψ_{op} and therefore characterizes the degree of local ordering in noncrystalline regions of polyethylenes. Two interesting peculiarities of these data are worthy of note. First, the dependence $V_{cl} = f(T_{tr} - T)^{1/2}$ has an inflection point at $T \cong 333$ K. It has been shown by Boyer [105] that at this temperature polyethylenes undergo a relaxation transition which the author called the 'glass transition I'. Second, Eqn (20) implies the condition $\psi_{op} = 0$ at $T = T_{tr}$. It follows from Fig. 4a that the identity $V_{cl} = 0$ is reached at $T = T_m$ but not at $T = T_g$. In other words, not only crystallites but also segments 'melt' at T_m and only the macromolecular interlacing network is preserved at temperatures above T_m [88]. Such a situation is due to the specificity of the local order formation in amorphous – crystalline polymers, such as polyethylenes, in which this process is 'forced', resulting from chain tension in the amorphous phase in the course of crystallization [96, 106]. It is worthwhile to note that the analogy between parameters ψ_{op} and V_{cl} rules out consideration of the entanglement sites as conventional interlacings [88] and suggests that they should be identified with the regions of local order (clusters) [107].

Density fluctuations $\langle \Delta\rho/\rho \rangle^2$ serve as a measure of polymer disorder and are defined in the following way [108, 109]

$$\left\langle \frac{\Delta\rho}{\rho} \right\rangle^2 = \frac{\langle (N - \langle N \rangle)^2 \rangle}{\langle N \rangle}, \tag{22}$$

where N is the number of electrons in an arbitrarily chosen volume ($\langle N \rangle$ stands for the mean value of N).

Sanditov and Bartenev [110] demonstrated that $\langle \Delta\rho/\rho \rangle^2$ depends on the relative fluctuation volume f_c in the following way

$$\left\langle \frac{\Delta\rho}{\rho} \right\rangle^2 = f_c \left(\frac{V_h}{V_a}\right), \tag{23}$$

where V_h is the volume of a microcavity in the fluctuation free volume, and V_a is the atomic volume.

Also, $\langle \Delta\rho/\rho \rangle^2$ can be found using the Poisson coefficient μ [110]:

$$\left\langle \frac{\Delta\rho}{\rho} \right\rangle^2 \cong \frac{(1 - 2\mu)^3}{6(1 + \mu)^2} . \tag{24}$$

The temperature dependences of $\langle \Delta\rho/\rho \rangle^2$, calculated by means of Eqns (23) and (24) for HDPE and LDPE, are presented in Fig. 4b. Despite the different absolute values of fluctuation density found from these equations, the temperature dependence patterns agree with the presently available data [111]. Characteristically, the dependences $\langle \Delta\rho/\rho \rangle^2(T)$ in this case too show inflection points at ~ 333 K as in Fig. 4a. Higher $\langle \Delta\rho/\rho \rangle^2$ values for LDPE are due to the larger V_h of this polymer [107].

Doping HDPE with a small amount (Z) of a highly dispersed Fe – FeO mixture results in a significant alteration

Table 3. Impact strength A_p, cracking resistance τ_{50}, and coefficient of gas (nitrogen) permeability P_{N_2} for HDPE + Z compositions [103].

Z content (weight percent)	A_p, kJ m^{-2}	τ_{50}, h	$P_{N_2} \times 10^{-17}$, $\frac{\text{mol m}^{-1}}{\text{m}^2\ \text{s Pa}}$
0	12.0	10	2.70
0.01	17.3	36	
0.05	37.4	250	0.16
0.10	12.0	38	
0.50	13.0		
1.0	19.6	3.9	1.70

of the polymer structure and properties [98, 103]. Table 3 shows the changes in such properties of an HDPE + Z composition as impact strength A_p, coefficient of gas permeability P_{N_2}, and cracking resistance τ_{50} in aggressive media. It is quite clear that such conspicuous changes of these (and a number of other [100]) properties must be associated with the corresponding restructuring of the HDPE + Z composition compared with original HDPE. In Ref. [103], structural changes in HDPE caused by the incorporated admixture of Z were examined by DSC, large- and small-angle X-ray diffraction, and IR spectroscopy. Some results were obtained in mechanical tests, by magnetic measurements, and in rheologic studies. Dramatic changes of the properties at $C_Z = 0.05$ wt % (see Table 3) suggest a decrease of the crystallite size at the given Z level [112]. This observation is confirmed by electron microscopy data.

Because the properties of melted HDPE and its compositions with Z are interrelated with the morphological structure of the material being formed during crystallization, the flow-behavior index (I_f) was measured and found to be minimal at a Z content of 0.05 wt %. It has been shown in Refs [98, 99] that a rise in viscosity of composite melts as compared with basic HDPE should be attributed to the enhanced density V_{cl} of a cluster network of entanglements resulting from the addition of the filler. According to current crystallization concepts [113], an increased number of molecular entanglement sites rejected from the regions undergoing crystallization interferes with the degraded continuity of this process and leads to a respective decrease in the crystallite size.

One more structural peculiarity of compositions containing 0.05 wt % of Z has been demonstrated by large-angle X-ray radiography. Evaluation of the C_Z-dependence of the fraction L_{or} of oriented crystallites revealed that it varies considerably with a change in the filler content (Table 4) and is of extreme character.

Analysis of small-angle X-ray scattering curves for specimens containing different amounts of Z has shown that maximum scattering occurs in composites with a larger fraction of oriented crystallites. Test pieces containing 0.05 wt % of Z exhibit the maximum intensity of small-angle scattering; the corresponding curve is characterized by the highest degree of symmetry and has the largest half-width. All these facts indicate that specimens of this composition have the most perfect (regular) polymer morphology with minimal dispersion, both in large period dimensions and in the dimensions of crystalline and amorphous regions. This is confirmed by the results of studies [114, 115] which suggest that enhanced crystallinity leads to a denser packing of crystallites, hence to a limited number of possible configurations that can be realized in noncrystalline regions. Specifically, as the distance between crystallites decreases, the chains in the noncrystalline regions have to align parallel to the crystallite surface (the so-called barrier effect).

Table 4. Fraction L_{or} of oriented crystallites and normalized magnetic susceptibility χ_m^n for HDPE compositions [103].

Z content, weight percent	L_{or}, %	χ_m^n, G g^{-1}
0	25	
0.01	27	0.30
0.05	44	0.23
0.10	36	
0.15	25	
0.20	24	0.18
0.50	27	
1.00	25	0.14
12.00		0.17

Table 4 shows the overall magnetic susceptibilities χ_m of specimens prepared from HDPE + Z compositions, which were calculated as follows [116]

$$\chi_m = \frac{M}{H}, \tag{25}$$

where M is the magnetic moment, and H is the magnetic field strength.

The dependences $M = f(H)$ for compositions containing Z at 0.01 and 0.05 wt % are characterized by a negative ingredient beyond the saturation point, which suggests a considerably enhanced (compared with other compositions) diamagnetic contribution (in absolute terms) to the overall magnetic moment [116]. It is known [117] that one of the causes of such a rise may be an increased number of conduction electrons or, in other words, an increase in the relative amount of free iron in a Fe–FeO mixture incorporated into a polymer matrix. It follows from these data that the parameter χ_m^n for PE compositions grows significantly at the beginning as the Z content increases, but thereafter (at $C_Z \geqslant 0.20$ wt %) reaches asymptotic values [101].

Taken together, the above results allow the following interpretation of the experimentally examined extremum in the physicomechanical characteristics of HDPE + Z compositions, related to an increase of V_e, in analogy with that proposed for single-phase metal-containing polymers [118]. If Z is incorporated into HDPE as described in Ref. [119], iron is reduced from its oxidized forms as schematically shown in the diagram below:

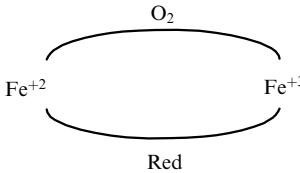

(26)

where Red is a reducer which may be a product of HDPE oxidation containing hydroxyl and carbonyl groups or mobile hydrogen. This speculation is confirmed by an increase in the diamagnetic contribution, a decrease in the size of Z particles, and higher χ_m^n values for compositions containing 0.01 and 0.05 wt % of Z. Because of the high dispersion of Z-particle sizes, a part of the Z fraction may fall into a size range accounting for the appearance of supermagnetic domains [120]. Naturally, the less the average size of the particles R_{av}, the more of them may become supermagnetic domains. The technology for the injection of metals into polymers, described in Ref. [118], implies

significantly smaller particle sizes for Z and the absence of its oxides. Nevertheless, it is obvious that there is a common tendency in the behavior of single-phase metal-containing polymers and HDPE + Z compositions. In particular, they share the property of a significantly decreased flow-behavior index [103].

Furthermore, the above results also suggest that Z particles initiate cluster-type entanglements (Fig. 1d) in noncrystalline regions of HDPE, because a magnetic field applied to a PE melt promotes ordering [121]. In addition, it can be expected that local magnetic fields of superparamagnetic particles will facilitate the formation of the regions of local order. From this standpoint, it is easy to explain the rise in τ_{50} and decrease of P_{N_2} for HDPE + Z compositions (see Table 3) because the enhanced amount of molecular interlacings must have an opposite effect as a result of structure loosing [122].

Figure 2b (curves *4*, *5*) shows the temperature dependences of functionality F for the sites of a network of molecular entanglements, determined with the help of Eqn (5) for HDPE and a composition containing Z at 0.05 wt %. For these polymers $F \geqslant 11$, whereas for conventional molecular interlacings $F = 4$ [66]. This also confirms clustering in noncrystalline regions of HDPE.

The foregoing can be summarized in the following way:

(1) sites of the network of macromolecular entanglements in noncrystalline regions of amorphous – crystalline polymers form regions of local order (clusters);

(2) density changes in the cluster network of entanglements have a marked effect on the HDPE structure and properties;

(3) there appears a possibility of goal-oriented regulation of V_{cl} and, consequently, of the properties of polymers belonging to this class.

Experimental evidence of the structural heterogeneity in the polymer amorphous state, consistent with the cluster model, has been obtained in Refs [86, 123] with the aid of the large-angle X-ray radiography used earlier for a similar purpose [124, 125]. As a rule, large-angle X-ray halos of amorphous polymers depart from an ideal shape, showing asymmetry, poorly distinguishable maximum, etc. This suggests the superposition of several scattering curves of a simpler form.

It is expected that the use of strictly monochromatic K_{α_1}-radiation broken free from the K_{α_2}-component may increase the resolving power of the X-ray technique and provide data in support of the above reasoning. Such a possibility has been demonstrated in a study of epoxy polymers as typical representatives of glassy cross-linked polymers [123].

Analysis of a typical diffraction pattern for epoxy polymers hardened with diamines (stoichiometric composition) [123] has demonstrated that they are best described on the assumption of the existence of two components. This finding once again confirms the above postulate of structural heterogeneity (microheterogeneity) of the polymer amorphous state. At the same time, the existence of two components allows the premises of the cluster model to be used. It is natural to associate a halo having the vertex at smaller scattering angles θ (and corresponding to a larger Bragg interval d_B) with the loose-packed matrix, while a halo at larger θ with clusters, i.e. a more closely packed component.

The knowledge of a Bragg interval for clusters and a loose-packed matrix provides the possibility to calculate the

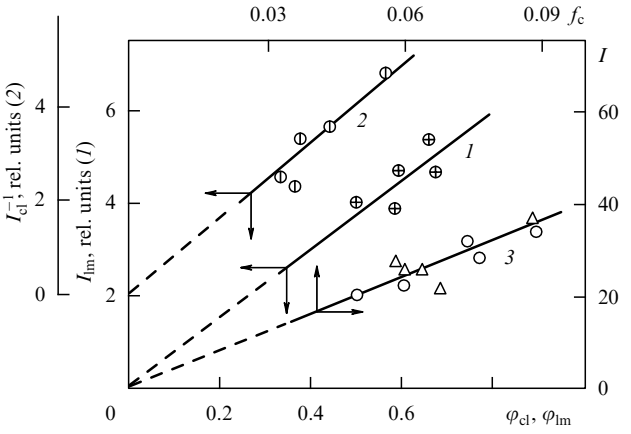

Figure 5. Plots of integral scattering curve intensity I_{lm} (*1*) for the loose-packed matrix and inverse integral scattering curve intensity I_{cl}^{-1} (*2*) vs. its relative portion φ_{lm} for epoxy polymers hardened with diamines [123], and of intensity I of large-angle roentgenograms vs. relative fluctuation free volume f_c (*3*) for epoxy polymers hardened with diamines (open circles) and anhydrides (triangles) [129].

appropriate characteristic intermolecular distance D because $D \cong 1.22 d_B$ [126]. The estimates obtained in Ref. [123] indicate that $D \cong 6$ Å for clusters, and $D \cong 7$ Å for the loose-packed matrix. Moreover, these distances are independent of the density ν_{cr} of cross-linking within the experimental error. Their absolute values agree fairly well with the generally accepted ones [126].

Figure 5 compares the integral scattering intensity I_{lm} of an amorphous halo component having the vertex at lower θ with the loose-packed matrix relative portion φ_{lm} estimated as [68]

$$\varphi_{lm} = 1 - \varphi_{cl} \,. \tag{27}$$

There is a definite growth of I_{lm} with increasing φ_{lm}. This dependence is linear and may be extrapolated to the origin of the coordinate system. An even more apparent correlation of this kind has been obtained for amplitude intensity. This gives additional evidence of the relationship between the scattering curve to which large d_B values correspond and a given structural component, namely, the loose-packed matrix [123].

To conclude, it should be noted that the existence of local order in the polymer amorphous state (regardless of the concrete model of its regions) is supported by rigorous mathematical arguments of the most general character. In accordance with the Ramsey theorem proved in the theory of numbers, any sufficiently large amount $i > R(i, j)$ of numbers, points, and objects (or statistical segments as is the case with this review) is sure to contain a highly ordered subsystem of $N_j \leqslant R(i, j)$ such segments. This makes improbable absolute disordering in large systems (structures) [127, 128].

3. The concept of a structural defect

It has been noted earlier that the cluster model of the polymer amorphous state allows for an essentially new interpretation of a structural defect (in the full sense of this term) for a given state [44, 129]. The structure of real solids is known to contain a large number of imperfections [34]. This concept constitutes the basis for the theory of dislocations, which is extensively employed to describe the behavior of crystalline solids.

Recent progress in this area accounts for the attempts of certain authors [35–40, 130, 131] to apply this concept to amorphous solids, too (specifically, to amorphous polymers). In this case, notions used to characterize crystal lattices are frequently extended to the structure of amorphous polymers. As a rule, this is done on the grounds of outward similarity between stress–strain ($\sigma-\varepsilon$) curves for crystalline and amorphous solids. The authors of Ref. [129] suggested that the essential structural differences rather than the formal resemblance of the behavior of a given type of solids should constitute the basis of the theory of structural defects.

The discussion concerning amorphous polymers has long been focused on whether they have or do not have local order. It has revealed a considerable controversy of opinion. The presence of local order may seriously influence the definition of a structural defect in amorphous polymers if, in the general case, the defect is understood as either an order–disorder transition or the reverse process. For example, in crystalline solids any distortion (break) of the long-range order represents a defect (dislocation, vacancy, etc.), whereas a single crystal with perfect long-range order constitutes an ideal structure showing no defects. It is known [132] that a sufficiently bulky polymer specimen with 100% crystallinity is impossible to synthesize, and all characteristics of such hypothetical polymers are deduced by extrapolation. For this reason, an ideal defect-free structure of the amorphous-state polymer is simulated by the 'felt' model proposed by Flory [70, 133]. According to this model, an amorphous polymer is made up of interpenetrating coiled macromolecules, i.e. the personification of complete disorder. In terms of this model, a defect in an amorphous polymer may be thought of as a disturbance (break) of the complete disorder — that is, the formation of local (or long-range) order [129]. It is also worth noting that the formal resemblance of $\sigma-\varepsilon$ curves for crystalline solids and amorphous polymers is far from fullness and their behavior reveals principal differences.

Returning to the proposed concept of an amorphous-polymer defect, it should be noted that a cluster segment may be regarded as a linear defect, i.e. an analogue of dislocation in crystalline solids. Because the length of such a segment in the cluster model is assumed to be equal to the length of the statistic segment l_{st}, and their number per unit volume equals the density V_{cl} of the network of cluster entanglements, the density of linear defects ρ_d per polymer unit volume can be expressed as [129]

$$\rho_d = V_{cl} l_{st} . \qquad (28)$$

This interpretation allows the well-developed mathematical apparatus of the dislocation theory to be applied to the description of mechanical properties of amorphous polymers. Of special interest here are the results of large-angle X-ray diffraction demonstrating an antibate change of the cluster fraction φ_{cl} (the degree of local order) and integral intensity I_{in} (area) of the total amorphous halo as a function of cross-link density ν_{cr} for epoxy polymers [123]. Viewed in the light of the analogy with crystalline solids, this inference seems unexpected because a rise in φ_{cl} must lead to the growth of I_{in} [134]. At the same time, this result can be fully accounted for by the proposed structural defect concept. In this case, the degree of disorder in a system (i.e. the degree of approximation to an ideal defect-free structure) may be the amount of fluctuation free volume f_c in the glassy state [135]. The dependence $I_{in}(f_c)$ in Fig. 5 (curve *3*) is linear and goes through the origin of the coordinate system. In other words, the quantity I_{in} characterizes the degree of disorder in the amorphous state of polymers, thus explaining the antibate dependences $\varphi_{cl}(\nu_{cr})$ and $I_{in}(\nu_{cr})$ mentioned earlier in this section and confirms the proposed structural defect concept. An essentially similar interpretation was proposed by Guinier [136]. He believed that a decrease of I_{in} for metals may be due to the formation of precrystallite structures in multicomponent melts.

Comparison of the results presented in Fig. 5 and available from the relevant publications on amorphous polymers indicates that the above reasoning is in line with observations of other authors. For example, a study of the effects of annealing temperature T_{ann} on the cellulose nitrate structure [137] revealed a systematic decrease of amorphous halo intensity and an increase of the large Bragg interval d_B with increasing T_{ann}. It is universally accepted that annealing of amorphous polymers at temperatures below T_g improves molecular packing [138]. Therefore, this process must intensify with increasing T_{ann}. Nonetheless paper [137] offers a different explanation of this effect, in which experimental data fit in the above interpretation. A decrease of I_{in} in the course of cluster formation was also documented in Ref. [139].

Generally speaking, it can be expected that the degree of disorder in a solid increases with temperature. If in addition the order is of thermofluctuation origin (as with the cluster model), this tendency becomes even more pronounced. However, studies of inorganic glasses (e.g., As_2Se_3 and GeS_2) by X-ray diffractometry and small-angle neutron scattering technique showed that a rise in temperature led to a higher intensity of the peak associated with the near-range order in the amorphous state [134]. It was hypothesized that the layered structure representing the near-range order in these glasses became even more regular upon raising the temperature. It is worth noting that Lin et al. [134] did not present other evidence, besides these analogies with the behavior of crystalline solids. The proposed interpretation appears to provide a more realistic explanation of this experimental finding. Also, it was shown in work [134] using different types of glasses that the closer the testing temperature to T_g of the glass, the higher the intensity of the peak mentioned. This observation is also consistent with the cluster model (see Fig. 2). Finally, a rise in the intensity of amorphous halos was also observed for polystyrene (PS) at temperatures both above and below T_g [140]. Evidently, there is no reason to expect an enhancement of the degree of local order with elevated temperature for this amorphous polymer [141]. Therefore, it should be recognized that the proposed interpretation of a structural defect provides a sufficiently general explanation of the experimental findings [134, 137, 139–141].

One striking experimental result was obtained with epoxy polymers experiencing deformation above the yield stress [142]. The authors observed an increase in the intensity of the amorphous halo by approximately 17%. This finding is also easy to explain in the context of the proposed interpretation because the cluster model implies (see below) that the flow process is associated with the decomposition of unstable clusters, hence with a decrease of V_{cl} and the degree of local order [143]. The amount of clusters of this type in Ref. [143] is approximately identical to that responsible for the rise in the amorphous halo intensity of epoxy polymers reported in paper [142]. For the intensity of the cluster-associated (see

Ref. [123]) second halo component (I_{cl}), there is linear correlation I_{cl}^{-1} (see Fig. 5, curve *2*), in agreement with the above considerations concerning a decrease of intensity with increasing degree of ordering in amorphous polymers.

We shall further consider the applicability of the proposed concept of structural defects to the description of flow in polymers. As a rule, earlier concepts of polymer defects were largely or even exclusively used to describe this process [35–40, 130, 131]. The theoretical shear strength of crystals was for the first time computed by Ya Frenkel' based on a simple model of two rows of atoms shifted relative to each other under the effect of shear stress. In accordance with this model, the critical shear stress τ_0 is given by [34]

$$\tau_0 = \frac{G}{2\pi}\,, \tag{29}$$

where G is the shear modulus.

In a slightly modified form, this model was applied to polymer fluidity in Ref. [37], where the following ratio was obtained:

$$\tau_0 = \frac{G}{\pi\sqrt{3}}\,. \tag{30}$$

Special attention should be given to an important fact characterizing the essentially different behavior of crystalline metals as compared with polymers. It has been shown [34, 144] that the ratio τ_{ann}/τ_y (where τ_y is an experimentally found shear stress in the case of yielding) for metals is significantly higher than for polymers. For five metals with face-centered cubic and hexagonal lattices $\tau_{ann}/\tau_y = 3740-22720$ (see Ref. [34]), whereas for five polymers this ratio is 2.9–6.3 [37]. As a matter of fact, the closeness of τ_{ann}/τ_y to unity is in itself a proof of the possibility of realization of the mechanism proposed by Frenkel' in polymers (as opposed to metals). A slight modification of the law of periodic changes of shear stress τ in polymers leads to τ_{ann}/τ_y practically equal to unity [145].

As shown by Kozlov and Novikov [145], dislocation analogies hold good for amorphous metals too. Indeed, Liu and Li [146] considered the distortion of the atomic arrangement (responsible for the appearance of elastic stress fields) as a linear defect (dislocation) incapable of motion. It is easy to see that such an approach is in excellent agreement with the concept proposed in this section. In the framework of this concept, the cluster (crystallite) cross section and a shift of segments as postulated by Frenkel' can be regarded as a mechanism limiting the fluidity of polymers. This view is supported by the results of Ref. [147] where it was shown experimentally that the flow in glassy polymers is realized in closely packed regions. Balankin et al. [128] also demonstrated that these closely packed regions are clusters. In other words, it may be argued that fluidity is associated with the loss of stability by clusters (crystallites) in a shear stress field.

Monograph [148] presents an asymmetric periodic function illustrating the dependence of shear stress τ on shear strain γ_{sh}. The asymmetry of such a function [144] and the corresponding decrease of the height of the energy barrier overcome by macromolecular segments in an elementary flow act is due to the cavity formation of fluctuation free volume cavity in the course of deformation (also being a specific feature of polymers [82]). These data indicate that the dependence of τ on their shift from zero to a maximum at the initial portion of the periodic curve can be simulated by a sinusoid with a smaller period. In this case, the function $\tau = f(x)$ can be represented as

$$\tau = k\sin\left(\frac{6\pi x}{b_i}\right)\,, \tag{31}$$

in perfect agreement with Frenkel's conclusion, excepting an arbitrary chosen numerical coefficient in parentheses (6 instead of 2).

The further calculation of τ_0 as described in Ref. [34] and its comparison with experimentally found values of τ_y revealed their close correlation in amorphous and amorphous–crystalline polymers. This confirms the possibility of realization of the above flow mechanism at the segmental level.

The lack of correspondence between τ_{ann} and τ_y in metals made researchers look for another mechanism of yield. At present, it is generally accepted that such a mechanism consists in the motion of dislocations over slip planes of the crystal [34]. This implies that interatomic interaction forces directed perpendicular to the crystallographic slip plane are overcome during a series of local displacements determined by the periodic lattice stress field. This mechanism is obviously different from a macroscopic shift in which all bonds are broken simultaneously (the Frenkel' model). It seems evident that the overall shear strain realized via dislocation motion requires a significantly smaller external stress than the process involving simultaneous disruption of all atomic bonds across the slip plane [34].

Peierls and Nabarro were the first to compute the shear stress τ_{sh} necessary for dislocation motion [34]. These authors used a sinusoidal approximation and showed that the quantity τ_{sh} is defined by the expression

$$\tau_{sh} = \frac{2G}{1-\mu}\exp\left[-\frac{2\pi a_i}{b_i(1-\mu)}\right]\,, \tag{32}$$

where μ is the Poisson coefficient, while the parameters a_i and b_i represent shifts in two mutually perpendicular directions.

The substitution of reasonable μ values, for instance, 0.35 [110] and the assumption of $a_i = b_i$ lead to $\tau_{sh} = 2\times10^{-4}G$. For metals, this figure is higher than the observed values of τ_y but significantly closer to them than the stress computed from the simple shift model (the Frenkel' model).

However, there is a reverse picture for polymers. A similar computation gives τ_{sh} of not higher than 0.2 MPa or roughly two orders of magnitude lower than the observed τ_y values.

Let us now consider the dislocation mean free path λ_d. It is known [34] that in metals, where mobile dislocations play the key role in plastic deformation, the quantity λ_d is of the order of $\sim 10^3$ nm. For polymers, this parameter can be estimated in the following way [149]

$$\lambda_d = \frac{\varepsilon_y}{b\rho_d}\,, \tag{33}$$

where ε_y is the yield strain, b is the Burgers vector, and ρ_d is the density of linear defects. The quantity ε_y is of the order of ~ 0.10 [150], the Burgers vector $b \cong 3\times10^{-10}$ m [40], and ρ_d can be found from Eqn (28).

With the help of Eqn (33), the value of λ_d for different polymers was estimated to be ~ 0.25 nm. A similar distance is covered by a macromolecular segment upon a shift as is easy to see from purely geometric considerations. Therefore, in this case too, there is no reason to speak about any significant value of dislocation mean free path in polymers. Rather, a

segment (or several segments) of a macromolecule passes from one quasi-equilibrium state to another [151].

It is well known [34, 148] that the Bailey–Hirsch relation between shear stress τ_y at yield and dislocation density ρ_d is fulfilled for crystalline materials:

$$\tau_y = \tau_i + \alpha G b \rho_d^{1/2}, \qquad (34)$$

where τ_i is the initial internal stress, and α is the efficiency constant.

Equation (34) also holds for amorphous metals [146]. In Ref. [145], this equation was used to describe the mechanical behavior of polymers belonging to major classes. For this purpose, the characteristics of amorphous glassy polyarylate (PAr) [91], amorphous–crystalline HDPE [98], and cross-linked epoxy polymers hardened with amines and anhydrides [143] were examined. Various loading schemes were employed including uniaxial tension [91], high-speed bending [98], and uniaxial compression [143]. An empirical relation was used to estimate the parameter b as [152]

$$b \cong \left(\frac{52.2}{C_\infty}\right)^{1/2}. \qquad (35)$$

Figure 6a illustrates the relationships between $Gb\rho_d^{1/2}$ and the experimentally obtained values of τ_y for the above polymers described by Eqn (34). It can be seen that these are linear relationships passing through the origin of the coordinates (i.e. $\tau_i = 0$), but the α values are different for linear and cross-linked polymers. It is therefore concluded that within the framework of the proposed defect concept the Bailey–Hirsch relation holds also true for polymers. This means that dislocation analogies are valid for any linear defect distorting the ideal structure of a material and creating an elastic stress field [145]. In this context, it is worthwhile to emphasize the high degree of imperfection in polymers, which reveals itself in $\rho_d \sim 10^{14}$ cm^{-2} [149] compared with $\rho_d \sim 10^{10}$ cm^{-2} for crystalline metals [34] and $\rho_d \sim 10^9$–10^{14} cm^{-2} for amorphous metals [146].

It can be concluded from the results reported in Ref. [145] that in polymers, unlike metals, the probability of flow by Frenkel' mechanism is much higher than its realization through the motion of defects. This inference is governed by the above-mentioned essential (and even diametrically opposite) structural difference between crystalline metals and polymers [129].

There is one more conceivable interpretation of structural defects in amorphous polymers, based on the premises of a new scientific discipline called synergetics [46] and concerned with self-organization processes in dissipative structures (DS). The possibility of DS realization in polymers was also considered in earlier studies [41–44]. Suffice it to note that the behavior of the regions of local order (clusters) and DS has much in common. To begin with, it is well known [138] that physical ageing of amorphous polymers leads to a higher degree of their local order, in agreement with the fact that a rise in DS energy dissipation with time ensures the stability of a strongly nonequilibrium system. It is also known [43, 153] that DS are formed when the system is rather far from equilibrium. This general proposition is also consistent with the cluster system behavior. It can be seen from Fig. 2 that the onset of cluster formation corresponds to a deviation from equilibrium (T_g). The rate of formation rapidly decreases in the $T < T_g$ region as T moves away from T_g. Such a behavior

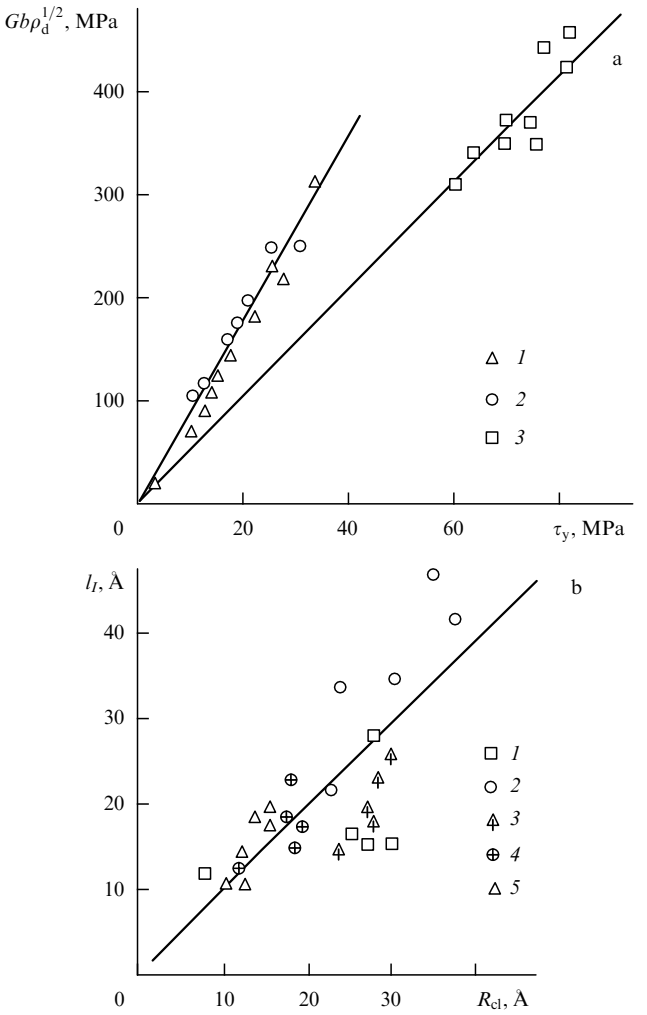

Figure 6. Relationships (a) between $Gb\rho_d^{1/2}$ and shear stress τ_y at yield, corresponding to Eqn (34), for PAr (*1*), HDPE (*2*), and EP (*3*) [145], and (b) of distances between dissipative structures l_I and clusters R_{cl} for: *1*, *2* — DF-10 polyarylate extruded parallel and perpendicular to the extrusion axis, respectively, *3* — amorphous glassy, *4* — amorphous–crystalline, and *5* — cross-linked polymers.

is typical of DS [153]. However, the most important common feature in the behavior of clusters and DS consist in that both represent a transition to an ordered state at the bifurcation point (T_g or T_m on the temperature scale [154]) and are of fluctuation origin [46]. This makes it possible to define a structural defect in the amorphous state of polymers as an element arising from a departure of the system from an ideal (equilibrium) condition towards a thermodynamically nonequilibrium one. In such an interpretation, the notions of ideal (defect-free) and equilibrium polymer structures coincide, since the two states are realized above the bifurcation point on the temperature scale and correspond to the structural model of interpenetrating Flory coils [133]. In other words, they are characterized by the absence of a 'frozen' local order. It needs to be shown that clusters and DS do not differ as structural entities, if the identity of the two defect interpretations considered in this section is to be confirmed.

As is well known [127], even in elastically isotropic solids there are at least three independent scales of length

$$l_p = a, \qquad l_\varepsilon = a\Lambda_0, \qquad l_I = l_\varepsilon \Lambda_i, \qquad (36)$$

which determine complex dynamics of self-organization processes in DS. There is every reason to anticipate [150, 156] that in amorphous-state polymers these scales must reflect three main structural levels — that is, molecular, segmental, and supersegmental (permolecular). If this suggestion is correct, l_p ought to be taken as a minimal independent dimension characterizing a macromolecule, i.e. the length of the skeletal bond l_0, the values of which for different polymers are reported in Ref. [73]. Another explicit scale of length for polymers is the length l_{st} of the statistic segment exhibiting the smallest fragment of a macromolecule with an interindependent orientation in space [157]. It follows from the comparison of Eqns (8) and (36) that

$$l_p = l_0 , \qquad \Lambda_0 = C_\infty . \tag{37}$$

The automodel coefficient Λ_i can be represented as follows [127]

$$\Lambda_i = \frac{l_{i+1}}{l_i} = \frac{2(1-\mu)}{1-2\mu} , \tag{38}$$

where l_{i+1} and l_i are the neighboring linear scales of DS, and μ is the Poisson coefficient.

Assuming that the next structural level in polymers is represented by DS separated by distances l_i, and taking into account Eqns (37) and (38), it is possible to write down [156]

$$\Lambda_i = \frac{l_I}{l_{st}} = \frac{2(1-\mu)}{1-2\mu} . \tag{39}$$

Equation (39) allows the value of l_I to be determined if the Poisson coefficient is known from the results of a mechanical test based on the equation [110]

$$\frac{\sigma_y}{E} = \frac{1-2\mu}{6(1+\mu)} , \tag{40}$$

where σ_y is the yield stress, and E is the modulus of elasticity.

The distance between clusters R_{cl} may be found from Eqn (18). Thus, within the framework of the two independent models, it is possible to estimate the distance between ordered elements of structure in the polymer amorphous state: l_I for DS, and R_{cl} for clusters. When these elements are the same structural units, the following evident identity must be satisfied:

$$l_I \cong R_{cl} . \tag{41}$$

The existence of two parallel structures with a similar characteristic scale of length on the order of a few tens of angstroms seems to be very unlikely. The comparison of l_I and R_{cl} for different polymers in Fig. 6b confirms the validity of identity (41) and suggests a similarity of clusters and DS. It should be noted that the formation of supersegmental structures (DS or clusters) in the amorphous state of polymers is encoded at the molecular level, since appropriate conditions are controlled by the parameters l_0 and C_∞ [see Eqn (37)].

The most important conclusion inferred from the materials presented in this section is that the three main approaches to the description of polymer amorphous state (local order model, structural defect concept, and fractal analysis discussed below) are based on a fundamental property of the glassy state, namely, its thermodynamically nonequilibrium character.

4. Analysis of experimental data (interpreted in the framework of the cluster model)

This section discusses experimental data and their interpretations showing that the cluster model does not contradict earlier findings and may serve as a unified model for their description. An indisputable advantage of this approach consists in that the parameters of the model inspected can be obtained in independent tests [55, 158].

Mooney – Rivlin equation. The possibility of using the Mooney – Rivlin equation for the description of local order in polymers has been considered in Ref. [159]. This approach is essentially different from the methods used in previous investigations into the properties of rubbers alone in that it is also applicable to solid glassy polymers. The empirical Mooney – Rivlin equation in its simplest variant has the form

$$f^* = 2C_1 + 2C_2\lambda^{-1} , \tag{42}$$

where f^* is the reduced stress, $2C_1$ and $2C_2$ are the equation constants, and λ is the degree of stretch.

The quantity f^* is defined by the ratio [161]

$$f^* = \frac{\sigma}{\lambda - \lambda^{-2}} , \tag{43}$$

where σ is the nominal stress, i.e. that calculated taking into consideration the initial cross-section area of a sample.

Equation (42) is extensively used to study the mechanical properties of rubber. Based on the analysis of a series of publications, Boyer [3] suggested that the $2C_2/2C_1$ ratio can serve as a measure of near-range order in the cross-linked rubbers and summarized in a table a variety of experimental data for polymers in the rubbery state that confirm this suggestion.

Typical dependences described by Eqns (42) and (43) for PC (tested at $T = 403$ K) and HDPE ($T = 293$ K) are presented in Fig. 7 (curves *1*, *2*). It can be seen that the Mooney – Rivlin equation is applicable to both amorphous

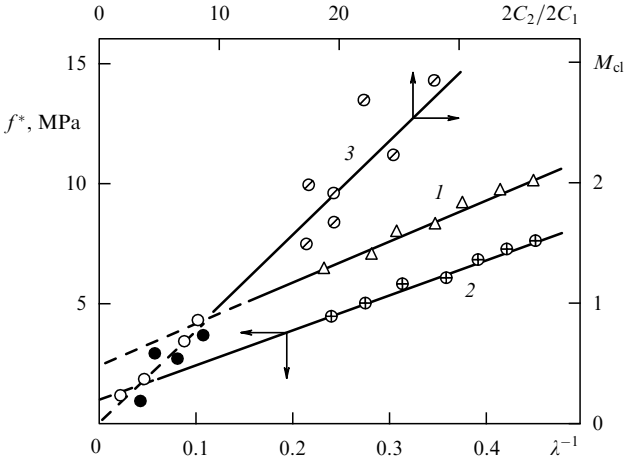

Figure 7. Plots of reduced stress f^* vs. degree of stretch for PC (*1*) and HDPE (*2*) [159] and of molecular weight M_{cl} of chain segments between clusters vs. the ratio of constants of the Mooney – Rivlin equation (*3*) for PC (open circles), PSf (full circles), and HDPE (crossed circles) [159].

and amorphous–crystalline polymers and gives reasonable absolute values of $2C_1$ and $2C_2$. This last inference is based on the following observation. It is known [160] that the constant

$$2C_1 = \frac{A\rho RT}{M_e}, \tag{44}$$

where A is the coefficient determined by the functionality of entanglement network sites.

The estimation of M_e from the known values of $2C_1$ using Eqn (44) has demonstrated a good agreement with analogous parameters computed with the help of relations (1) and (2). Characteristically, the values of $2C_1$ thus obtained are in correspondence with M_{cl} (but not with M_e values for a molecular entanglement network, which are one or two orders of magnitude higher).

It follows from the dependence of M_{cl} on the $2C_2/2C_1$ ratio (Fig. 7, curve *3*) that the parameters in question are related by a linear correlation, which confirms Boyer's suggestion about the possibility of using the $2C_2/2C_1$ ratio as a measure of near-range (local) order in polymers. However, Boyer [3] believed that a rise in the absolute $2C_2/2C_1$ value reflects the enhanced degree of the near-range order in rubbers. For the polymers studied in Ref. [159], a rise in M_{cl} with increasing $2C_2/2C_1$ means a decrease in the density of entanglement network [see Eqn (3)], the number of segments in a cluster, and therefore the degree of local order. In other words, a rise in $2C_2/2C_1$ for amorphous glassy and amorphous–crystalline polymers reflects an effect opposite to that observed in rubbers. Such a discrepancy is no mere coincidence, it rather reflects structural differences between these classes of polymers. In rubbers, the cross-link density and the potential for the chain fragment packing between cross-link sites are associated with different structural elements and display the opposite trend [3]. For polymers of this study, the density of entanglement network and the degree of local order undergo symbate variations, as follows from the cluster model. In other words, analogies between structural and mechanical properties of truly cross-linked rubbers and linear polymers studied in Ref. [159] may be regarded as relevant only with some reservation.

Grüneisen parameter. In the physics of liquids and glasses, there has recently been increasing interest in the Grüneisen parameter γ which enters the equation of state and serves as a measure of anharmonicity of quasi-lattice vibrations and nonlinearity of interatomic interaction forces [47, 48]. The Grüneisen parameter has been successfully used for the analysis of cluster formation and molecular ordering in liquids [162–164]. The liquid and glassy states being structurally indistinguishable [165], it is of interest to apply the Grüneisen parameter to the study of local order in glassy systems. Paper [166] offers an interpretation of the temperature dependence of γ in amorphous polymers within the framework of the cluster model.

Knopoff and Shapiro [162] have demonstrated that a decrease of γ with increasing specific volume V for water and mercury can be ascribed to a change of the mean number N of molecules in the cluster. They posed a semiquantitative one-dimensional model to describe the volume dependence of γ. It was assumed that γ is a sum of two components [162]:

$$\gamma = \gamma_D + \xi \left.\frac{\partial \ln N}{\partial \ln V}\right|_P, \tag{45}$$

where γ_D is the component of γ corresponding to the Debye theory of heat capacity, and ξ is the N-dependent factor.

Equation (45) describes variations of γ with changing pressure P. However, it can also be used to estimate the temperature dependence of γ at a constant pressure, by virtue of the equivalence of variables P and T in the equation of state. In this case the subscript P in Eqn (45) is replaced by T.

The Debye component γ_D of the Grüneisen parameter may be expressed as [162]

$$\gamma_D = -\xi \left(\frac{\partial \ln \omega_D}{\partial \ln V}\right)_P, \tag{46}$$

where $\omega_D = \pi\omega_0$ is the Debye vibration frequency of a polymer chain, and

$$\omega_0 = \frac{U}{M}. \tag{47}$$

Here, M is the mass of a vibrating kinetic unit of the chain, and U is the potential interaction energy of two kinetic units (segments) in a cluster, which may be estimated in the framework of the structural defect concept discussed in the previous section as follows [152, 156]

$$U = \frac{Gb^2 l_{st}}{4\pi(1-\mu)} \ln\left(\frac{r}{r_0}\right), \tag{48}$$

where r and r_0 are the outer and inner radii of the linear defect (dislocation) field of forces, respectively. The radius r is assumed to be equal to the distance between clusters R_{cl}, and the radius r_0 to the Burgers vector length determined in Ref. [152].

The temperature dependence of the specific volume V_{red} is calculated by means of the equation [164]

$$V_{red}^{1/3} - 1 = \frac{\alpha T}{3(1+\alpha T)}, \tag{49}$$

where $V_{red} = V/V^*$ is the reduced specific volume, V^* is the characteristic specific volume, and α is the coefficient of volumetric thermal expansion, whose temperature dependence is determined in the following way [166]

$$\left(\frac{\partial \alpha}{\partial T}\right)_P = (7 + 4\alpha T)\frac{\alpha^2}{3}. \tag{50}$$

Taking the value of α at $T = 293$ K [166] and characteristic volume V^* as the density inverse ρ^{-1}, it is possible to derive the relation $\ln \omega_D = f(\ln V)$ which is shown in Fig. 8a (curves *1*, *2*) for polyarylate (PAr) and polysulfone (PSf). It can be seen that the relationship between the logarithms of ω_D and V is fairly well approximated by a linear correlation. This means, in accordance with Eqn (46), that γ_D remains constant over a temperature range of 293–453 K for PAr, and of 293–433 K for PSf. Absolute γ_D values can be obtained from the slopes of the straight lines in Fig. 8a regardless of the choice of V^*. For PAr one finds $\gamma_D = 12$, and for PSf $\gamma_D = 13.75$, i.e. they are close to the values for polymers of the same class obtained in earlier studies [167].

To summarize, the above results indicate that the following condition [see Eqn (45)] must be fulfilled when the mean number of segments in a cluster is independent of T [166]:

$$\gamma = \gamma_D = \text{const}. \tag{51}$$

It has been shown in a previous study [47] that γ decreases with increasing T [47], which suggests that $dN \neq 0$; hence the necessity to evaluate the second term in Eqn (45). It follows

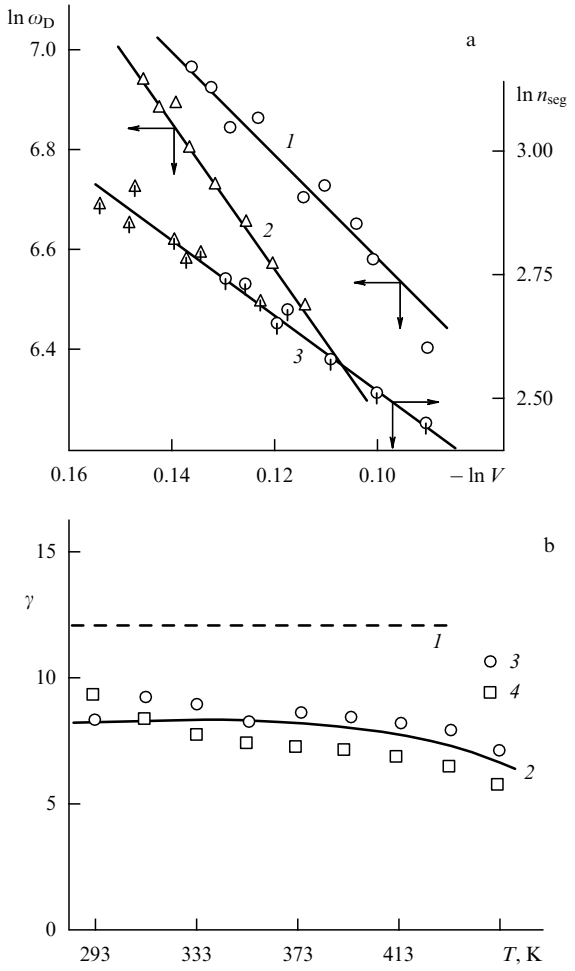

Figure 8. Changes of (a) Debye frequency ω_D (*1*, *2*) and mean number n_{seg} (*3*) of segments in a cluster depending on the specific volume V for PAr (crossed circles) and PSf (triangles) [166], and (b) Grüneisen parameter γ for PAr depending on temperature T: Debye component γ_D (*1*) [calculations using equations (45) (*2*), (53) (*3*), and (54) (*4*)] [166].

from the discussion in Section 2 that $N = n_{seg} = F/2$. Figure 8a (curve *3*) depicts the dependences $\ln n_{seg} = f(\ln V)$ for PAr and PSf. Both are described by a single linear relation, thus providing the possibility to evaluate $\partial(\ln n_{seg})/\partial(\ln V) \cong 6.5$. Parameter ξ in Eqn (45) at temperatures above the Debye temperature for large n_{seg} is approximated by the following expansion in a series [162]:

$$\xi = 0.6942 + \frac{0.03780}{n_{seg}} + \ldots \tag{52}$$

The temperature dependence of γ computed by Eqn (45) for PAr is presented in Fig. 8b (curve *2*).

The value of γ may also be obtained by the following two independent methods. One of them uses a simple relation for the temperature dependence of the modulus of elasticity E [168]:

$$E = E_0(1 - \gamma\alpha T)\,, \tag{53}$$

where E_0 is the value of E extrapolated to $T = 0$ K. The other is based on the Sharma equation [164]

$$\gamma = 1 + \frac{1}{2\alpha T} - \frac{1}{3}\,(5V_{red}^{1/3} - 2)\,. \tag{54}$$

The values of γ calculated from Eqns (53) and (54) for PAr are also shown in Fig. 8b (curves *3*, *4*). Similar dependences have been obtained for PSf as well.

In the past, a decrease of γ with rising temperature used to be ascribed to a concomitant fall in the modulus of elasticity. The latter, in turn, was accounted for by a reduced cluster network density, i.e. by a decrease of n_{seg} [91]. Therefore, the above results are consistent with the explanation of the observed effect, suggested by earlier workers. Equations (45), (53), and (54) give an adequate description of $\gamma(T)$ in terms of both the general tendency and absolute values. This, in its turn, confirms the correctness of the cluster model and the utility of using the Grüneisen parameter for the description of local ordering in glassy polymers [166].

Fluctuation free volume. The fluctuation free volume model was extensively employed for the description of physical properties of liquids and glasses [110, 169, 170]. However, the physical sense of many parameters of the model remains obscure. Moreover, difficulties are encountered in explaining temperature dependences of kinetic properties, such as viscosity at a fixed system volume [171]. In the framework of the cluster model, the fluctuation volume is known to be concentrated in a loose-packed matrix. In terms of the theory of fluctuation free volume, removal of a kinetic unit (an atom or group of atoms) from a cluster results in formation of a fluctuation microcavity ('hole'), whereas the attachment of another kinetic unit fills this void. This suggests that a fluctuation-related change of the free volume with a rise in temperature can be, in principle, realized at a constant system volume by means of 'hole' exchange between clusters and loose-packed matrix. Such an understanding of the mechanism of creation and migration of fluctuation microcavities helps to overcome the difficulty in explaining the temperature dependence of viscosity at a fixed system volume [171].

Specifically, a critical fraction of the fluctuation free volume f_g corresponding to T_g is determined from viscosity measurements in the glass transition region [110, 170]. Knowing f_g, it is possible to calculate the energy ε_h of formation of a minimal microcavity [110]:

$$\varepsilon_h = kT_g \ln\left(\frac{1}{f_g}\right). \tag{55}$$

It can be seen from Fig. 2 that a rise in temperature is paralleled by a symbate decrease of the cluster network density V_{cl} and cluster functionality F for amorphous glassy polymers. Analysis of these data leads to the conclusion that the number of clusters per unit volume of the polymer does not significantly change with a rise of temperature, whereas the number of segments in each cluster decreases. However, clusters are subject to degradation over the glass transition temperature range $T = T_g$, because $V_{cl} = 0$. An excess fluctuation free volume amounts to a critical value ($f_c \geqslant f_g$).

In the light of these observations, devitrification (softening) of a glassy polymer is due to cluster breakdown (annihilation of local order). Therefore, the energy of cluster formation or dissociation U must be on the order of the mean thermal energy of a kinetic unit (statistic segment) at the softening temperature, i.e. $U \cong (i/2)kT_g$, where i is the number of the degrees of freedom of a kinetic unit. Bearing in mind that each segment consists of many atoms, i must be equal in the first approximation to the number of degrees of freedom of a polyatomic molecule, i.e. $i \cong 6$ [171].

As expected, the segment separation energy from a cluster, defined by Eqn (48), turned out to be proportional to the polymer vitrification temperature. Interestingly, the slope of the straight line $U \sim kT_g$ practically coincides with the coefficient of proportionality between the energy of formation of a minimal fluctuation microcavity and the glass transition temperature [see Eqn (55)]: $U \cong 3.3kT_g$ and $\varepsilon_h \cong 3.5kT_g$, respectively, where it is taken into account that f_g for glassy polymers is generally accepted to equal 0.025, and $\ln(1/f_g) \cong 3.5$ [171]. Therefore, the energy of formation of a fluctuation microcavity is practically coincident with the interaction energy between segments in a cluster ($\varepsilon_h \cong U$).

From this standpoint, the formation and collapse of a fluctuation microcavity in amorphous polymers are the results of degradation and creation, respectively, of the sites in the fluctuation network (clusters). The energy of microcavity formation equals the work of separation of parallel segments from each other due to the rupture of intermolecular bonds keeping them together. The linear size of a microcavity is $\cong 4-5$ Å, i.e. of the same order of magnitude as the ultimate elastic strain of intermolecular bonds between the segments. 'The inner radius of the defect (dislocation) field of force' takes approximately the same value $r_0 \cong b \cong 3-5$ Å and can be determined from Eqn (35) [171].

Equation (48) suggests a decrease of U with rising testing temperature owing to the existence of temperature dependences $G(T)$ and $\mu(T)$. It can be shown that, for glassy polymers, the quantity f_g increases (even if insignificantly) as the temperature rises [135], leading to a corresponding decrease of ε_h. It should be noted, however, that the temperature dependences of energies ε_h and U are rather weak [171]. This can probably be accounted for by the fact that the parameters ε_h and U are characteristics of the near-range (local) order in glasses, which is virtually insensitive to temperature variation (at least at $T < T_g$ [55]).

Besides the correspondence between the cluster model and the kinetic theory of fluctuation free volume, the former offers a number of new ideas concerning free volume–structure relationships [172]. For example, Fig. 9 (curve *1*) shows the dependences of the relative amount of fluctuation free volume f_c on the loose-packed matrix fraction φ_{lm} for two linear amorphous polymers PC and PAr. These dependences are linear, and their extrapolation to $\varphi_{lm} = 0$ give $f_c = 0$. Therefore, in this case, the amorphous polymer is actually a giant cluster having no fluctuation free volume. It is understandable that this property does not exclude the presence of the geometric free volume [173]. At $\varphi_{lm} = 1.0$, f_c is extrapolated to a finite quantity roughly equal to 0.14 and corresponding to $f_c = f_g$ at glass transition temperature T_g [174].

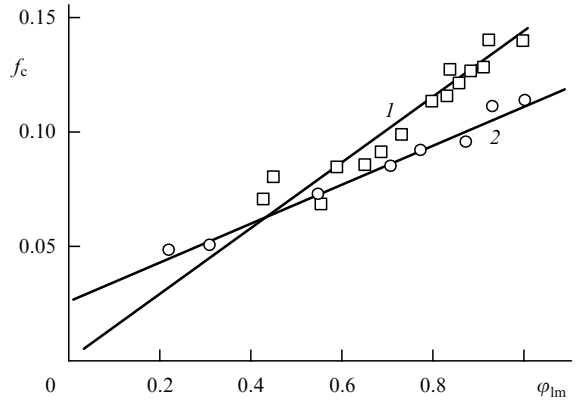

Figure 9. Plots of relative fluctuation free volume f_c vs. volume fraction of the loose-packed matrix φ_{lm} for linear amorphous (PC and PAr) (*1*) and cross-linked (EP) (*2*) polymers]172].

The $f_c(\varphi_{lm})$ dependences for cross-linked polymers differ from those described in preceding paragraphs (Fig. 9, curve *2*). They are well approximated by a straight line, similar to those for linear amorphous polymers. However, this line does not pass through the origin of the coordinate system and, in the case of $\varphi_{lm} = 0$, cuts off an intercept $f_c = 0.024$. It seems plausible that f_c is related to the presence of chemical bond network sites. Therefore, the relative fluctuation free volume in cross-linked polymers, unlike that in linear ones, consists of two components. One is of constant magnitude and is associated with regions of chemical bond sites, while the other is a linear function of φ_{lm} and depends on the supersegmental (cluster) structure. Different f_c components are responsible for the specific properties of polymers. The variable component of f_c controls the elasticity and local plasticity, whereas the total f_c determines the properties in the macroscopic fluidity region [175].

To sum up, correlations obtained with the aid of the cluster model of the amorphous polymer structure indicate that the amount of the fluctuation free volume and its variations under the effect of structure factors are to a large extent dependent on the polymer type [172].

Model of amorphous–crystalline polymer. The two presently available cluster models provide an experimentally verified tool for the interpretation of amorphous–crystalline polymers and allow for the validation of theoretical calculations using the model described in paper [55]. It has been shown in Refs [57, 176] that paramagnetic resonance (PMR) spectra obtained from the devitrified regions in amorphous–crystalline polyethylenes comprise two components. The broad one is due to the contributions of crystallites and the remaining devitrified amorphous fragments (clusters, in terms of the model posed in Ref. [55]). The narrow component results from amorphous portions involved in intense micro-Brownian motion (i.e. devitrified). The ratio of the narrow spectral component area to the total spectrum area (C_m) gives the relative number of devitrified regions at each temperature (the so-called 'mobile fraction' [176]).

Another interpretation was proposed in Refs [177, 178], according to which the formation of a certain number of primary crystallites in amorphous–crystalline polymers is followed by chain folding which gives rise to secondary crystallites in the form of fringed micelles (cluster analogues).

Thus, the fractions of clusters φ_{cl} and loose-packed matrix φ_{lm} evaluated in the framework of the cluster model can be compared with the experimentally found relative amounts of secondary crystallites m_{sc} (by DSC [177]) and the 'mobile fraction' C_m (PMR technique [176]), respectively. The quantitative assessment of φ_{cl} is possible by means of Eqn (10), and that of φ_{lm} from the evident relation [179]

$$\varphi_{lm} = 1 - \varphi_{cl} - K, \tag{56}$$

where K is the degree of crystallinity.

Collation of φ_{cl} calculated by Eqn (10) and m_{sc} taken from paper [177] has demonstrated a good correspondence between their absolute values as well as similar trends of their temperature-dependent changes, despite the use of different HDPE for the evaluation of these parameters. Such

a correspondence was not unexpected, knowing the structural identity of clusters [55] and secondary crystallites [177, 178].

The comparison of φ_{lm} and C_m for HDPE and LDPE also showed a significant correlation between the theoretical and observed values. This gives reason to associate the 'mobile fraction' [57, 176] with the loose-packed matrix of the polyethylene amorphous phase [55, 68].

Thus, paper [179] confirms the correctness of the cluster model by up-to-date experimental techniques of DSC and PMR.

The Poisson coefficient is one of the main characteristics of polymers, determining many of their thermodynamic and mechanical properties [45, 110]. It is natural to predict a close relationship between this parameter and the polymer structure. However, such a correlation remains to be demonstrated. Nevertheless, the application of the cluster model allowed the analytical relationship between the structure and Poisson coefficient to be obtained for polyarylate sulfone as an example, a typical representative of amorphous glassy polymers [180].

One of the laws underlying the classical theory of continuous medium elasticity is the experimentally found Poisson's relation which postulates a lateral strain ($\varepsilon_\perp$) effect [181]:

$$\varepsilon_\perp = \mu\varepsilon_{ii}\,, \tag{57}$$

where μ is the Poisson coefficient, and ε_{ii} is the longitudinal strain.

The coefficient μ can be found using Eqn (40) which was confirmed in experiment [182]. This equation is rather a strict relation derived from the polymer equation of state [110]. However, it does not reflect the relationship between μ and the polymer structure. It is quite clear that an accurate structural identification is needed if the desired relationship is to be obtained. It has been mentioned in the foregoing that the regions of local order (clusters) may be regarded as a departure from an ideal structure, i.e. a defect. In this interpretation with the use of mathematical apparatus of dislocation theory, it is possible to write down [129]

$$\frac{\sigma_y}{\sqrt{3}} = \frac{Eb}{4\pi(1+\mu)}\sqrt{\rho}\,. \tag{58}$$

A combination of Eqns (8), (28), (35), (40), and (58) provides the following expression for μ taking into consideration only the structural characteristics of the polymer [180]:

$$\mu = 0.5 - 2.985\times 10^{-10}(V_{cl}\,l_0)^{1/2}\,, \tag{59}$$

where V_{cl} is measured in m^{-3}, and l_0 in m.

Comparison of the calculated temperature dependence μ [Eqn (59)] and functions $\mu(T)$ derived from Eqn (40) in the event of impact and quasi-static tests for polyarylate sulfone (PArSf) showed that μ increased with increasing T in all the three experimental series [183]. The maximum discrepancy between theoretical μ values and those observed in impact tests did not exceed 20%. It was even smaller (less than 10%) for quasi-static extension. Therefore, the data reported in Ref. [180] indicate that the Poisson coefficient computed from the structural parameters of an amorphous polymer alone is in good correspondence with the values obtained by other methods. It should be noted that Eqn (59) used for the computation of μ includes only structural characteristics in the absence of an adjustable parameter.

The photochromic mark method is extensively employed to study free volume parameters in polymers [184, 185]. It provided qualitatively new information about their free volume and allowed it to be compared with various theoretical models (see, for example, Ref. [186]). Paper [187] collates experimental findings obtained by this method and predictions of the cluster model for epoxy polymers hardened with diamines (EPD) or anhydrides (EPAh), and aged anhydride-hardened epoxy polymer ($EPAh_{ag}$).

The photochromic mark method allows us to measure the free volume size and its distribution for structurally different portions of cross-linked polymers, viz. in the free (dangling) chains, fragments enclosed between neighboring backbone chains and those of hardener (cross-link sites). In all these cases different marks are used [184, 185]. Specifically, in a study [185] with an epoxy oligomer (diglycidilether bisphenol A) hardened with diaminodiphenylsulfone (previously used in paper [187]), the reactive monoamine p, p′-aminoazobenzene (AA) was used to mark the first of the said portions. A derivative of p, p′-diaminoazobenzene (DAA) in which four amine hydrogens were fully substituted with ethyl groups (designated as tt-DAA) and unmodified DAA incorporated into the net-shaped skeleton as a cross-linking agent were used as the marks for the second and third structural portions, respectively. The authors of Ref. [185] had to invoke at least two processes with substantially different (by approximately a factor of 100) rate constants to describe the photoisomerization kinetics of these epoxy skeleton portions above the gelation point. They interpreted the fraction of the 'rapid' process α_s as an integral area under the curve of the free volume distribution for an individual mark. It was assumed that a critical size of the free volume cavity around the mark is necessary for its photoisomerization. For this reason, the method in question evaluates the characteristics of different portions of the epoxy polymer structure, surrounding the mark (i.e. in its immediate neighborhood [185]).

According to Ref. [185], the radius of a free volume cavity in epoxy polymers averages 6.5 Å. Positron spectroscopy yielded somewhat lower figures [188, 189]. The estimates given in Ref. [187] indicate that the distance between cluster centers R_{cl} [see Eqn (18)] in these epoxy polymers varies from approximately 19 to 31 Å. The size of a portion of the loose-packed matrix enclosed between two neighboring clusters is even smaller. Therefore, the size of a free volume microcavity is comparable with the distance from the nearest cluster. This means (using the terminology adopted by Lamarre and Sung [184]) that such a portion of the loose-packed matrix may be regarded as the immediate vicinity of the free volume microcavity contained in it. Hence the possibility to identify the 'rapid' process fraction α_s in an epoxy polymer with the loose-packed matrix fraction φ_{lm}. Another reason for such a correlation is given by the proportionality between φ_{lm} and the relative fluctuation free volume f_c in epoxy polymers (see Fig. 9, curve *2*) [135, 172]. Finally, it is worthwhile mentioning one more finding in support of the identification of α_s as φ_{lm}. Works [184, 185] showed that such factors affecting a polymer as an increased temperature, plasticization, and deformation lead to an enhancement of α_s, while physical ageing causes its decrease. The quantity φ_{lm} behaves in exactly the same manner when a polymer experiences the effect of the same factors [47, 166, 171].

Figure 10 shows the dependences of α_s on the glass transition temperature T_g for the cross-linked skeletons of AA (curve *1*) and tt-DAA (curve *2*), using data from

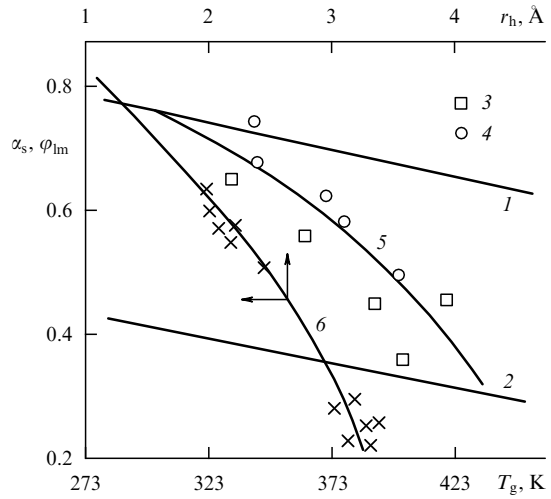

Figure 10. Dependences of the 'rapid' fraction α_s for marks AA (*1*) and tt-DAA (*2*) and loose-packed matrix fraction φ_{lm} (*3–5*) on the glass transition temperature T_g, and of φ_{lm} on the mean radius r_h (*6*) of free volume microcavities for epoxy polymers. Curve *5* depicts the supposed transition of sites with the largest amount of free volume cavities [187].

experimental study [185]. Similarly, the T_g-dependence of φ_{lm} is represented based on the results of Ref. [175]. It can be seen that the records of φ_{lm} fall between curves *1* and *2* and undergo a shift from curve *1* to *2* with an increasing cross-link density (or T_g growth). Evidently, the number of dangling chains must decrease with growing T_g (and ν_{cr}) due to their cross-linking and incorporation into the skeleton. Accordingly, the free volume fraction attributable to them must decrease too. As a result, a key role in a rather closely cross-linked skeleton (where the molecular weight may reach 10^4 g mol^{-1} [190]) will be played by the free volume between the chain segments fixed at both ends by chemical cross-link sites. This hypothetical process is depicted by curve *5* in Fig. 10.

Paper [185] also reports the dependence of α_s on the free volume microcavity radius r_h, which has the meaning of the distribution curve. Figure 10 presents an analogous curve $\varphi_{lm}(r_h)$ (curve *6*), with r_h calculated from the size of the free volume microcavity V_h (on the assumption of its spherical shape) [110]:

$$V_h = 3\,\frac{(1-\mu)kT_g}{f_c E}\,, \tag{60}$$

$$f_c \cong 0.017\,\frac{1+\mu}{1-2\mu}\,. \tag{61}$$

Plot $\varphi_{lm}(r_h)$ in Fig. 10 (curve *6*) has a somewhat different physical sense than plot $\alpha_s(r_h)$ [185]. Because the former correlation includes data for different epoxy polymers, it may reflect characteristic patterns of variation of the free volume hole size r_h upon the alteration of the magnitude of departure from thermodynamically equilibrium structure of these polymers. For example, an enhancement of the degree of local order (decrease of φ_{lm}) leads to the growth of r_h. Figure 10 also presents data for an anhydride-hardened epoxy polymer aged at 293 K for 1.5 hours. As expected, φ_{lm} decreases parallel to the growth of r_h, which suggests a well-known [140] enhancement of the degree of departure from thermodynamic equilibrium in epoxy polymers experiencing physical ageing.

To conclude, the results reported in paper [187] suggest the possibility of identifying the 'rapid' fraction α_s (measured by the photochromic mark method) with the loose-packed matrix fraction φ_{lm} in the framework of the cluster model, in excellent agreement with the physical sense of α_s. Figure 10 indicates that not only the relative fluctuation free volume f_c (regarded as the disorder parameter [135]) but also the mean size of its microcavity (r_h or V_h) can serve as a measure of departure from thermodynamic equilibrium for the cross-linked polymer structure. It should be noted that the authors of Ref. [185] also accepted the proposed interpretation of the parameter α_s, considering it to be associated with the high segmental mobility of lower-density regions in a solid polymer.

Percolation models are extensively used to consider a large number of physical problems [191] including those pertinent to polymers [192, 193]. These models are simple and demonstrable [191], and their application to the description of polymer structure and properties permits one to exploit their well-developed mathematical apparatus. The formation of a cluster structure at T_g results in a sharp change of the properties of an amorphous polymer which becomes as rigid as a genuine solid [55]. It may therefore be suggested that in this case T_g determines the percolation threshold [194] at which an infinite (within the sample length) cluster forms. In work [195], these processes were studied for the EPD and EPAh epoxy polymers discussed in the preceding paragraphs.

It has been shown in review [191] that the critical behavior of the infinite cluster capacity P_∞ (the probability for a site to enter this cluster) near a percolation threshold x_g is described by the scaling relation

$$P_\infty \propto (x - x_g)^\beta\,. \tag{62}$$

In the framework of the cluster model, the obvious choice for P_∞ is the cluster fraction φ_{cl} [196], while the glass transition temperature T_g is taken as x_g (see above). In this case, the testing temperature T is regarded as the current probability x, and equation (62) can be rewritten as

$$\varphi_{cl} \propto (T_g - T)^\beta\,, \tag{63}$$

where the exchange of positions of T and T_g is due to the inequality $T_g > T$. It is worth noting that, because all the tests of epoxy polymers in Ref. [195] were carried out at $T = 293$ K, Eqn (63) actually gives the appropriate dependence of φ_{cl} on T_g. Figure 11 shows the dependences of φ_{cl} on $(T_g - T) = \Delta T$

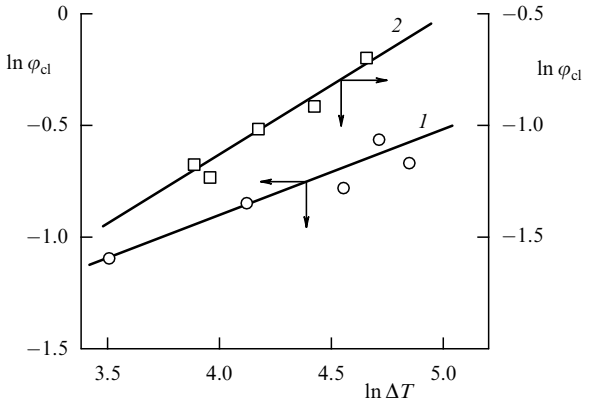

Figure 11. Plots of cluster fraction φ_{cl} vs. temperature difference $\Delta T = T_g - T$ in double logarithmic coordinates for epoxy polymers EPD (*1*) and (EPAh) (*2*) [195].

Table 5. Characteristics of percolation clusters in epoxy polymers [195].

Parameter	Experimental values		Calculated values [191]
	EPD	EPAh	
β	0.36	0.58	0.40
γ	1.28	2.28	1.84

in double logarithmic coordinates for EPD and EPAh. These plots are linear, permitting the calculation of β. It proved to be 0.36 for EPD, and 0.58 for EPAh (Table 5), i.e. rather close to the theoretical 'geometric' value of $\beta = 0.40$ [191]. Therefore, the cluster structure of epoxy polymers being considered is a percolation cluster with the percolation threshold T_g. This means that the vitrification of cross-linked polymers represents a phase (nonequilibrium) transition, and φ_{cl} is an order parameter. This confirms an earlier conclusion [80, 170] and suggests that the epoxy polymer structure may be described proceeding from the general premises of the percolation theory [191]. For example, the number of sites s in a finite cluster depends on the dimensionless deviation of concentration τ_{con} from a critical value $\{\tau_{con} = (x - x_g)/x_g\}$ [191] when $\tau_{con} \to 0$ as

$$s \propto |\tau_{con}|^{-\gamma_{con}} . \tag{64}$$

For the cluster structure, s should be the number of segments $n_{seg} = F/2$ in one cluster, while τ_{con} is the parameter $(T_g - T)/T_g$ [195]. The calculated values of γ are presented in Table 5 which shows that they agree fairly well with the theoretical 'geometric' parameter γ for a three-dimensional percolation cluster [191].

Thus, the results reported in Ref. [195] indicate that a new element — a percolation cluster described by the cluster model — is formed in the epoxy polymer structure at the glass transition temperature T_g. This implies that the vitrification of epoxy polymers proceeds as a nonequilibrium phase transition, and the quantity φ_{cl} is an order parameter in the strict physical sense of this term [195].

Shear and crazing. As is well known [197, 198] shear and crazing are the two key mechanisms of plastic deformation in amorphous glassy polymers. The relationship between these mechanisms governs the polymer plasticity. As a rule, a more intense crazing enhances polymer brittleness, whereas the propensity for shear contributes to its plasticity [199, 200]. The recognition of this fact gave impetus to a large number of studies having the objective to elucidate these mechanisms and competition between them, in which the phenomenon of testing temperature dependence was extensively employed to characterize their relative importance.

Donald and Kramer [201 – 203] posed a micromechanical crazing model for amorphous polymers, in which the probability of one or the other mechanism of plastic deformation is determined by a structural factor, i.e. the density V_e of the network of macromolecular entanglements. The authors demonstrated in the framework of this model that a rise in V_e intensifies the shear mechanism and proportionally suppresses crazing. Kramer [204] derived the following formula for the effective surface energy Γ:

$$\Gamma = \gamma_w + \frac{1}{4} d_e V_e U_w , \tag{65}$$

where γ_w is the van der Waals surface energy, d_e is the distance between cross-link sites, and U_w is the bond dissociation energy in the main chain.

A rise in V_e (other things being equal) facilitates Γ growth and therefore enhances fibrillation stress and suppresses crazing. Henkee and Kramer [205] have also demonstrated that the formation of craze fibrils requires the 'geometrically necessary entanglement loss' which occurs by two mechanisms: either through molecular-chain scission or macromolecular slip followed by their disentanglement.

An advantage of the Donald and Kramer model [201] consists in that it relates the craze structure to such an important structural characteristic of a bulk polymer as the density of the network of macromolecular entanglements. It should be noted that both V_e as a structural characteristic and crazing as the mechanism of plastic deformation are specific features of the polymeric state of matter. This suggests a relationship between these parameters. The predictive value of the model being considered is increased by virtue of correlations between entanglement network characteristics and molecular properties of polymers, found in Refs [66, 73]. At the same time, a variant of the macromolecular entanglement network (the network of 'interlacings') chosen by the authors imposes apparent constraints on the application of the model. It is known from Refs [88, 207] that V_e is evaluated based on the results of mechanical testing of polymers at temperatures above T_g. The value thus obtained is taken as constant over the entire temperature range within which the polymer remains in the glassy state, i.e. at $T \leqslant T_g$.

It is understandable that the possibility of explaining the temperature dependence of the crazing mechanism was restricted from the very beginning by the polymer structure model adopted for the purpose. It was assumed that the 'geometrically necessary entanglement loss' is realized at relatively low molecular-chain scission temperatures (close to room temperature). At higher temperatures, the same effect is achieved via 'untangling' — that is, chain disengagement from the entanglement network. Donald [207] posed another model for the explanation of the high-temperature shear – crazing transition based on the temperature dependences of yield (shear) σ_y and crazing σ_c stresses. The disentanglement of macromolecules in high-molecular-weight polystyrene (PS) encounters difficulty. For this reason, the crazing stress σ_c falls with rising temperature slower than in a low-molecular polymer [see Eqn (65)]. Once the yield stress σ_y is higher than σ_c, crazing is favored over shear deformation; if $\sigma_y < \sigma_c$, shear becomes increasingly important. It is assumed [207] that σ_y is unrelated to the molecular weight of the polymer. Since the degree of stretch λ_c of craze fibrils is a function of molecular weight M_e, it was proposed to explain a rise in λ_c with increasing T by enhanced disentanglement of macromolecules at elevated temperature [208, 209]. In accordance with this concept, the friction coefficient S_0 of macromolecules is high at relatively low temperatures and the applied load breaks the main chain. As T is raised, S_0 decreases and the load enabling macromolecules to slip becomes smaller than the chemical bond strength. This accounts for the predominance of the former process. Macromolecular slip along the surrounding 'tube' leads to 'disentanglement' or reduction in V_e, hence to a decrease of σ_c. This concept was used to explain the experimentally found temperature dependences of λ_c and Γ [209, 210].

For all that, the concept just discussed raises a number of objections. Some of them are listed below:

(1) As is well known [211, 212], crazing stress is a function of temperature and monotonically grows as T drops. In PS, for example, it increases three-fold as T falls

from 300 to 100 K [212]. If the 'geometrically necessary entanglement loss' even at room temperature is due exclusively to the molecular-chain scission, the cause of such a rise in σ_c is unclear.

(2) The ratio of σ_y and σ_c, and the more so their absolute values should not be taken as the sole evidence for the simplicity of realization of one or the other mechanism. It has been shown in Refs [98, 103] that the modification and cross-linking of HDPE result in a 2–3-fold increase of the degree of shear as is easy to see from the 'shear lip' sizes at the damaged sample surfaces. Simultaneously, σ_y remains unaltered or increases by 5–10%, while crazing is completely suppressed [98].

(3) The independence of σ_y from the molecular weight of the polymer, postulated by Donald [207], is questioned by other authors [213].

(4) The slippage of a macromolecule along the 'tube' under the effect of load and its resulting disentanglement can hardly be regarded as a unidirectional process. A hypothetical three-stage model has been posed for its explanation. First, a local equilibrium is established without slip, then stretching of the chain takes place, and finally recovery of the statistical ball configuration under micro-Brownian motion. This three-stage model accounts for the situation in a polymer melt. For a glassy polymer, Donald [207] found it appropriate to consider the first two stages only and regard the third one as missing due to the appearance of the prolate chain. It should be recalled, however, that the active zone at the bulk–craze interface is involved, with enhanced molecular mobility owing to the proximity to the free surface and/or mechanical devitrification of the polymer [89]. Also, it is worthwhile to note that the formation of macromolecular entanglements in the course of polymer craze 'healing' by diffusion is known to occur even in the stressed state [214, 215].

(5) Evaluation of the temperature dependence of σ_c for PS under shock loading [216] revealed its decrease from 25 to 18 MPa with a rise in T from 193 to 252 K. Moreover, a maximum of σ_c corresponding to the β-transition in PS was recorded at $T \cong 313$ K [217]. Berger and Kramer [208] estimated the macromolecular disentanglement time τ_{dis} at $\sim 10^2-10^3$ s. The deformation time for PS samples in an impact test was 5–6 orders of magnitude smaller, which makes the disentanglement process unlikely. Nevertheless, the energy of craze formation in PS in a temperature range of 313–353 K was significantly lower than at $T < 313$ K [216].

(6) Finally, the main reason for an alternative interpretation of the temperature-dependent shear and crazing mechanisms is the inconsistency of the results obtained by Kambour and Gruner [218–220] and that in the framework of the Donald model [207]. The authors of Refs [218–220] empirically found linear correlations between crazing parameters (crazing strain ε_c, major principal stress σ_{yy}, hydrostatic stretching P_s) and essential characteristics of bulk polymers (T_g and cohesive energy density W_c) as well as σ_y and E in the form

$$\varepsilon_c \propto \frac{W_c(T_g - T)}{E}, \tag{66}$$

$$\varepsilon_c \propto \frac{W_c(T_g - T)}{\sigma_y}, \tag{67}$$

$$\sigma_{yy} \propto W_c(T_g - T), \tag{68}$$

$$P_s \propto W_c(T_g - T). \tag{69}$$

The analogy between Eqn (63) and relations (66)–(69) is worth mentioning since it provides an additional argument in favor of an alternative interpretation discussed below.

Today, correlations between E and W_c [221, 222], E and σ_y [223], W_c and T_g [224] are well known. Therefore, relations (66)–(69) to the first approximation reflect the dependence of ε_c (or σ_{yy} and P_s) on the temperature difference $\Delta T = T_g - T$, i.e. the degree of closeness of testing temperature to T_g. In Fig. 12 (curves *1*, *2*), this approximation is confirmed by relevant correlations for $\varepsilon_c = f(\Delta T)$ and $P_s = f(\Delta T)$ constructed from the data of Refs [219, 220], respectively. Despite a larger scatter of points compared with correlations (66) and (69), these plots demonstrate a tendency in ε_c and P_s to increase with rising ΔT. The enhanced scatter of points is due to the departure of the results obtained in the correlations $E = f(W_c)$ and $T_g = f(W_c)$ from the straight line. The physical grounds of such deviations are subjected to a detailed analysis in Refs [221, 222, 224]. Evidently, an increase of ε_c, σ_{yy}, and P_s indicates that crazing becomes progressively more difficult to realize. It is just as clear that all polymers must have equal probability of craze formation at similar ΔT. In terms of the model posed by Donald and Kramer [201–203], this condition must imply similar V_e values. However, it has been shown above that the macromolecular entanglement network is 'frozen' over the entire temperature range corresponding to the glassy polymer state, i.e. V_e remains constant. This discrepancy is resolved by the assumption of chain slippage and withdrawal from the entanglements with rising T [207–210].

Plastic deformation. Let us now consider an alternative interpretation of the temperature dependence of the plastic strain mechanism, based on the premises of the cluster model. It is known [225] that the limiting degree of stretch λ of polymers (the same as the quantity λ_c for craze fibrils, and λ_{dz} for deformation zones (DZ) [226]) is determined by the length

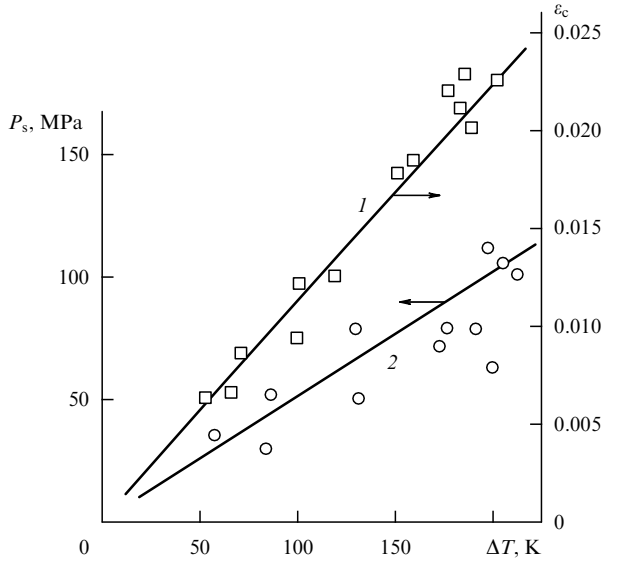

Figure 12. Plots of crazing strain ε_c (*1*) and hydrostatic stretching P_s (*2*) vs. temperature difference $\Delta T = T_g - T$, based on the data from works [219, 220].

of the macromolecular segment l_e between entanglement sites. In qualitative terms, this relationship implies that a rise in M_e leads to the growth of λ. The strain ε magnitude in crazes or deformation zones can be expressed as [227]

$$\varepsilon = \ln\left(\frac{r_p + \delta_c}{r_p - \delta_c}\right), \tag{70}$$

where r_p and δ_c are the craze (or DZ) length and opening displacement, respectively.

The quantity λ is found from the following simple relation [228]

$$\lambda = 1 + \varepsilon. \tag{71}$$

Plummer and Donald [209] measured the degrees of stretch λ_c and λ_{dz} for PS crazes and deformation zones, respectively. Parameter λ_c was found to grow rapidly at $T \cong 383$ K, while λ_{dz} remained unaltered. Theoretical estimation of the maximum degree of stretch in a craze (λ_c) or deformation zone (λ_{dz}) is feasible using a relation proposed by Donald and Kramer [201, 202]:

$$\lambda_c \text{ (or } \lambda_{dz}) = \frac{l_e}{R_{cl}}. \tag{72}$$

In the framework of the cluster model, the quantity l_e is easy to obtain from the known M_{cl} values, based on the relationship between the molecular weight and the chain volume [229] and the macromolecular cross-section area [230]. Quantity R_{cl} may be found by means of Eqn (18). The results of such λ_c and λ_{dz} calculations for PS were compared with the experimental findings of Plummer and Donald [209]. It turned out that the onset of crazing in PS coincided with T_g'. There was an excellent agreement between the observed and theoretical λ_c values, which was rather unexpected bearing in mind that the results had been obtained in different laboratories and with different PS species. In the deformation zone ($T \leqslant 343$ K), the λ_{dz} values exhibited a similarly good correlation on absolute scale and as functions of temperature (the difference between experimental and theoretical data did not exceed 15%). However, the most remarkable result was obtained from the collation of the observed and calculated parameters in the DZ – craze transition region ($T = 333 - 373$ K). It indicated that the reduction in the density of the network of macromolecular entanglements necessary for the realization of such a transition and the associated increase of λ depend exclusively on the thermofluctuation decomposition of clusters with rising T [229].

Molecular orientation. Investigations into the properties of oriented polymers have always been in the focus of attention by virtue of their important practical implications [231]. In this respect, amorphous – crystalline polymers are considered to be superior to amorphous ones because they are much easier to orient, yielding a higher degree of chain stretch, and therefore have better properties. This difference can be accounted for by dissimilarities found in supermolecular structures of the two classes of polymers. Nevertheless, oriented amorphous polymers received as much attention as their semicrystalline counterparts, one of the reasons, apart from practical considerations, being the possibility of producing orientation – property relationships taking advantage of the simpler structure of these compounds containing no crystalline components. Molecular orientation is usually described in terms of two deformation schemes: the so-called 'affine' and 'pseudoaffine'. Papers [232, 233] provide detailed characteristics of these schemes and their potential applications to work with real polymers. It came to be known, however, that neither theoretical scheme is really adequate to describe many aspects of the behavior of real oriented polymers, hence the large number of their modifications [232, 233]. An indispensable element of all these modified and unmodified schemes is the molecular entanglement skeleton [234, 235]. It is therefore appropriate to recall three specific characteristics of the cluster entanglement network important for further discussion, which distinguish it from the conventional network of macromolecular interlacings:

(1) The sites of the cluster network have a well-defined finite size equivalent to the polymer statistic segment length [166].

(2) The cluster network density V_{cl} is a function of temperature. It decreases as T is raised; the cluster network is completely disintegrated at T_g. The growth of V_{cl} with decreasing T is markedly slowed down at $T \leqslant T_g$.

(3) The density V_{cl} exceeds the corresponding parameter of a macromolecular entanglement skeleton by approximately one order of magnitude.

It is worthy of note that the regions of local order, i.e. clusters, influence the orientation behavior of amorphous polymers (see works [236, 237]). A careful check of the results reported in Refs [232 – 238] revealed a number of specific behavioral features of oriented polymers, which are unaccountable in the framework of the macromolecular entanglement skeleton concept and thus preclude the straightforward application of the two aforementioned deformation schemes. These features are listed below:

(1) the qualitative difference between the dependences governing molecular orientations below and above T_g on the degree of stretch λ;

(2) the density V_{cl} for polymethyl methacrylate (PMMA) below $T \cong 50\,^\circ$C is practically constant;

(3) a change of the shrinkage stress at temperatures above T_g implies the existence of a permanent 'residual' skeleton;

(4) it is supposed that the molecular orientation can be described on the assumption of a single mechanism involving changes of entanglement density with temperature and strain;

(5) it is suggested [232] that orientation in polyethylene terephthalate (PETP) is associated with microcrystallites of dimensions comparable to or smaller than the Brillouin light scattering wavelength;

(6) the small n_{st} (the number of statistic segments between entanglement sites) accounting for the high skeleton densities.

It has been mentioned in a preceding paragraph that the behavior of real polymers did not always obey the theoretical schemes for their deformation mechanisms which had to be modified. One such modification is described by the equation [234]

$$\Delta n = C V_0 \alpha_p (\lambda^2 - \lambda^{-1}) \exp(-k_d \lambda), \tag{73}$$

where Δn is the path difference in birefringence measurements, characterizing the degree of molecular orientation; V_0 is the molecular skeleton density; α_p is the difference between statistic segment polarizabilities parallel and perpendicular to its axis, and k_d is the parameter characterizing the degree of degradation of the sites involved in molecular skeleton during

the course of stretching. The constant C is defined as [235]

$$C = \frac{2\pi}{45} \frac{(n_{av}^2 + 2)^2}{n_{av}}, \quad (74)$$

where n_{av} is the average refractive index.

Botto, Duckett and Ward [233] noticed that Eqn (73) fairly well describes experimental findings at $T < T_g$ but is not adequate to describe the situation for $T > T_g$. They proposed the following modification of Eqn (73):

$$\Delta n = \alpha_p C \left\{ V_p + V_t \exp\left[-k_d(\lambda - 1)\right] \right\} (\lambda^2 - \lambda^{-1}), \quad (75)$$

which implies the existence of two molecular entanglement skeletons (permanent and 'temporary') with densities V_p and V_t, respectively.

Despite successful applications of Eqn (75) to the description of experimental data for PMMA (both at $T < T_g$ and $T > T_g$) [233], it is worthwhile to note the following:

(1) the quantities V_p, V_t, and k_d were obtained by adjusting to experimental values; the absence of independent methods for measuring V_p and V_t significantly compromises the value of Eqn (75);

(2) V_t values turned out to be an order of magnitude higher than V_e of the entanglement network.

To our knowledge, the model of a molecular skeleton maintained through the agency of electrostatic interactions [234] has never been used in subsequent studies, although it is difficult to recognize that a macromolecular skeleton of such density does not influence other polymer properties. The treatment of two macromolecular skeletons in terms of the cluster model looks much more natural. In this case, $V_p \cong V_e$ and $V_t \cong V_{cl}$. Then, the macromolecular skeleton density is $V_{cl} + V_e$ at $T < T_g$, and V_e at $T > T_g$. It is easy to see that the proposed interpretation removes all the aforementioned discrepancies between real and theoretical behavior of molecular orientations.

Table 6 collates the macromolecular skeleton densities obtained by fitting to experimental results [233, 235] and by an independent method [152]. It can be seen that there is an almost 2-fold difference between $V_0(V_t)$ obtained in Refs [233, 235], which reflects their adjustable character. At the same time, pairs of V_p from Ref. [233] and V_e as well as V_t and V_{cl} are in good agreement. Thus, our interpretation actually uses the two-skeleton model posed in Ref. [233] but has the advantage of accurate physical identification and independent skeleton density assessment for these structures.

Table 6. Structural PMMA parameters used in calculations by means of Eqns (73) and (75).

T, K	Ref. [235]		Ref. [233]			Ref. [152]		
	V_0	k_d	V_p	V_t	k_d	V_{cl}	$V_{cl} + V_e$	k_p
303 – 323	15.1	1.42	—	—	—	9.23	9.7	2.0
363	8.4	1.22	0.38	4.70	0.89	3.83	4.3	2.0
373	6.4	1.18	—	—	—	1.33	1.8	1.3
390	2.4	0.58	—	—	—	—	0.47	—
408	—	—	0.31	9.31	0.61	—	0.47	—

Note: The values of V_0, V_p, V_t, V_{cl}, and $(V_{cl} + V_e)$ are given in 10^{26} m^{-3}.

Figure 13 (curve *1*) compares calculated [see Eqn (75)] and experimental [233] $|\Delta n|$ values as functions of λ for PMMA. Because the experiments had been carried out at 408 K, i.e. at

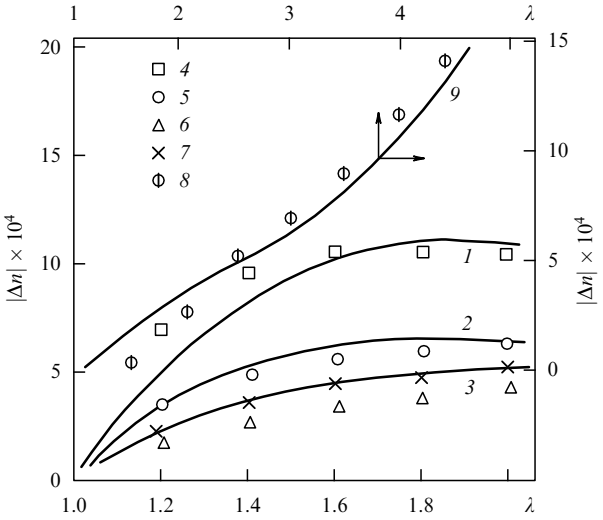

Figure 13. Birefringence $|\Delta n|$ vs. macroscopic degree of stretch λ at $T = 303$ K (*1*, *4*), 363 K (*2*, *5*), 373 K (*3*, *6*, *7*), and 408 K (*8*, *9*) for PMMA: *1–3* — experimental data [235], *4–6* — calculated by Eqn (75) with $k_d = 2.0$, *7* — calculated by Eqn (75) with $k_d = 1.3$ for $T = 373$ K, *8* — experiment, *9* — calculated by Eqn (75).

$T > T_g$ ($T_g = 378$ K for PMMA [235]), the calculations were made at $V_p = V_e$, $V_t = V_{cl} = 0$, and $k_d = 0$. It can be seen that the theoretical and experimental results are in rather good agreement.

Figure 13 (curves *2–9*) also compares experimental [235] and calculated with equation (75) dependences $|\Delta n|(\lambda)$ for test-pieces stretched at 303, 363, and 373 K. PMMA orientation having been effected at $T < T_g$, the calculation was made at $V_p = V_e$, $V_t = V_{cl}$, and $k_d = 2.0$. Here again, there is a good agreement between the theoretical and observed values. A small discrepancy (a somewhat lower calculated $|\Delta n|$ compared with experimental values at elevated stretching temperatures) is easily resolved by lowering k_d as demonstrated for curve $|\Delta n|(\lambda)$ at $T = 373$ K by the choice of $k_d = 1.3$. Therefore, the above results indicate that cluster entanglement network parameters determined by an independent method are in close correlation with experimental data on the molecular orientation in PMMA.

To conclude, it should be noted that the cluster model revealed its consistence with a wealth of experimental materials obtained by different techniques. It is important that this model provides quantitative interpretations using no adjustable parameters.

5. Local order and processes in glassy polymers

In the pages that follow, we shall demonstrate the application of the cluster model to the description of various processes in polymers under different influences and discuss the major parameters controlling them. Again, this description will be quantitative. It should be noted that the cluster model not infrequently offers quite a new fundamental interpretation of one or another process (e.g., yielding). Bearing in mind the large volume of materials to be discussed, this section is divided into subsections to consider each set of results in turn, for the reader's convenience.

Elasticity. The modulus of elasticity E was first described in terms of the cluster model in paper [91]. Figure 14a shows the dependence of E on V_{cl} for polyarylate sulfone (PArSf).

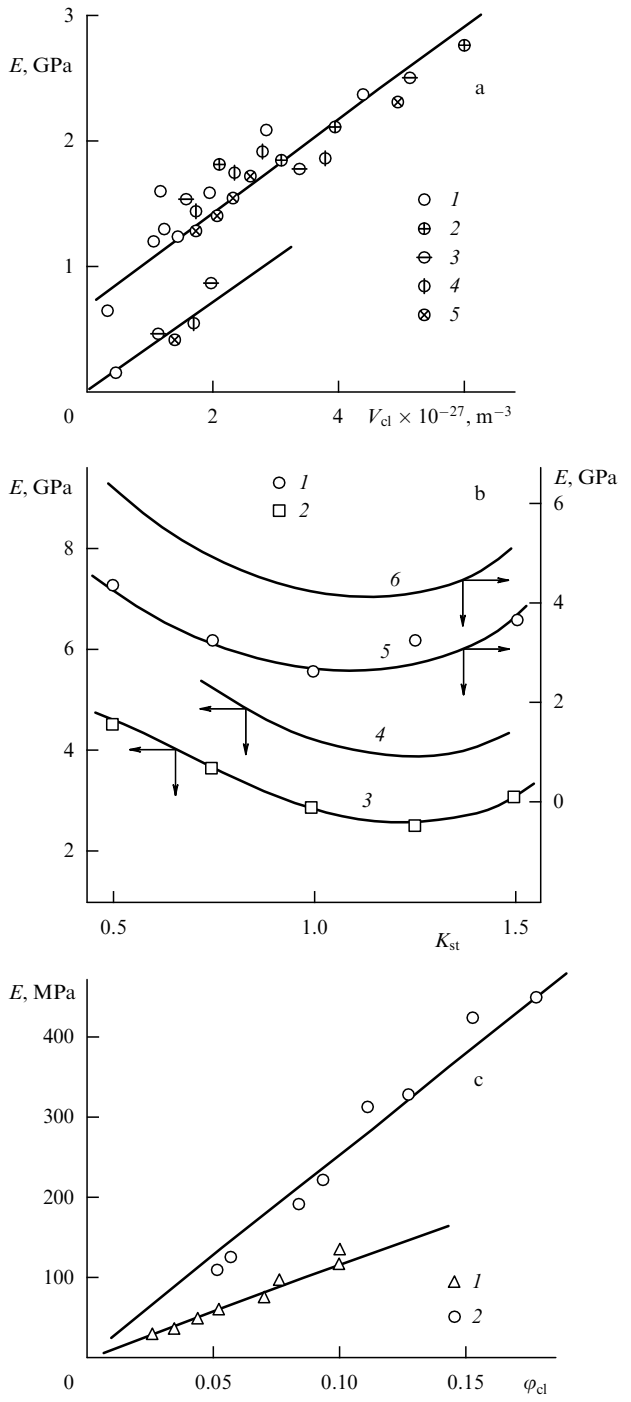

Figure 14. Plots of elastic modulus E vs. (a) density V_{cl} of cluster entanglement network for PArSf films casted from solutions in tetrachloroethane (*1*), tetrahydrophthalate (*2*), chloroform (*3*), dimethyl formamide (*4*), and methylene chloride (*5*) [91]; (b) hardener/oligomer ratio K_{st} for the epoxy polymer hardened with amine at 0.1 MPa (*3*, *4*) and 200 MPa (*5*, *6*). Curves *3*, *5* — calculation by Eqn (78) using f_c', curves *4*, *6* — using f_c [175], *1*, *2* — experimental values, and (c) cluster fraction φ_{cl} for LDPE (*1*) and HDPE (*2*).

Such a correlation is easy to explain in the framework of the cluster model according to which increased V_{cl} means a greater number of close-packed segments and the corresponding intensification of intermolecular interactions between them, leading to a rise in E [222].

A remarkable finding is that the dependence of E on V_{cl} shows two parallel portions of the curves. T_g for PArSf is ~ 475 K [229]; hence, $T_g' \cong 425$ K. Therefore, curve *2* (Fig. 14a) corresponding to the temperature interval $T < T_g'$ indicates that the quantity E in this interval consists of two components: a modulus corresponding to close-packed polymer (clusters) and proportional to V_{cl}, and a relatively constant modulus of loose-packed matrix at $V_{cl} \cong 0$. At 443 K (i.e. for $T > T_g'$), the loose-packed matrix undergoes devitrification, its modulus on the scale of Fig. 14a falls to zero, and the cluster network remains the sole determinant of polymer rigidity. It is worthwhile to note that in terms of the theory of rubber-like elasticity, the modulus of elasticity E is proportional to V_{cl} [58], which is also true of PArSf, to within a constant factor, over the entire temperature range employed in the test [91].

It is known [57] that deformation of amorphous glassy polymers, intermediate between liquids and solids in terms of structure, is fairly well described by both molecular-kinetic (liquid-phase) and solid-state models. The quantitative relationship between them may be established with the aid of the kinetic theory of fluctuation free volume [110] or the cluster model (identified as type 1 and 2 models, respectively). The interrelation of these concepts has been demonstrated in the previous section, while Sanditov and Kozlov [152] used them to describe the temperature dependence of shear modulus G for two amorphous glassy polymers, PC and PAr. This dependence is easy to obtain by combining Eqns (8), (40), (48), (51), and (61) in the form

$$G = \frac{4\pi(1-\mu)T_g\, k \ln(1/f_c)}{b^2 l_0 C_\infty \ln(r/r_0)} \,. \tag{76}$$

Parameters T_g, k, b, l_0, and C_∞ for one polymer are constants, therefore the experimentally established changes of G at different temperatures are fully attributable to the temperature dependences of μ and f_c. Equation (76) is characteristic in that it demonstrates the necessity of variation of μ and f_c [related to each other by expression (61)] with temperature. Also, it shows that the interpretation of the constancy of these parameters below T_g as an indication of a 'frozen' structure is too rough an approximation [32].

The results of estimating the temperature dependence of shear modulus G by means of Eqn (76) for PC and PAr show that even a small change in absolute values of μ and f_c may have a marked effect on the mechanical properties of polymers [152].

The specific relationship between cross-link polymer structure and modulus of its elasticity was examined in Ref. [175], taking into consideration the aforementioned division of the fluctuation free volume of epoxy polymers into two components: f_c^g attributable to the presence of chemical cross-link sites, and f_c' arising from cluster decomposition, i.e. the fluctuation component proper ($f_c = f_c^g + f_c'$) [135, 172]. In monograph [110], the following relation between microrigidity H_μ and E was suggested:

$$\frac{H_\mu}{E} = \frac{1-2\mu}{6(1+\mu)} \,. \tag{77}$$

Despite the seeming identity of formulas (40) and (77), they yield dissimilar H_μ and σ_y values, because the quantities μ entering them differ for various deformation zones in the polymer. It follows from Eqns (61) and (77) that

$$E \cong 35.3 f_c H_\mu \,. \tag{78}$$

In work [175], this relation was used for calculating the dependences of E on the hardener/oligomer ratio K_{st}. Comparison of calculated and observed dependences $E(K_{st})$ for an epoxy polymer hardened with amines at different pressures revealed their symbate character (Fig. 14b). The use of f_c' in the calculations of E from formula (78) gave a better quantitative correspondence than f_c. Similar results were obtained for epoxy polymers hardened with anhydrides.

The data presented in Fig. 14b explain the better correlation between E and V_{cl} than between E and v_{cr} for the case of epoxy polymers [175]. It appears that the mechanical properties of epoxy polymers in the elastic deformation zone are governed only by that fraction of the total free volume which is related to the assembly of segments into clusters or their dissociation from them. It should be emphasized that polymer properties are under the control of different structural regions at various stages of deformation. For example, the influence of the loose-packed matrix (f_c') is largely apparent in the elasticity (E) and local plasticity (H_μ) intervals. In the case of macroscopic fluidity (σ_y), its action is supplemented by that of chemical cross-link sites, i.e. matrix ($f_c = f_c' + f_c^g$). This accounts for the different σ_y and H_μ values derived from Eqns (40) and (77) despite the apparent similarity of these formulas [175].

There are several concepts explaining the relationship between polymer structure and the modulus of elasticity for amorphous–crystalline polymers, e.g., low-density (LDPE) and high-density polyethylenes (HDPE). One of them considers either polymer to be a two-phase composite made up of alternating crystalline and amorphous regions [239]. Due to this circumstance, E is largely determined by the high elastic modulus characteristic of the crystalline phase. Because this phase is more rigid than the other, a major part of the strain affecting a bulk sample must be realized in the amorphous interlayers. Moreover, in the general case, polymeric molecules have to pass through both crystalline and amorphous regions. Therefore, crystallites function similarly to cross-links, i.e. preclude slippage of macromolecules relative to one another. Thus, the structural organization of amorphous–crystalline polymers and elastomeric skeletons displays certain common features. The validity of this concept is seriously doubted on the grounds of the significantly smaller calculated moduli of elasticity compared with that observed. Krigbaum and co-workers [240] have modified this approach. They believe that the formation of crystallites must result in considerable tension of the remaining amorphous chains. This means that an increase in the modulus of elasticity throughout crystallization is due to the fact that the skeleton chains are almost fully stretched even in the absence of external load. Mandelkern et al. [241, 242] have studied various polyethylenes and showed that crystallinity alone cannot adequately account for the elastic modulus values inherent in amorphous–crystalline polymers. In terms of concepts framed in works [240–242], they are largely dependent on the molecular structure of amorphous regions. Thus, crystallinity affects amorphous interlayers which in turn induce changes of E.

Pakhomov and co-workers [243] postulated that the elastic modulus E of amorphous–crystalline polymers is fully determined by their conformational state, namely, the concentration of *trans*-conformations. The latter were compared in Ref. [244] with the data for LDPE and HDPE in the context of the cluster model.

Variations of the LDPE and HDPE elastic moduli as functions of the parameter $1/(1-k)$, where k is the degree of crystallinity, are in good agreement with the calculated values obtained by Krigbaum et al. [240]. Some discrepancy may be due to a failure to take into account changes of crystallite size with temperature [239]. Anyway, the observed correspondence confirms the validity of the model [240].

Comparison of experimental E values with those computed in the framework of the theory of rubber elasticity [see Eqn (2)] has demonstrated that the former are approximately 30–150 times higher than the latter [244]. In terms of the model posed in work [240], this means that stated N_r-fold rise is due to the tension of macromolecular chains in amorphous regions, accompanying the crystallization of polyethylenes.

It is worthy of note that temperature dependences of N_r and bulk crystallinity k [192] variations are very similar. As expected from the above reasoning, these parameters are in good correspondence. Rathje and Ruland [109] have recently reported the analysis of small-angle X-ray diffraction patterns suggesting significant temperature-dependent changes in the thickness of polyethylene amorphous and crystalline regions. Specifically, the thickness of amorphous interlayers increases from 30 Å at room temperature to 150–200 Å near the melting point. This means in turn that the amorphous chain tension decreases with rising temperature.

As is mentioned above, the relative number of clusters φ_{cl} characterizes the degree of local order in the amorphous state of polymers [68]. The relation $E = f(\varphi_{cl})$ for LDPE and HDPE is presented in Fig. 14c. It shows that the dependences are linear and extrapolated to $E = 0$ at $\varphi_{cl} = 0$, notwithstanding the presence of the crystalline phase. Levene et al. [245] reported maximum E values for nonoriented polyethylenes as functions of their densities at 1.45 MHz — that is, for a case in which the viscoelastic contribution to E may be neglected. These E values are in perfect agreement with experimental ones at $\varphi_{cl} = 1.0$ (see Fig. 14c, where $E = 1.3$ and 1.1 GPa for LDPE, and 2.8 and 2.6 GPa for HDPE). The above results indicate that in nonoriented polyethylenes E is controlled by noncrystalline regions, which in turn depend on the crystalline morphology [240–242].

Paper [244] reports calculated levels C_t of LDPE and HDPE transconformations obtained by using the method outlined earlier [243]. As expected, C_t decreases with increasing temperature [244]. This observation gives reason to argue that the elasticity modulus of polyethylenes is related to the stiffness of noncrystalline regions. This property depends on the crystalline morphology which alters the topological and conformational characteristics of amorphous chains, compared with the macromolecular characteristics of hypothetical fully amorphous polyethylene.

Flow. The flow behavior in amorphous glassy polymers is frequently regarded as their mechanical devitrification [89]. However, analysis of a typical stress–strain ($\sigma-\varepsilon$) curve for such polymers shows that the forced rubber-like elasticity plateau stress σ_{re} beyond the yield stress σ_y is practically equivalent to σ_y. In other words, it is of the order of a few tens of MPa, whereas in a devitrified polymer this parameter is at least a factor of 10 lower. Moreover, σ_{re} is a function of the testing temperature T, in contrast with a devitrified polymer for which this dependence must be much weaker and, above all, display the opposite tendency (a rise in σ_{re} with increasing T). This discrepancy is easily removed within the framework of the cluster model which implies that the flow occurs when only the loose-packed matrix undergoes devitrification [129].

It is worth noting that the model posed by Kozlov et al. [129, 246] assumes that the number of close-packed segments in a cluster per unit volume of the polymer is equivalent to the density V_{cl} of cluster entanglement network, determined from the parameters of the plateau of forced rubber-like elasticity, over which V_{cl} remains unaltered. In this interpretation, the forced rubber-like elasticity (cold flow) of the polymer is related to the deformation of the devitrified loose-packed matrix with 'floating' clusters. However, thermal devitrification of the loose-packed matrix occurs at T_g', i.e. approximately 50 K below T_g [60]. It should therefore be expected that the application of a very small stress (on the order of 1 MPa) must cause a flow (deformation) of an amorphous polymer over the entire temperature range $T_g' - T_g$. However, such a flow is not observed. This means that devitrification of the loose-packed matrix is a result rather than a realization criterion of flow. Moreover, it is known [147] that the flow occurs in close-packed regions (clusters) of an amorphous polymer [128]. Thus, it may be speculated that a sufficient condition for polymer flow is provided by the loss of stability in locally ordered regions, after which the deformation proceeds without a further (at least nominal) rise in stress σ. This situation differs from the strain process continuing until a yield stress is reached and accompanied by a monotonic growth of σ.

The model developed in Ref. [247] shows that clusters lose stability when the stress generated in a polymer reaches a macroscopic yield stress σ_y. Because clusters are assumed to be an array of close-packed collinear segments and should be expected to have randomly oriented axes relative to the applied stress σ, they can be simulated by 'inclined plates' (IP) [247]. The following expression holds for IP:

$$\tau_y < \tau_{ip} = 24 G_{cl} \varepsilon_0 \frac{1+\mu_2}{2-\mu_2}\,, \tag{79}$$

where τ_y is the shear stress at the yield point, τ_{ip} is the shear stress in IP (cluster), G_{cl} is the shear modulus accounted for by the presence of clusters and determined from plots similar to those in Fig. 14a [i.e. $G = f(V_{cl})$], ε_0 is the intrinsic IP deformation, and μ_2 is the Poisson coefficient for clusters.

Quantities σ_y and τ_y are related by a simple expression [36]

$$\tau_y = \frac{\sigma_y}{\sqrt{3}}\,. \tag{80}$$

Because Eqn (79) characterizes the plastic strain of the clusters, it is possible to assume $\mu_2 = 0.5$. Furthermore (assuming $\tau_y = \tau_{ip}$), an expression is derived for the minimal intrinsic deformation ε_0^{min} [taking into account the inequality in the left-hand side of Eqn (79)]:

$$\varepsilon_0^{min} = \frac{\tau_y}{\sqrt{24}\, G_{cl}}\,. \tag{81}$$

The stability condition for clusters (IP) has the form [247]

$$q = \sqrt{\frac{3}{2}}\,\frac{\varepsilon_0}{\tau_y}\left[\left|1+\frac{\varepsilon_0'}{\varepsilon}\right| - \sqrt{\frac{3}{8}}\,\frac{\tau_y}{G_{cl}\varepsilon_0(1+\mu_2)}\right], \tag{82}$$

where q is the parameter characterizing the plastic strain, and ε_0' is the proper deformation of the loose-packed matrix.

Cluster stability is disturbed if the following inequality is fulfilled:

$$q \leqslant 0\,. \tag{83}$$

Comparison of relations (82) and (83) gives the following instability criterion for IP (clusters):

$$\left|1+\frac{\varepsilon_0'}{\varepsilon_0}\right| = \sqrt{\frac{3}{8}}\,\frac{\tau_y^{th}}{G_{cl}\varepsilon_0(1+\mu_2)}\,, \tag{84}$$

whence the theoretical stress $\sigma_y(\sigma_y^{th})$ is determined, at which criterion (83) is satisfied.

Quantitative assessments require that two simplifying assumptions be made [246]. First, the condition [247]

$$0 \leqslant \sin^2\theta_n\,\frac{\varepsilon_0'}{\varepsilon_0} \leqslant 1 \tag{85}$$

must be fulfilled for IP, where θ_n is the angle between the perpendicular to IP and the principal axis of intrinsic strain.

Because $\sin^2\theta_n = 0.5$ for arbitrarily oriented IP (clusters), condition (85) is met if $\varepsilon_0'/\varepsilon_0 = 1$. Second, Eqn (81) gives a minimal ε_0 value; for the convenience of calculations, τ_y and G_{cl} were substituted by σ_y and E, respectively. The elasticity modulus E is bigger than the appropriate modulus of elasticity E_{cl} accounted for by the presence of clusters, as follows from Fig. 14a. Therefore, the strain ε_0 determined by Eqn (81) must be doubled to compensate for these two effects. In the end, this leads to [246]

$$\varepsilon_0 \cong 0.638\,\frac{\sigma_y}{E} = 0.638\varepsilon_{el}\,, \tag{86}$$

where ε_{el} is the elastic component of macroscopic yield strain [248] with the physical sense of strains ε_0 and ε_0' [247].

A combination of Eqns (80), (84), (86) and plots similar to those in Fig. 14a [whence $E_{cl}(G_{cl})$ can be derived) allows for the theoretical estimation of the yield stress $\sigma_y^{th}(\sigma_y^{th} = \sqrt{3}\,\tau_y^{th})$ and its comparison with experimentally found σ_y values. Such a comparison has demonstrated fairly good agreement between σ_y^{th} and σ_y, and thus confirmed the validity of assumptions made in Ref. [246] and the above reasoning in general.

By this means flow of amorphous glassy polymers requires stable clusters and is followed by devitrification of the loose-packed matrix [246]. A similar criterion was obtained for amorphous–crystalline polymers [249].

It has been shown in Refs [143, 250] that the flowing behavior of cross-linked polymers is essentially the same as that of linear PC and PAr. However, further progress in the study of this phenomenon in cross-linked polymers encounters at least two obstacles: the overestimation of the role of chemical cross-links, and the absence of a quantitative structural model. Kozlov et al. [250] proposed a mechanism of flow and forced rubber-like elasticity in cross-linked polymers, based on the premises of the cluster model and the latest developments in synergetics of deformable materials [127] for the example of two epoxy polymers, EPD and EPAh, discussed above.

It follows from $\sigma-\varepsilon$ curves for EPAh that uniaxial compression applied to a test piece until it is destroyed or subjected to strain ε in excess of the yield strain ε_y results in a sequential 'yield tooth' suppression with a constant stress σ_{re} of forced rubber-like elasticity plateau [250]. Large σ_{re} suggests a correspondingly high density V_{cl}^{st} of the stable cluster entanglement network, much higher than the chemically cross-linked network density ν_{cr} [175]. For this reason, a network of stable clusters is retained for the given portion of the $\sigma-\varepsilon$ curve, although the behavior of the cross-linked

polymer at the forced rubber-like elasticity plateau is described in the framework of the theories of rubber elasticity. Only unstable clusters undergo decomposition which ensures devitrification of the loose-packed matrix. The process of unstable cluster decomposition starts at a stress equivalent to the proportionality limit, in agreement with the results of Ref. [182] where this stress and temperature $T_2 \approx T_g'$ are assumed to have analogous effects. The analogy between flow and glass transition is only partial since a single structural component (the loose-packed matrix) undergoes devitrification. Moreover, the complete decomposition of unstable clusters occurs at the origin of the plateau of forced rubber-like elasticity σ_{re} and not at the point of yield strain σ_y. This means that the flow is unrelated to the devitrification of the loose-packed matrix, being regulated by a different mechanism. It has been shown above that this mechanism may consist of the loss of cluster stability as is equally well known from the vanishing of the derivative $d\sigma/d\varepsilon$ at the yield point [150].

According to monograph [127], the critical strain γ_* terminating in the loss of shear stability by a solid is given by

$$\gamma_* = \frac{1}{mn}, \tag{87}$$

where m and n are indices in the Mie equation [110] relating the interaction energy and the distance between particles. The quantity $1/mn$ can be expressed through the Poisson coefficient μ [110]:

$$\frac{1}{mn} = \frac{1-2\mu}{6(1+\mu)}. \tag{88}$$

It follows from Eqns (40) and (88) that

$$\frac{1}{mn} = \gamma_* = \frac{\sigma_y}{E}. \tag{89}$$

Equation (89) gives the strain magnitude regardless of viscoelastic effects (departure of the $\sigma-\varepsilon$ curve from linearity outside proportionality limit).

The σ_y/E ratio may also be expressed through the Grüneisen parameter γ [110]:

$$\frac{\sigma_y}{E} = \frac{1}{6\gamma}. \tag{90}$$

Taking into consideration that $\varepsilon_y \approx 0.5/\gamma$ [150] and the shear strain is ~ 0.66 of the tensile deformation [40] gives the theoretical yield strain [250]:

$$\varepsilon_y^{th} = 2\gamma_*. \tag{91}$$

Comparison of the experimental yield strain ε_y and ε_y^{th} derived from Eqn (89) revealed their rough equality suggesting the association of flowing quality with the loss of stability by polymers (strictly, by clusters because μ depends on the density V_{cl} of a cluster network of macromolecular entanglements [see Eqn (59)] and σ_y is proportional to V_{cl} [91]).

Paper [251] demonstrated accelerated stress relaxation in epoxy polymers loaded as described above. The authors explained this effect by a partial breaking of chemical bonds. To verify this conclusion, the experiment was reproduced by subjecting samples first to compression until the plateau of forced rubber-like elasticity was reached and then to annealing at $T < T_g$ [250]. These procedures resulted in the reappearance of the yield tooth in the $\sigma-\varepsilon$ curve, probably due to the recovery of unstable clusters (the restoration of disrupted chemical bonds at $T < T_g$ being unlikely). In connection with this, it should be noted that suppression of the yield tooth as a result of preliminary plastic deformation was also observed in linear amorphous polymers, e.g., polycarbonate [82], known to be having no network of chemical bonds.

According to Filyanov [182], the yield tooth $\Delta\sigma$ in epoxy polymers decreases with increasing T_g. It is also true of the systems studied in Ref. [250]. However, the dependence $\Delta\sigma(T_g)$ is not universal. For EPD, $\Delta\sigma$ are significantly smaller than for EPAh at the same T_g. In the case of $K_{st} > 1.0$ and comparable T_g, $\Delta\sigma$ is higher than that at $K_{st} \leqslant 1.0$. In other words, an excess of the hardener promotes formation of a larger number of unstable clusters.

Analysis of the relationship between the experimentally found width of the temperature range ΔT_g over which the glass transition occurs and the unstable cluster network density V_{cl}^{us} derived from the equation [250]

$$\Delta\sigma = \frac{1.73Eb\sqrt{l_0 C_\infty V_{cl}^{us}}}{4\pi(1+\mu)} \tag{92}$$

has shown that the correlation between $\Delta\sigma$ and ΔT_g is due to the presence of unstable clusters [182].

The personification of processes proceeding during the cold flow of amorphous polymers is also possible in the framework of the cluster model [250]. They may be interpreted as the movements of stable clusters interconnected by penetrating chains in the devitrified loose-packed matrix, the high viscosity of which is one of the causes of the transition to the turbulent regime [250, 252]. Such a qualitative deformation model for amorphous glassy polymers was constructed by Bekichev [22, 254].

The behavior of a deformable solid experiencing mechanical action is underlain with the processes of formation and evolution of dissipative structures (DS) which ensure optimal dissipation of the energy incoming from the outside [127, 255]. In the case of metals, this approach is universally accepted even though there is no concerted opinion on the mechanism of structural rearrangement in the deformable material [256]. For polymers, this problem is virtually unexplored although they have been shown to contain DS [41–43]. Meanwhile, its solution may be instrumental in addressing polymer deformation based on fundamental physical principles of nonequilibrium thermodynamics [257]. The application of these principles is possible if a quantitative structural model is available. In what follows, the cluster model will be used for the purpose, in which DS are characterized as the regions of local order.

It has been shown by Balankin et al. [128] that the flow process in linear amorphous polymers is initiated after an effective Poisson coefficient $\mu_y \approx 0.41$ is reached. Assuming this inference to be correct for cross-linked polymers too and using the formula relating μ to V_{cl} [see Eqn (59)], the authors of Ref. [44] computed V_{cl}^{y} as the yield stress σ_y is reached. The results are presented in Fig. 15a along with V_{cl} values for undistorted epoxy polymers EPD and EPAh as a function of K_{st}. It can be seen that the V_{cl}^{y} values are independent of K_{st} and practically identical in EPD and EPAh owing to the initial choice of μ_y. At the same time, they are significantly lower than V_{cl}. This means that for the flow process to be realized in cross-linked polymers, a certain number of clusters (DS) must disintegrate. Such a situation is diametrically

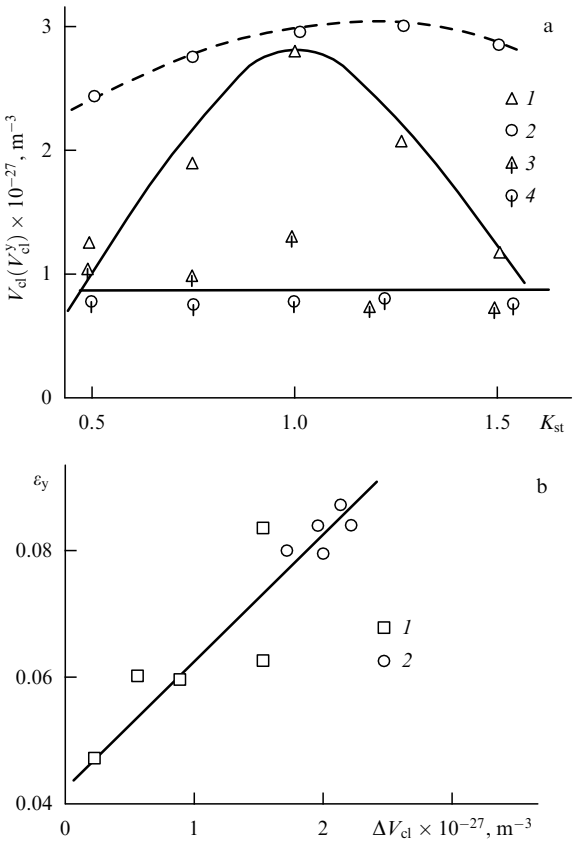

Figure 15. Plots of (a) cluster network density V_{cl} in the unstrained state (*1*, *2*) and after yielding V_{cl}^{y} (*3*, *4*) vs. hardener/oligomer ratio K_{st}, and (b) yield strain ε_y vs. difference between cluster network density ΔV_{cl} before and after yield initiation for epoxy polymers hardened with diamine (*1*) and anhydride (*2*) [44].

opposite to deformation processes in metals during which DS (dislocation substructures) are formed [127, 257]. This difference is fundamental, being due to distinct notions of ideal (defect-free) structures of the materials compared.

It should be expected that these structural changes must influence parameters which characterize the flowing quality in cross-linked polymers. We shall consider this situation taking the yield strain ε_y as an example. It is natural to suggest that the more DS undergoes decomposition throughout the flow process, the higher ε_y must be. The amount of DS involved in the process can be evaluated as the difference between the cluster network density before (V_{cl}) and after (V_{cl}^{y}) initiation of yielding: $\Delta V_{cl} = V_{cl} - V_{cl}^{y}$ which is easy to determine from plots in Fig. 15a. The correlation $\varepsilon_y(\Delta V_{cl})$ that confirms this suggestion is presented in Fig. 15b.

Relations (37) – (39) taken together with Eqn (18) may be used to assess the cluster functionality F for epoxy polymers before and after yielding is induced. The most characteristic difference between the dependences $F(K_{st})$ being compared consists in a significant increase of F as the yield stress is achieved. A parallel decrease of V_{cl} and increase of F upon polymer deformation prior to the yield stress indicate the decomposition of unstable clusters having low F. As a result only stable clusters with high F are preserved at σ_y. Decomposition of unstable clusters leads to mechanical devitrification of the loose-packed matrix, accounting for the rubber-like behavior of the polymer on the plateau of forced high elasticity (cold flow).

Let us now estimate the energy cost of cluster decomposition under the action of external load. The energy U necessary for the association (dissociation) of a pair of segments in a cluster can be calculated from Eqn (48). Then, the total energy U_y spent to impose yield strain ε_y is given by [44]

$$U_y = U\Delta V_{cl} . \tag{93}$$

On the other hand, U_y may be derived from the $\sigma - \varepsilon$ curve, assuming it to remain roughly triangular until the yield point is reached:

$$U_y = \frac{\varepsilon_y \sigma_y}{2} . \tag{94}$$

By equating formulas (93) and (94), it is possible to find a theoretical yield stress σ_y^{th} and compare it with the experimental σ_y. The good agreement between σ_y^{th} and σ_y obtained in Ref. [44] means that the yield strength actually depends on the decomposition energy of unstable clusters. It is concluded that the flowing quality of cross-linked polymers is described in the framework of synergetics of a strained material, namely, by dissipative structure evolution.

Let us consider specific features of flow process in amorphous – crystalline polymers [213, 258, 259]. Practically all the properties of a polymer of this class have been shown to depend on the degree of crystallinity [112]. It is therefore recognized that the crystalline phase makes the main contribution to the polymer properties. For certain obvious reasons, plastic deformation of amorphous – crystalline polymers is of special interest [241, 242]. Unlike amorphous glassy polymers discussed above on which there is no concerted opinion as regards flowing quality, its mechanism in amorphous – crystalline polymers raises no controversy amongst researchers, starting from the early treatment of flow as partial melting and recrystallization of crystalline regions [260]. The authors of the latest studies appear to share this view of amorphous – crystalline polymer flowing quality without any serious modification [64, 241].

Investigations based on this general concept brought about correlations of flow and stretch characteristics with crystalline phase properties of amorphous – crystalline polymers. Examples of such correlations are provided by the relationship between yield stress σ_y and the degree of crystallinity [241], between σ_y and the melting heat [64], etc. It is generally believed that noncrystalline regions have no effect on flowing quality or stretching. However, a number of studies published in the last decade suggest that the influence of noncrystalline regions on the aggregate of properties of amorphous – crystalline polymers has long been underestimated [114, 258].

The flow concept for amorphous – crystalline polymers is consistent with the treatment of their behavior as related to the presence of dislocations. The advocates of such an interpretation are usually focused on crystalline phase defects analogous to dislocations in crystal lattices. Analysis of effects of the amorphous phase of amorphous – crystalline polymers on their mechanical properties in the framework of dislocation analogies requires a revision of the defect concept as applied to the original amorphous phase (see above). Without violating the generality of the definition, dislocation may be regarded as a linear entity that affects the initial arrangement of the elements comprising an ideal structure.

Associated with this entity is the strain energy of the surrounding medium [see Eqn (48)]. In terms of the interpretation being considered, both clusters formed in the initially 'fully amorphous' polymer matrix (melt or solution) and crystallites are the defects of the amorphous structure. For obvious reasons, their formation leads to elastic disturbances in the matrix with which they are connected by penetrating (entering neither clusters nor crystallites) chains. Therefore, macromolecular segments in crystallites and clusters may be treated as linear defects formally analogous to dislocations in a fully crystalline material [159].

The temperature dependences of σ_y for HDPE and PP calculated by means of Eqns (8), (35), (58) and obtained in experiment are presented in Fig. 16a. As expected, the σ_y values computed from the cluster network density in noncrystalline regions (σ_y^{nc}) are significantly lower than the experimental σ_y. This can be accounted for by the fact that flow in amorphous–crystalline polymers involves both noncrystalline and crystalline regions [258, 261].

The contribution of crystalline regions to σ_y in amorphous–crystalline polymers can be evaluated in the following way. The linear defect density ρ_d^c corresponding to crystalline regions is defined as the length of macromolecules entering them [cf. Eqn (7)] [259]:

$$\rho_d^c = \frac{K}{S}, \tag{95}$$

where K is the degree of crystallinity, and S is the macromolecular cross-section area.

By substituting ρ_d^c into Eqn (58), it is possible to calculate the contribution of crystalline regions (σ_y^c) to the total σ_y. Figure 16a also compares experimental σ_y values and the calculated sum ($\sigma_y^{nc} + \sigma_y^c$) and demonstrates a good correlation between these parameters.

It is concluded that the model suggested by Belousov et al. [259] based on the revised structural defect concept [129] allows for the quantitative assessment of the contributions of crystalline and noncrystalline regions to flowing quality in amorphous–crystalline polymers.

Let us consider the dependence of the yield strain ε_y on the structural characteristics of polymers. This dependence has actually been neglected until recently by researchers even though an early study [89] demonstrated its importance in the deformation of amorphous glassy polymers. There are several definitions of this parameter. For example, ε_y has been defined as the ratio of yield stress σ_y to the modulus of elasticity E or as a degree of deformation at which a yield point is reached [47]. In what follows, the latter definition will be used. Also, we shall demonstrate the functional relation of yield strain ε_y to structural and molecular characteristics of amorphous glassy polymers for the example of PC and PAr.

Earlier authors believed that ε_y is either the same for different polymers [89] or depends on a change of free volume f_c in the course of polymer dilation under deformation [262]. It was also shown that ε_y relates to the degree of anharmonicity of intermolecular bonds, i.e. the Grüneisen parameter γ, by the following simple expression [47]

$$\varepsilon_y = \frac{1}{2\gamma}. \tag{96}$$

Nevertheless, both f_c and γ are indirect characteristics of the structure of an unstrained polymer and its changes under deformation. Therefore, it would be important to obtain, e.g. in the framework of the cluster model, expressions relating the mechanical properties of polymers to parameters which have a direct bearing on their structural features.

The quantity ε_y was related to the polymer structural characteristics by Eqn (90) taking into consideration Eqn (96). This gave

$$\varepsilon_y = \frac{3\sigma_y}{E}, \tag{97}$$

which clearly shows the relationship between yield strains in terms of the above definitions.

The authors of Ref. [263] substituted f_c-dependent parameter A for coefficient 2 in Eqn (96). As a result of this refinement, Eqn (97) acquired the form

$$\varepsilon_y = \frac{6\sigma_y}{AE}, \tag{98}$$

where

$$A = \frac{9}{\ln(1/f_c)}. \tag{99}$$

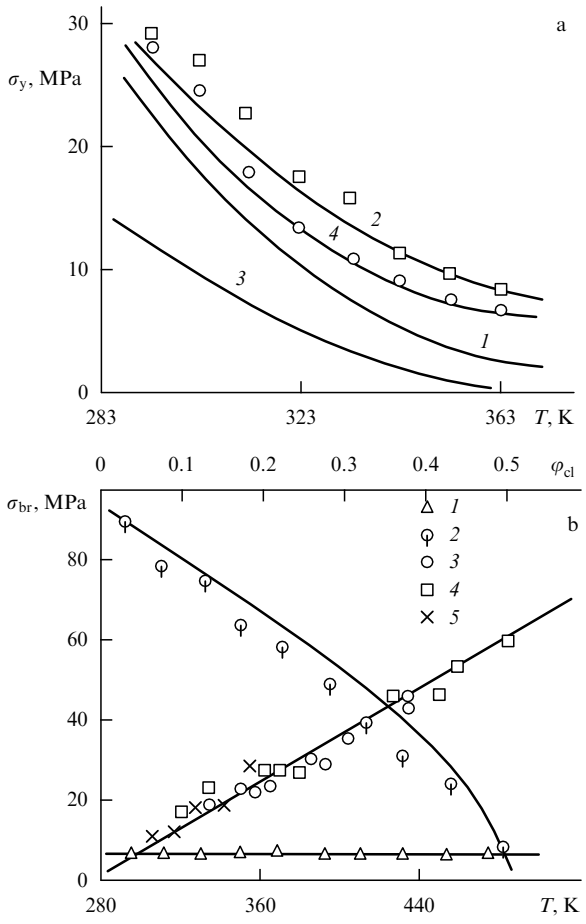

Figure 16. Plots of (a) yield stress σ_y of polyethylene (*1*, *2*) and polypropylene (*3*, *4*) vs. temperature T (points show experimental data, curve *1* — estimates for noncrystalline regions, *2* — estimates taking into account the contribution of crystalline regions [259]), and (b) breaking stress σ_{br} vs. testing temperature T [for the entanglement network (*1*) and cluster network (*2*)] and cluster fraction φ_{cl} [for PC (*3*), PAr (*4*) and HDPE (*5*)]; the upper curve depicts the experimental dependence [267]).

Thus, it follows from Eqns (98) and (99) that the definition $\varepsilon_y = \sigma_y/E$ ignores the presence of free volume in a polymer, while quantitative differences between ε_y determined by the two methods actually depend on f_c.

A combination of Eqns (8), (28), (58), (98), and (99) allows the final expression for the calculation of ε_y to be obtained in the form

$$\varepsilon_T = \frac{\sqrt{2}\,\ln(1/f_c)b(l_0 C_\infty V_{cl})^{1/2}}{4\pi(1+\mu)}\,. \tag{100}$$

The relation (100) indicates that ε_y depends in rather a complicated manner on three groups of factors. One includes molecular characteristics b, l_0, and C_∞ of the polymer. The physical sense of b and l_0 was commented on in preceding paragraphs, while C_∞ is the automodel coefficient of the supersegmental polymer structure [155, 156]. The second group comprises the quantities A and μ determined by the fluctuation free volume of the polymer. Finally, the quantity V_{cl} is a purely structural characteristic showing the degree of local order in an amorphous polymer. This parameter is largely responsible for the temperature dependence of ε_y and also its dependence on structural changes throughout the thermal treatment of the polymer.

It has been shown in Ref. [150] that, within a single polymer class, ε_y increases as the glass transition temperature T_g is raised at a constant testing temperature T and strain rate ε. Equation (100) explains this dependence because a rise in V_{cl} in these polymers at practically similar C_∞ values is a function of T_g [80].

In conclusion, it is worthwhile to note that the quantities A and μ in the end depend on V_{cl}, too. Due to this circumstance, Eqn (100) gives the dependence of ε_y practically on two groups of factors. One comprises molecular factors which can to the first approximation be regarded as independent of thermal prehistory of the sample and testing conditions. The other is represented by the structural parameter V_{cl} which takes into account both T and ε changes and previous treatments of the sample (thermal treatment, film formation by casting from solvents, etc.). Furthermore, it follows from Eqn (100) that the condition $V_{cl} = 0$ must be fulfilled if ε_y is to be reduced to zero. Because ε_y vanishes at T_g [262, 264], it may be concluded that polymer devitrification is due to cluster decomposition under the effect of thermal fluctuations.

Destruction. According to monograph [62], the deformation – strength behavior of polymers depends on their macromolecular entanglement networks. It is therefore speculated that the strength of nonoriented glassy polymers is a function of the amount of entanglements per unit area in the plane perpendicular to the external force direction. Bersted [265] expressed the stress-at-break σ_{br} as

$$\sigma_{br} = \frac{Q(T,\varepsilon)}{2}\left(\frac{2}{3}\right)^{5/6} N_A^{1/3}(E_0 S U_b)^{1/2}\left[\frac{\rho}{M_c}\left(1-\frac{M_c}{M_n}\right)\right]^{5/6}, \tag{101}$$

where Q is the correction factor taking into account changes of the strain rate ε and the difference between the testing temperature T and the temperature at which mobility of macromolecules is completely terminated, N_A is the Avogadro constant, E_0 is the modulus of longitudinal elasticity of the crystal lattice, M_n is the average molecular weight, and M_c is the critical molecular weight which, once achieved, gives rise to the molecular entanglement network. The last quantity is expressed as [73]

$$M_c \cong 2M_e\,. \tag{102}$$

In conformity with the cluster model [55], the amorphous polymer structure is a mesh of clusters tied by 'penetrating' chains and the intercluster (loose-packed) matrix incorporating interlaced chains. In this situation, the substitution of M_e measured by different techniques into Eqn (100) may be used to elucidate what type of entanglements is responsible for polymer durability and check up the validity of the cluster molecular entanglement network concept.

Narasawa [62] substituted different E_0, S, and U_b values to simplify Eqn (100) for the calculation of σ_{br} based on the data for polyethylene and polyethylene terephthalate:

$$\sigma_{br} = 1.4\times 10^5\left[\frac{\rho}{M_c}\left(1-\frac{M_c}{M_n}\right)\right]^{5/6}, \tag{103}$$

where σ_{br} is given in Pa.

Of all the parameters enumerated, E_0 is characterized by the largest data spread. Even for polyethylene, in which it was measured by different methods, E_0 varies over a range of 40 – 400 GPa [266]. For this reason, the constant of Eqn (103) was assumed in Ref. [267] to be 1.17×10^5 for both PC and PAr and used as an adjustable parameter. It should be emphasized that M_e for the network of interlacings was measured at $T > T_g$ and therefore considered to be constant over a temperature range below T_g. Because the fracture stress is a function of temperature [262], Bersted [265] took it into account with the aid of coefficient Q, which looks like a speculative assumption. The value of M_{cl} for the cluster network is a function of T and grows with its rising [see Fig. 2 and Eqn (3)]. Therefore, it seems more natural to think that a decrease of σ_{br} at elevated T is due in this case to a rise in M_{cl}.

In Ref. [267], the true stress-at-break σ_{br}^{true} was taken as a polymer strength characteristic and determined from Eqn (36):

$$\sigma_{br}^{true} = \sigma_{br}^{n}\lambda_{br}\,, \tag{104}$$

where σ_{br}^{n} is the nominal breaking stress, and λ_{br} is the degree of stretch leading to polymer destruction. The value of λ_{br} was in turn found from the breaking strain ε_{br} with the use of relation (71).

Comparison of the temperature dependences of σ_{br}^{true} for PAr obtained in experiment (solid line) and estimated by Eqn (103) (curves *1*, *2*) is shown in Fig. 16b. It can be seen that the substitution of M_{cl} for the cluster network into Eqn (103) gives a $\sigma_{br}^{true}(T)$ value close to the experimental one. A similar operation using M_e for the conventional interlacing network fails to produce an equally good agreement of estimated σ_{br}^{true} with experimental data both on an absolute scale and as a function of temperature [267]. It is worthy of note that σ_{br}^{true} values for $M_e(M_{cl})$ determined by both methods coincide only at $T = 493$ K, i.e. at the glass transition temperature for PAr [267]. This can be accounted for by the disintegration of the cluster network at T_g, leaving intact the conventional polymer interlacing network.

For PC, the calculation was made in the reverse order — that is, M_e was found from experimental σ_{br}^{true} values with the help of Eqn (103). Comparison of M_e thus obtained and

corresponding M_{cl} values computed by Eqns (1) and (2) indicated that it was clustering of chain segments that correlated with the experimentally established PC tensile strength both on an absolute scale and as a function of temperature [267].

It may be concluded that the degree of strength of amorphous glassy polymers is due to the presence of the high-density cluster entanglement network alone, the density of which is almost two orders of magnitude higher compared with the conventional interlacing network [267]. Similar results were obtained in Ref. [268] using the model of Mikos and Peppas [269] who had demonstrated that the strength of amorphous–crystalline polyethylenes under impact destruction is a function of V_{cl}. Moreover, it was shown in Ref. [270] using data for PArSf that λ_{br} is also under the control of cluster network parameters.

One more approach to the evaluation of polymer strength is based on the concept of a quasi-two-phase (microheterogeneous) structure of the polymer amorphous state [86]. The following empirical equation was derived for strength σ_{br} of filled polymers [271]:

$$\sigma_{br} = a - c\varphi_{fill}\,, \tag{105}$$

where a and c are constants, and φ_{fill} is the volume fraction of the filler.

Figure 16b (curves *3–5*) presents the dependences of breaking stress σ_{br} on the cluster volume fraction φ_{cl} for three polymers: PC, PAr, and HDPE. The data for HDPE were obtained in impact tests. It follows from the figure that the strength of these polymers is described by a simple relation [86]:

$$\sigma_{br} \cong 119\varphi_{cl}\ [\text{MPa}]\,, \tag{106}$$

which is analogous to Eqn (105) at $a = 0$ and $c = -119$, with an increase in φ_{cl} (unlike φ_{fill}) leading to higher polymer strength.

Glass transition. It has been repeatedly emphasized that in the framework of the cluster model the polymer vitrification at T_g (more precisely, in a certain temperature interval ΔT around T_g) is considered to be a nonequilibrium phase transition associated with the thermofluctuation breakdown of the regions of local order (clusters). It is important to note that the cluster model postulates a 'frozen' local order. It is underlain by the high viscosity of the polymer matrix, although the degree of order 'freezing' is a function of temperature (see Fig. 2). Local ordering in the regions of this type is characterized by a long lifetime. Local order makes itself evident just as well at temperatures above T_g, as was many times suggested for rubbers [56, 57] and has recently been confirmed in experiment [272]. The last study revealed 'dynamic' local order whose regions (associates) possess short lifetimes. In this context, it should be recalled that Lobanov and Frenkel' [273] posed what appears to be the most relevant model of the fluctuation molecular entanglement network on the condition that it contains multifunctional entanglement sites. These authors hypothesized that the three-dimensional physical network (identified with macromolecular entanglements for the purpose of this discussion) is thermally reversible as it passes through T_{ll} (the so-called 'liquid I–liquid II' transition temperature). In other words, there is every reason to consider the transition T_{ll} as resulting from the formation of the fluctuation macromolecular entanglement network [274]. Quantities T_{ll} and T_g are related by the following approximation [57]

$$T_{ll} \cong 1.21T_g\,. \tag{107}$$

Boyer [275] demonstrated the temperature dependence of polystyrene (PS) viscosity which suggests a sharp change in the slope of linear plots at $T = 443$ K. In other words, this change actually coincides with T_{ll} equal to ~ 435 K for PS. This means that the polymer melt viscosity is governed by two factors: the viscosity of a 'structureless macromolecular ensemble' proper ($T > T_{ll}$), and the viscosity stemming from the fluctuation entanglement network formed under definite conditions ($T < T_{ll}$). Polymer treatment should be carried out at temperatures above T_{ll} [or above T_u — an analogue of T_{ll} for amorphous–crystalline polymers — related to melting temperature T_m similar to Eqn (107)] [274].

Bearing in mind the fluctuation nature of the macromolecular entanglement network, it appears appropriate to examine its relation to density fluctuations $\psi(V)$ in polymers, which are formally described by Eqn (22). It is known from statistical mechanics that for a liquid in equilibrium $\psi(V)$ (when $V \to \infty$, i.e. in the thermodynamic limit) is given as [108]

$$\psi(\infty) = \rho kT\chi_T\,, \tag{108}$$

where χ_T is the isothermal compressibility.

Equation (108) indicates that density fluctuations are due to thermal atomic motions with energy kT but limited by bulk stiffness (χ_T^{-1}). Estimation of $\psi(\infty)$ at $T_{ll}(T_u)$ using data for ρ and χ_T from reference materials [276] shows that $\psi(\infty)$ for certain polymers is roughly constant at these temperatures. This observation suggests that once a critical $\psi(\infty)$ value is reached, the formation of the regions of local order, i.e. a fluctuation macromolecular entanglement network, becomes impracticable because of the high thermal mobility of macromolecules. Conversely, at $\psi(\infty)$ below the critical value, regions of local order (clusters) are formed in a polymer melt, which the cluster model treats as multifunctional entanglement network sites. In other words, the situation takes place described by Boyer as a 'liquid with fixed structure' [275]. The calculated critical temperature T_{crt} [274] at which the critical $\psi(\infty)$ value is reached (assumed to be constant) is in good agreement with $T_{ll}(T_u)$ for a number of amorphous and amorphous–crystalline polymers, the maximum difference being not more than 6% (Table 7).

Table 7. Calculated T_{crt}, $T_{ll}(T_u)$ and their relative deviations Δ [274].

Polymer	T_{crt}, K	$T_{ll}(T_u)$, K	Δ, %
Polymethyl methacrylate	398	415	4.1
Polystyrene	462	433	6.2
Polycarbonate	488	502	2.8
Low-density polyethylene	488	480	1.7
High-density polyethylene	496	480	3.3
Polypropylene	510	528	3.4
Polyamide-6	635	600	5.8

Thus, the fluctuation macromolecular entanglement network may be regarded as a percolation system formed upon cooling the polymer melt as a certain critical fluctuation density, i.e. critical thermal mobility of macromolecules, is achieved. In this case, the percolation threshold on the

temperature scale is T_{ll} for amorphous, and T_u for amorphous – crystalline polymers [274].

When the glass transition in amorphous and amorphous – crystalline polymers is considered within the framework of the cluster model, it is accepted [277] that the elevated density of the chemical cross-link sites v_{cr} leads to a rise in T_g for cross-linked polymers. Such a dependence is due to the restriction of molecular chain mobility by chemical cross-link sites [277, 278]. This inference is confirmed by a number of experimental findings showing symbate changes of v_{cr} and T_g [278]. At the same time, the following observations are worth noting. According to Chang and Brittain [279], thermal ageing of epoxy polymers at $T < T_g$ increases T_g but does not affect v_{cr}. This suggests the absence of a direct relationship between T_g and v_{cr}. It is realized, if at all, at the supermolecular level of structural organization of cross-linked polymers.

Kozlov et al. [280] studied two series of epoxy polymers, one immediately after manufacture (EPAh) and the other after natural ageing in the air for three years ($EPAh_{ag}$). Appropriate vales of T_g, v_{cr}, and V_{cl} for these epoxy polymers are shown in Table 8. It can be seen that ageing of the majority of test pieces resulted in a reduction of v_{cr} and increase of V_{cl} especially in the case of a large deviation of epoxide compositions from the stoichiometric ratio. Thus, a change in the polymer structure throughout thermal ageing may be interpreted in terms of the cluster model as an enhanced degree of local order characterized by V_{cl} [166]. Because this reflects a trend towards a more equilibrium structure, such an interpretation is consistent with current concepts [138]. A rise in V_{cl} also suggests a reduction in the fluctuation free volume f_c for cross-linked polymers [172], in agreement with modern views of epoxy polymer ageing [279].

T_g values for aged epoxy polymers are higher than for fresh ones (Table 8). Analysis of data included in Table 8 shows symbate changes of V_{cl} and T_g in the course of ageing, and the absence of a similar relationship between v_{cr} and T_g. Hence, T_g is not directly dependent on v_{cr}, being a function of the characteristics of the supersegmental structure.

Table 8. Characteristics of epoxy polymers before and after ageing [280].

K_{st}	T_g, K	v_{cr}, 10^{-26} m^{-3}	V_{cl}, 10^{-27} m^{-3}
0.50	342/363	4/3	1.3/4.7
0.75	372/383	10/5.3	2.3/5.4
1.0	399/408	11/7.44	3.3/5.8
1.25	378/398	10/11.7	2.4/6.0
1.50	343/408	8/10.4	1.6/5.7

Note: numerator — for EPAh, denominator — for $EPAh_{ag}$ samples.

Figure 17a shows the dependences $T_g(V_{cl})$ for both EPAh series, which are linear and fall on the same straight line, which allows the devitrification of cross-linked polymers to be regarded as the thermal breakdown of the 'frozen' local order [41, 42]. Thus, the results of Ref. [280] indicate that the behavior of the glass transition temperature for cross-linked polymers is governed by the density of cluster macromolecular entanglement network.

It is known at present that the modulus of elasticity E and the glass transition temperature T_g in linear amorphous polymers undergo symbate variations [110]. This can be accounted for by the dependence of these parameters on symbate changes of such characteristics as cohesive energy and chain stiffness, respectively [81]. However, in cross-linked

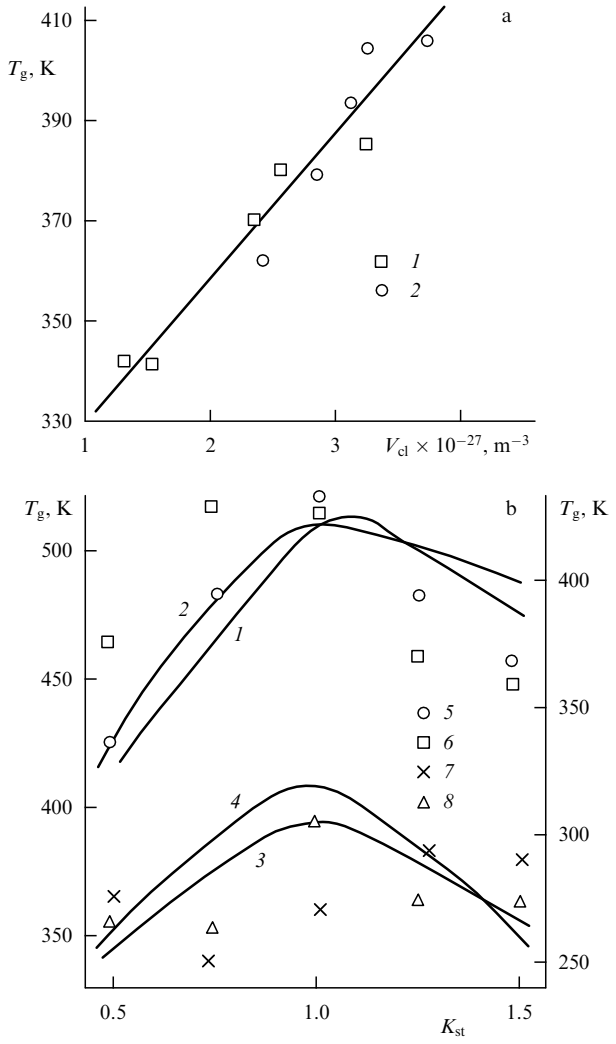

Figure 17. Plots of glass transition temperature T_g (a) vs. cluster entanglement network density V_{cl} for an epoxy polymer hardened with anhydrides (*1* — original specimens, *2* — after ageing [280]), and (b) vs. hardener/oligomer ratio K_{st} obtained in experiment (*1*–*4*) and calculated from Eqn (111) (*5*–*8*) for epoxy polymers hardened with diamine (*1*, *2*, *5*, *6*) and anhydride (*3*, *4*, *7*, *8*) at 0.1 MPa (*1*, *3*, *5*, *7*) and 200 MPa (*2*, *4*, *6*, *8*) [81].

polymers, including epoxy species, E and T_g can show different (e.g. antibate) behavior. For example, it has been shown in Refs [175, 281, 282] that a change of the site concentration in the chemical network by means of K_{st} variation brings about antibate (with respect to T_g) changes of the bulk compressibility modulus and the velocity of longitudinal ultrasound waves. This effect was explained in Ref. [81] based on the fluctuation density $\psi(\infty)$ concept. Estimation of $\psi(\infty)$ for certain polymers from available literature data [276] has shown that $\psi(\infty)$ remains virtually constant not only at T_{ll} but also at T_g as was expected bearing in mind relation (107). This fact allowed Eqn (108) to be rewritten taking into account the relation $\chi^{-1} = K_T$ (K_T is the isothermal bulk compression modulus) as [81]

$$\psi_{crt} = \frac{\rho k T_g}{K_T}\,, \tag{109}$$

where ψ_{crt} is the critical $\psi(\infty)$ value at T_g.

Because the approximate equality $K_T \cong E$ is fulfilled at $\mu \cong 0.33$ characteristic of glassy polymers, it follows from

Eqn (109) that the criterion for constant ψ_{crt} is inapplicable to the vitrification of epoxy polymers studied in Refs [175, 281, 282]. A decrease of E must result in a fall of T_g, at variance with known experimental data. This apparent controversy is explained in Ref. [81] on the assumption that chemical bond network sites restrict fluctuations of cluster segments and are thus responsible for lowering density fluctuations. This explanation does not undermine the key postulate of the model, according to which polymer devitrification is controlled by the breakdown of the 'frozen' local order. A similar line of reasoning can be found in a work of Flory [283] who hypothesized that physical entanglements in rubbers (regarded by many authors as 'short-lived' regions of local order) place strong constraints on fluctuations of chemical cross-link sites. A direct relationship between v_{cr} and T_g appears unlikely because the glass transition is a critical phenomenon associated with a substantial modification of all polymer properties, whereas v_{cr} does not change as the temperature passes through T_g. For this reason, it is assumed, as before, that chemical cross-linking in polymers influences the formation of physical supersegmental structure manifest as V_{cl}; hence, its effect on T_g.

It is difficult to describe the effect of v_{cr} on ψ_{crt} in analytical terms. However, it may be thought that a growing v_{cr} imposes progressively stronger constraints on ψ_{crt} which becomes lower. The authors of Ref. [81] empirically took these constraints into account (as Flory [283] done earlier) by introducing a factor Cv_{cr}^n into the right-hand part of Eqn (109), where C and n are constants. In this case, Eqn (109) for cross-linked systems assumes the form (taking into consideration a well-known relation between K_T and E [110]):

$$\psi_{crt} = \frac{3\rho k T_g (1 - 2\mu)}{E C v_{cr}^n} . \qquad (110)$$

Based on a few simple assumptions described by Beloshenko et al. [81], Eqn (110) can be rewritten as

$$T_g \cong 4.45 \times 10^{-21} K_T v_{cr}^{1/2} , \qquad (111)$$

where T_g is in kelvins, K_T in Pa, and v_{cr} in m^{-3}.

Figure 17b shows the experimental dependences $T_g(K_{st})$ for epoxy polymers, which on the whole exhibit a good correlation. The discrepancies apparent in the EPAh system appear to be related to the approximations used in the study.

Thus, the network of chemical bond sites not only affects the degree of local order (parameter V_{cl}) as was noticed earlier in Ref. [284] but also restricts thermal fluctuations of cluster segments. This effect plays an important role in the formation of the properties of cross-linked systems. For example, it explains the observed antibate variations of E and T_g [81].

Let us now turn to the interpretation of characteristic temperatures for amorphous–crystalline polymers in the framework of the cluster model. The complex structure of these materials as compared with amorphous polymers made certain authors question the applicability of the notion of the general nature of α- and β-transitions to highly crystalline polymers [57]. Analysis of a large number of theoretical and experimental studies on relaxation transitions in polyethylenes shows that their interpretation is apparently contradictory and many important aspects remain a matter of controversy [57]. We do not consider here the pros and cons of the implications of relaxation transitions in amorphous–crystalline polymers because they have been discussed at length in many previous works [57, 285, 286]. Suffice it to recall some major prerequisites for cluster formation in these materials. It has been mentioned before that the amorphous chain tension at the time of crystallization gives rise to the regions of local order (clusters) by analogy with the formation of liquid–crystalline order [287]. This means that clustering at $T < T_m$ is also due to 'freezing' molecular mobility by mechanical chain tension [288]. As the temperature is raised, the tension falls leading to a decrease of the local order level and the corresponding growth of $C_m(\varphi_{lm})$. It is appropriate to recall that, in the case of polyethylenes, the 'mobile fraction' C_m (or the devitrified loose-packed matrix in the amorphous phase) appears at temperatures roughly between 140 and 170 K [57]. On approaching T_m, the degree of crystallinity decreases as a result of crystallite surface melting and intensified chain slippage through crystallites. These processes lead to cluster decomposition and devitrification of the amorphous phase which acquires high elasticity. This process is completed at the polymer melting point. Therefore, devitrification of both the amorphous phase and the bulk material in amorphous–crystalline polymers is associated with the breakdown of the 'frozen' local order (cluster decomposition) as in amorphous glassy polymers [171]. In the framework of such a structural interpretation, the glass transition occurs over a very wide temperature range, from $\sim 140-170$ K to ~ 410 K for polyethylenes [289]. In fact, in terms of the cluster model, the transition at $\sim 140-170$ K in polyethylenes is an analogue of T_g', while T_m is an analogue of T_g. In this aspect, T_g should be regarded as the achievement of an 'ideal' polymer structural state in which there is neither local nor long-range order [129, 259].

Diffusion. The free volume theory is successfully employed for the interpretation of diffusion processes in polymers above glass transition temperature. However, its application to the glassy state encounters difficulty [290]. Polymer diffusive properties below T_g were considered in Refs [66, 166] in terms of two interrelated models: the fluctuation free volume model [110] and the cluster model [55].

The specific patterns of the dependence of the nitrogen-based permeability coefficient P_{N_2} on the amount of fractional fluctuation free volume f_c estimated from Eqn (61) suggests a close relationship between diffusion processes and free volume fractions in polymer materials. An admixture of 0.05 wt % Z in HDPE results in a dramatic decrease of P_{N_2} (see Table 3). Selected structural characteristics of three most common HDPE + Z systems are presented in Table 9. At the practically invariable degree of crystallinity K, the nitrogen-based permeability coefficient for HDPE + Z compositions is almost a factor of 17 smaller than for uncontaminated HDPE. A $\sim 16\%$ decrease of K in HDPE + Z containing 1.0 wt % of Z (compared with original HDPE) leads to a decrease in P_{N_2} rather than to an increase. This means that an explanation for the effect in question should be sought in structural changes of noncrystalline regions. As is known from Ref. [291], transfer processes in amorphous–crystalline

Table 9. Degree of crystallinity K and crystallite size L_{002} for HDPE + Z compositions.

Z content, weight percent	K	L_{002}, Å
0	0.68	280
0.05	0.65	250
1.0	0.52	265

polymers, such as HDPE, are as a rule mediated through amorphous regions. It may be suggested that these processes occur in the loose-packed matrix, since it accumulates the entire fluctuation free volume available. The dependence of P_{N_2} on φ_{lm} is also linear [166]. This confirms that the above structural interpretation of the diffusion processes in polyethylenes is correct [68].

There is a definite relationship between the fluctuation free volume size and the ratio of the diffusion activation energy to the diameter squared of the diffusing particle, E_D/d_D^2 [290]. This relationship turned out to be linear and, as expected, a rise in f_c results in a decrease of E_D/d_D^2. These data were obtained at temperature 293 K. Taking into account the linear dependence $f_c(\varphi_{lm})$ (see Fig. 9), it may be argued that E_D/d_D^2 and φ_{lm} are related to each other by an analogous correlation.

Thermodynamic properties. Let us consider the influence of cluster structural parameters on certain thermodynamic characteristics of polymers. Interesting physical information, apart from necessary technical data, has been obtained in a study of thermal expansion of polymers [292]. Slutsker and Filippov [293] noticed different patterns of micro- and macroexpansion in amorphous polymers and assigned them to a certain degree of ordering in chain macromolecules. In other words, these authors established a relationship between thermal expansion and the supermolecular structure of selected amorphous polymers. However, they were unable to specify this relationship for the lack of an adequate quantitative structural model. A potential relationship between thermal expansion and the cluster structure in epoxy polymers EPD and EPAh will be considered below.

Analysis of large-angle X-ray patterns for these epoxy polymers revealed a systematic displacement of the center of gravity of the amorphous halo along axis θ as K_{st} was varied. This suggested a corresponding change of the Bragg interval d_b over a distance scale of 4.48 – 4.82 Å [96]. It may be concluded from the halo shift in amorphous polymers [294] and from d_b values that the X-ray technique measured distances between the axes of roughly parallel neighboring macromolecules, i.e. interchain distances D_{int}, which can be obtained from the well-known Keesome formula [294]

$$D_{int} \cong 1.22 d_b \,. \tag{112}$$

In these works, as in Ref. [293], microdilations (α_μ) and macrodilations (α_m) were measured, the former being counted from the state at $K_{st} = 1.0$ for EPD, and at $K_{st} = 1.25$ for EPAh, where d_b were minimal. The dependences $\alpha_\mu(K_{st})$ and $\alpha_m(K_{st})$ for the two systems examined (and for linear amorphous polymers) exhibited a much higher degree of α_μ variations compared with α_m, although their general trend was identical [293]. This difference can be explained in the framework of the cluster model analogous to that employed in Ref. [293], setting apart the regions of local order. Slutsker and Filippov proposed to consider these regions as analogues of folded-chain crystallites, and clusters as PCC analogs [55]. Following the line of reasoning adopted in Ref. [293] it may be concluded that thermal expansion of a cluster is strongly anisotropic and can be described by the following equation

$$3\alpha_{ml} = 2\alpha_{\mu\perp} + 2\alpha_{\mu\parallel} \,, \tag{113}$$

where α_{ml} is the quantity obtained by dilatometric measurements, and $\alpha_{\mu\perp}$ the quantity determined by X-ray diffraction analysis. Equation (113) allows $\alpha_{\mu\parallel}$ to be found. All measured α values are listed in Table 10 which shows that α_{ml}, $\alpha_{\mu\perp}$, and $\alpha_{\mu\parallel}$ are very close to the analogous characteristics reported in Ref. [293] both on an absolute scale and in terms of the tendency in changes. For all that, there is an important difference such that $\alpha_{\mu\parallel}$ may be either positive or negative in sign. The authors of Ref. [293] maintain that one of the factors accounting for the negative sign of $\alpha_{\mu\parallel}$ may be *trans-hauche* conformation transitions contributing to the longitudinal contraction of a macromolecule. Evidently, the positive sign and rather high absolute values of $\alpha_{\mu\parallel}$ suggest a sufficiently high probability of reverse (*hauche-trans*) transitions in epoxy polymers with changing K_{st}. The wavelength λ_v for a nonstretchable strand as a model of a macromolecular segment in the case of sinusoidal vibrations can be written as [293]

$$\lambda_v = \pi d_b \sqrt{\frac{\alpha_{\mu\perp}}{|\alpha_\mu|}} \,, \tag{114}$$

where α_μ is the overall polymer microstate.

Table 10. Dynamic characteristics of cross-linked polymers.

Composition	K_{st}	$\alpha_{\mu\perp} \times 10^2$	$\alpha_{\mu\parallel} \times 10^2$	$\alpha_m \times 10^2$
EPD	0.50	4.15	−2.03	2.09
	0.75	3.94	−2.09	1.93
	1.25	1.04	3.83	1.97
	1.50	2.07	1.83	1.99
EPAh	0.75	1.08	2.81	2.23
	1.0	0.43	4.30	1.72
	1.50	3.03	0.24	2.10

There have been many studies on the heat of solution concerning amorphous polymers [292, 295, 296]. It is believed that a major contribution to the heat of solution ΔH_s comes from the thermal effect of system transition from the metastable glassy state to a quasi-equilibrium solution [296]. Of crucial importance here may be the contribution from a component associated with the polymer structure, in particular, the presence of ordered regions [295]. It is natural to check this inference in terms of the cluster model.

A few general features of ΔH_s behavior were noticed in Ref. [295]. First, ΔH_s does not depend on the solution temperature T above the glass transition temperature T_g of the polymer. It has been mentioned above that the cluster model implies thermofluctuation cluster decomposition at T_g. In other words, this process may be supposed to control variations of ΔH_s at T_g. Second, a rise in T_g is accompanied by an increase of ΔH_s at a fixed T [in the framework of the cluster model, polymers with higher T_g have larger V_{cl} at constant temperature T, see Eqn (63)]. Third, a rise in solution temperature leads to a fall in ΔH_s because in the cluster model V_{cl} decreases as T is raised (see Fig. 2). However, the most remarkable finding is the linear dependence of ΔH_s on the $T_g - T$ difference, observed in Ref. [295]. This dependence suggests that ΔH_s is unrelated to the structural features of amorphous polymers and is determined by the degree of proximity to T_g alone. Treating a cluster segment as a linear defect, one can calculate its dissociation energy U with the help of Eqn (48). Then, the dissociation energy U_{dis} per unit volume of the polymer is found in the following way

$$U_{dis} = U V_{cl} \,. \tag{115}$$

The evaluated U_{dis} and the linear dependence $\Delta H_s = f(T_g - T)$ for PMMA, PC, and PAr [295] give reason

to regard ΔH_s as an energy necessary for cluster dissociation. This means polymer transition from the metastable glassy state to the quasi-equilibrium one (solution or melt).

Finally, a jump of heat capacity ΔC_p at the glass transition temperature T_g can be estimated as described by Wunderlich [297]:

$$\Delta C_p = R \frac{v_0}{v_h} \left(\frac{E_h}{RT_g} \right)^2 \exp\left(-\frac{E_h}{RT_g} \right), \quad (116)$$

where R is the gas constant, v_0 is the molar volume occupied by macromolecules, v_h is the molar free volume, and E_h is the energy of the free-volume microcavity formation.

The estimate is facilitated by simplifying formula (116) and assuming $v_0/v_h = 5$ [297], $E_h/RT_g = \ln(1/f_c)$ [110], and $\exp(-E_h/RT_g) = f_c$ [110]. The resultant ΔC_p values are presented in Table 11. Their correctness can be checked by independent determination of ΔC_p using the Boyer empirical relation [298]

$$\Delta C_p \cong \frac{104.25 \text{ J g}^{-1}}{T_g}. \quad (117)$$

Table 11 shows rather close ΔC_p values derived from Eqns (116) and (117). It is also easy to see that the calculation of ΔC_p by means of Eqn (116) requires a single parameter f_c. It may be argued based on the linear correlation $f_c(\varphi_{lm})$ (see Fig. 9) that a similar ΔC_p value will be obtained in the framework of the cluster model.

Table 11. Comparison of heat capacity discontinuity ΔC_p at T_g, estimated from Eqns (116) and (117) for epoxy polymers.

Polymer	K_{st}	ΔC_p, J g^{-1} K^{-1}	
		from Eqn (116)	from Eqn (117)
EPD	0.50	32.6	32.0
	0.75	26.6	28.6
	1.0	21.8	24.6
	1.25	18.8	25.7
	1.50	24.8	26.7
EPAh	0.50	29.3	30.4
	0.75	24.4	28.0
	1.0	22.9	26.1
	1.25	25.2	27.5
	1.50	31.0	30.2

Scaling of molecular characteristics. Molecular weight characteristics are specific parameters of the polymers, having a definitive influence on all their properties [299]. It has been shown in the foregoing pages that an admixture of Z in HDPE results in a dramatic change of many HDPE properties. This prompted a study of molecular weight effects in HDPE + Z compositions [300].

Following Popova et al. [301], the average molecular weight M_w of HDPE can be estimated from an empirical relation

$$\lg M_w = \lg 129000 - 0.263 \lg(I_{21.6}^{190}), \quad (118)$$

where the superscript and subscript on I denote the temperature in °C and the imposed load in N, respectively.

The dependence $M_w(C_Z)$ found from Eqn (118) exhibits a maximum at $C_Z = 0.05\%$, when M_w is approximately 25% higher than the molecular weight of unmodified HDPE (Table 12). According to these data, admission of Z into HDPE results in a marked increase of the polymer molecular weight. This rise is paralleled by a change of mechanical characteristics, such as would be caused by M_w modulation. Thus, Table 12 shows C_Z-dependence of the Sharpy impact strength (A_p) having a maximum. Also, Ref. [301] proposes a formula relating HDPE viscosity at impact tension (a_p) to I:

$$\lg a_p = 1.492 - 0.22 \lg(I_{21.6}^{190}). \quad (119)$$

Table 12. Molecular and mechanical characteristics of HDPE + Z compositions [300].

Z content, weight percent	$M_w \times 10^{-5}$, g mol^{-1}	A_p, kJ m^{-2}	a_p, kJ m^{-2}
0	1.56	19.5	34.5
0.01	1.48	15.8	34.1
0.03	1.70	23.5	39.5
0.05	1.93	37.2	44.8
0.07	1.76	29.8	40.5
0.10	1.45	11.7	34.0
0.15	1.44	12.5	33.9
0.20	1.40	14.8	33.5
0.50	1.47	13.4	34.0
1.00	1.42	19.2	33.5

Note: M_w was calculated using Eqn (118).

The dependence of a_p on C_Z, governed by Eqn (119) (see Table 12), is also analogous to the dependence $M_w(C_Z)$.

However, these data do not actually indicate that an admixture of Z in HDPE results in a higher M_w [99]. After boiling of HDPE + Z in xylene for 5 h, I (hence M_w) practically returned to the initial values at C_Z of 0.01–0.15%, as follows from Eqn (118) [99, 300]. The treatment regimes for HDPE + Z compositions in *n*-xylene (temperature and duration) were chosen such that only van der Waals intermolecular bonds were broken, while covalent bonds remained intact as indicated by the equality of I for original HDPE prior to and after boiling in *n*-xylene. It is therefore assumed that incorporation of Z into HDPE has no effect on its molecular weight. A drastic change of M_w estimated with the use of Eqn (118) may be attributed to the enhancement of V_{cl}.

Kavassalus and Noolandi [302] showed that the following relation is true within the framework of scaling concepts:

$$\frac{M_w^3}{M_p^2} \propto \eta_0, \quad (120)$$

where η_0 is the polymer melt viscosity at zero shear.

To a good approximation, η_0 can be characterized by I because measurement of the latter parameter is not associated with marked shear stress. The reciprocal of the I quantity is more convenient to use for the purpose because its increase corresponds to η_0 growth. In this approach, I^{-1} reflects a cumulative change of both molecular mass and macromolecular entanglement network density of the polymer [300].

The dependence of molecular characteristics on η_0 in the form of Eqn (120) is linear and goes through the origin of the coordinate system. In other words, the cluster entanglement network in HDPE + Z compositions may be described in the framework of the scaling theory [302].

To conclude, Mills et al. [303] treated polyethylenes as a rubber-like amorphous matrix in which crystallites played the role of molecular entanglement network sites. However, measurements of I indicated that the maximum viscosity of

HDPE + Z compositions is also retained in a melt at 190 °C, when crystallites are nonexistent. Moreover, there is a linear correlation between I ($T = 190$ °C) and M_{cl} ($T = 20$ °C) [99]. These observations support the role of cluster entanglements in polyethylenes.

Structural relaxation. Structural changes accompanying relaxation of amorphous glassy and amorphous–crystalline polymers are referred to as structural relaxation. The principles of structural relaxation in amorphous polymers are demonstrated by Fig. 18a which shows the dependences of the modulus of elasticity E and equilibrium modulus E_∞ on V_{cl} for PC and PAr, respectively. The dependences $E(V_{cl})$ split into two linear portions each bounded by the glass transition temperature T_g' of the loose-packed matrix [60]. This means that at temperatures below T_g' E is determined by the collective contribution of the clusters and loose-packed matrix, and only by clusters above T_g' [91]. Such a situation is easy to explain. Specifically, at temperatures above T_g' the modulus of elasticity of the devitrified matrix is around 2 MPa [65] or practically zero on the scale of Fig. 18a. Of special interest is that the contribution of the loose-packed matrix to E, determined by the extrapolation of plot $E(V_{cl})$ to $V_{cl} = 0$, is independent of temperature. Such a situation is not a mere coincidence, being underlain by fundamental processes worthy of special consideration. The dependence $E_\infty(V_{cl})$ for PC, also shown in Fig. 18a, is distinct from $E(V_{cl})$ at $T < T_g'$ only in the zero contribution of the loose-packed matrix. In fact, there is a parallel shift of the plot $E(V_{cl})$, suggesting that relaxation processes in amorphous polymers at $T < T_g'$ are actually confined to the loose-packed matrix.

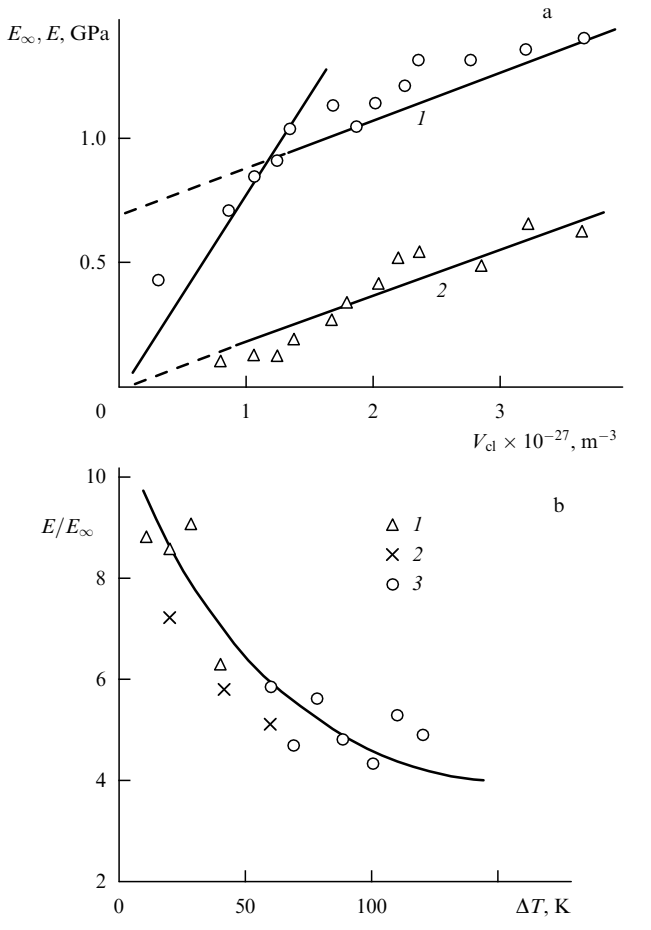

Figure 18. Plots of (a) elastic modulus E (*1*) and equilibrium modulus E_∞ (*2*) vs. cluster entanglement network density V_{cl} for PC, and (b) E/E_∞ ratio vs. temperature difference $\Delta T = T_g - T$ for PC (*1*) and PAr (*2*), and vs. $(T_m - T)$ for HDPE (*3*).

The dependences $E(V_{cl})$ and $E_\infty(V_{cl})$ for HDPE, derived from the results of quasi-static tensile tests, present quite a different picture compared with the behavior of PC and PAr at $T < T_g'$. The course of relaxation is reflected in a change of the slope of the plot $E_\infty(V_{cl})$ as compared with $E(V_{cl})$. The vanishing of E and E_∞ at $V_{cl} = 0$ is due to the low elastic modulus (~ 2.1 MPa [65]) of the loose-packed matrix which is devitrified at the temperatures (293–363 K) used in the test [57]. A decline in the slope, in turn, signifies a modulation of the structural relaxation mechanism now biased in favor of the second constituent structure, viz. clusters.

Let us now consider factors that may be responsible for a change in the mechanism of structural relaxation. Earlier studies [254, 304] revealed two potential mechanisms functioning in the deformation of amorphous polymers: one corresponds to the appearance and 'freezing' of nonequilibrium macromolecular conformations (mechanism I), and the other to mutual displacement of elements of the supermolecular structure tied by penetrating chains (mechanism II). In essence, relaxation processes are opposite to deformation, which allows the above interpretation to be used to explain the available data. Evidently, in the case of a vitrified loose-packed matrix, structural relaxation due to cluster motion encounters difficulty (or, at least, is time-consuming). For this reason, the relaxation occurs via the transition of nonequilibrium chain conformations back to equilibrium ones (mechanism I). When generating a stress, this mechanism is readily realized in a loose-packed matrix having high f_c. In the case of a devitrified loose-packed matrix (PC and PAr at $T > T_g'$, and HDPE), relaxation is a rapid process, its viscosity markedly decreases [110], and clusters are capable of motion. Thus, structural relaxation is supported by mechanism II. The dependences $E(V_{cl})$ and $E_\infty(V_{cl})$ at $T > T_g'$ for PC and HDPE practically coincide, which confirms the identity of the structural relaxation mechanisms. It is worthwhile to note that the coincidence of E and E_∞ dependences on V_{cl} for PC at $T > T_g'$ and HDPE also provides indirect evidence in support of the aforementioned temperature transitions for HDPE, in which the interval $T \sim 140-170$ K is associated with T_m, and T with T_g.

Another argument in favor of possible identity comes from the results of impact tests using HDPE. The longer the notch, the shorter the period over which the test piece is destroyed and the larger the growth of E due to the incompleteness of relaxation processes [47]. Simultaneously, a part of the loose-packed matrix undergoes mechanical vitrification and therefore makes an important contribution to E.

Works [182, 305] used the inverse relative stress decrease during a certain period of its relaxation β as a parameter characterizing the temperature dependence of relaxation properties:

$$\frac{1}{\beta} = \frac{\sigma_1}{\sigma_1 - \sigma_r}\,, \tag{121}$$

where σ_1 is the stress at the time of loading, which becomes σ_r after a certain period of relaxation.

In terms of the proposed mechanisms of structural relaxation, a decrease of the cluster size with increasing T

may be expected to promote the process governed by mechanism II. Hence, a correlation between $1/\beta$ and F may be anticipated (it should be recalled that the number of segments in one cluster is $F/2$ [55]). This was confirmed in the work [166] which also showed that $1/\beta$ tends to unity in the course of complete thermofluctuation cluster decomposition, i.e. as $F \to 2$ and $T \to T_g$.

The intensity of relaxation processes can be expressed through the ratio E/E_∞. The smaller E_∞, the more complete the relaxation processes and the higher E/E_∞. A similar interpretation was proposed by Boyd [285, 286] who demonstrated that the height of the peaks of secondary relaxation depends on the difference $E - E_\infty$. Figure 18b shows the dependence of E/E_∞ on the temperature difference $T_g - T$ ($T_m - T$ for HDPE), i.e. the degree of T approach to T_g (T_m). It follows from the figure that the degree of process completeness for all the three polymers grows on approaching T_g (T_m). This may be due either to a drop in viscosity of the devitrified matrix or to a decrease of the cluster volume with increasing T. Both causes promote cluster displacement in mechanism II.

It is concluded that the cluster model is useful for the identification of structural relaxation mechanisms in polymers. In the case of a vitrified loose-packed matrix, the relaxation process occurs through its conformational restructuring (mechanism I); in a devitrified matrix the relaxation is realized via relative displacements of the clusters (mechanism II).

Crazing. It has been shown above that amorphous glassy polymers experience deformation by such local plastic strain mechanisms as crazing [306] and shear bands [307]. These may be considered to reflect the structural inhomogeneity of polymers under the effect of force fields. Nevertheless, the behavior of these polymers under certain strain conditions is not infrequently described in terms of polymer mechanical continuity [197] which raises the problem of the size scale on which a given polymer may still be regarded as a homogeneous solid. Fellers and Huang [87] have shown [see Eqn (17)] that structural inhomogeneity of a polymer determines its propensity for crazing — that is, the higher the degree of inhomogeneity, the more amenable the polymer to crazing. Hence the possibility of establishing a direct relationship between the polymer structure and the susceptibility to crazing. In the paragraphs that follow, this will be done based on the fluctuation theory [87].

In terms of Eqn (17), the 'interlacing'-free volume V_0 is considered to be a random quantity which rules out its relation to the polymer structure. In the framework of the cluster model, volume V_0 can be treated as a cubic volume of the loose-packed matrix (devoid of cluster network sites by definition) bounded by eight clusters at the cube vertices. Its volume V_{str} is easy to determine as the inverse number of clusters N_{cl} per unit volume of the polymer. Flory [56] proposed the following formulas for N_{cl}:

$$N_{cl} = \frac{2V_{cl}}{F}\,, \tag{122}$$

and

$$V_{str} = \frac{F}{2V_{cl}}\,. \tag{123}$$

The quantity V_{str} thus obtained can be compared with V_0, namely, the volume necessary for the creation of a craze cavity between fibrils, which can be found from Eqn (17). Let us consider the physical meaning of the parameters entering this equation. The crazing stress σ_c admits of several interpretations. It is conceivable that there is craze nucleation stress, craze elimination stress, etc. [308, 309]. In the interpretation under discussion, the major principal stress σ_{yy} for the cluster nucleation was chosen as σ_c [309]. Such a choice is justified by the necessity to consider cavity (hence, craze) initiation.

Experimental measurement of the modulus of elasticity E (which is approximately equal to the bulk modulus B in Eqn (17) at $\mu \sim 0.33$, see above) deserves a more detailed discussion. Polymer impact tests [47, 310] revealed the strong dependence of E on the strain ε due to the anharmonicity of intermolecular bonds. So far as craze nucleation is concerned, it is correct to choose E at the craze nucleation strain ε_c. For PC and PAr, ε_c may be assumed to equal ~ 0.02 [220]. Comparison of E values found from the slope of the linear portion of the load–time ($P-t$) curve in impact tests and evaluated by the elastic recoil technique [47] at $\varepsilon \cong 0.02$ indicates that the former are significantly (approximately 1.5-fold) higher than the latter. This difference interferes with the results of V_0 determination by means of Eqn (17). Finally, the glass transition temperature T_g is taken as T_0 (see above).

Calculations of V_0 with the help of Eqn (17) using E values found from the slope of the linear portion of $P-t$ curve give figures higher than V_{str}. Nevertheless, in this case too, V_0 and V_{str} are of the same order of magnitude, with similar patterns of temperature dependences. For the reasons presented above, the correlation is improved using E values obtained at $\varepsilon \cong \varepsilon_c$. In this case, the difference does not exceed $\sim 22\%$.

Characteristically, V_{str} does not change with temperature and is therefore an intrinsic polymer property. The relations between V_{cl} and F for PC and PAr are well approximated by straight lines [221]. This means that a rise in V_{cl} with decreasing temperature (Fig. 2a) is mediated through segment attachment to the existing clusters rather than through the formation of new clusters. Extrapolation of $V_{cl}(F)$ plots to $F = 0$ yields a finite V_e as a characteristic of the network of interlaced chains with density $\sim 0.4 \times 10^{27}$ m^{-3}, i.e. close to the experimentally found V_e [66].

An essentially similar interpretation of the association of crazing with the entanglement network (network of overlapping chains) is proposed in Ref. [311]. It is however qualitative and speculative unlike the model discussed in the previous paragraphs.

It may be concluded that V_{str}, by virtue of its correspondence to V_0, characterizes the propensity of a polymer to crazing. It is especially well apparent from the comparison of V_0 for PC and PAr ($\sim 6.0 \times 10^3$ Å^3 and $\sim 3.9 \times 10^3$ Å^3, respectively) and also from the V_0 values for polystyrene (PS) obtained in work [87] ($\sim 450 \times 10^3$ Å^3). Evidently, PS exhibits a much stronger tendency to crazing than either PC or PAr, as has been shown in numerous experiments [312, 313]. Another observation worth noting consists in that a decrease of V_0 leads to the lowering of the critical size level above which the polymer may be treated in terms of continuity concepts. In practice, it is realized via deformation by diffuse shear in PC [314] and by strongly localized 'coarse' shear bands in PS [307].

Physical (thermal) ageing. Thermal (physical) ageing of amorphous polymers has been investigated in numerous studies. Many of them used PC and thus provide good

materials for comparison. It has been shown that the influence of thermal ageing on the structure and properties of amorphous polymers is due to departure of the glassy state from thermodynamic equilibrium. This gives grounds to consider polymer ageing as the slow approach toward equilibrium of a system with a broad distribution of relaxation times [315]. The available results [138, 316] suggest that ageing of amorphous polymers at temperatures below the glass transition temperature T_g increases the density of their fluid-like packing and thus facilitates the approach of their structure to the equilibrium glassy state. There are two major concepts of the mechanism of this process. One [317] postulates that ageing affects free volume, the other [318] maintains that ageing effects result from thermoreversible molecular restructuring. It is specified in Ref. [319] that these effects in the event of PC are associated with a decreased mobility of phenyl groups and further ordering of polymer chains. One more hypothesis was formulated by Bubeck and Yusar [320]. The authors speculate that ageing leads to relatively fine conformational changes weaker than, for instance, a *cis-trans* transition. They also argue that the decreased free volume is a result of ageing rather than the main cause of altered polymer physical properties. It will be shown below, using data for PC, to what extent this hypothesis is consistent with the cluster model.

The dependences of cluster network density V_{cl} on testing temperature T for original and aged PC indicate that V_{cl} of the latter material is higher than of the former. In other words, aged PC is characterized by a higher degree of local ordering. This trend is fully consistent with the approach of the structure of amorphous polymers experiencing thermal ageing to equilibrium, i.e. a perfectly ordered state. Comparison of the dependences $V_{cl}(T)$ and $F(T)$ shows that the number of clusters per unit volume in an ageing polymer remains roughly constant, but the number of segments in one cluster increases, suggesting greater stability of the clusters. Moreover, the increase in the number of cluster segments in the course of ageing agrees with the conclusion of Ref. [320] to the effect that the concomitant restructuring is due to relatively slight conformational changes.

The T-dependence of the fluctuation free volume (f_c) is illustrated by Fig. 19 showing that f_c of original PC is bigger than in the aged polymer over the entire temperature range. This agrees with the results of Morgan and O'Neal [317]. Antibate plots $V_{cl}(T)$ and $f_c(T)$ suggest the possibility of correlation between these parameters, which is confirmed by curves *3* and *4* in Fig. 19. However, original and aged PC exhibit different dependences $f_c(V_{cl})$. At equal V_{cl}, f_c of the aged polymer is smaller than of the initial one. Because the entire fluctuation free volume is enclosed in the loose-packed matrix, these findings indicate that it undergoes compaction in the course of thermal ageing. This conclusion is in excellent agreement with the data for annealed PAr obtained by the positron annihilation technique [147]. Also interesting is the extrapolation of plots in Fig. 19 (curves *3*, *4*) to $f_c = 0$ and $V_{cl} = 0$. It is obvious that at $f_c = 0$ the polymer forms a close-packed structure, actually one giant cluster [171, 321]. By analogy with Eqn (9), V_{cl} of such a structure can be expressed as L/l_{st} which is 7.04×10^{27} m^{-3} for both fresh and aged PC. Extrapolation to $f_c = 0$ gives a close value equal to $\sim 6.8 \times 10^{27}$ m^{-3} [321]. Extrapolation of the dependence $f_c(V_{cl})$ to $V_{cl} = 0$ yields the fluctuation free volume of the polymer at the glass transition temperature T_g. Its values are ~ 0.150 for fresh and ~ 0.133 for aged PC. They are higher

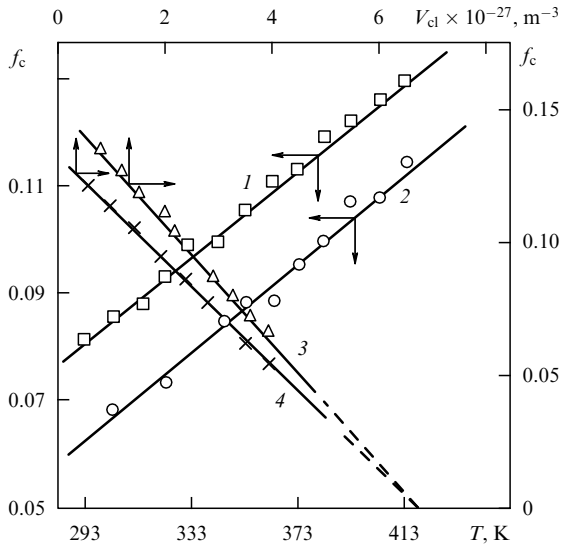

Figure 19. Plots of relative fluctuation free volume f_c vs. temperature T (*1*, *2*) and cluster entanglement network density V_{cl} (*3*, *4*) for original (*1*, *3*) and aged (*2*, *4*) PC [321].

than the universal Simha – Boyer quantity (~ 0.113 [298]) but fully agree with the calculations of Sanchez (0.105 – 0.159) [174].

As is known [140], the majority of amorphous glassy polymers fail to meet the Prigogine – Defay criterion. This means that the order parameter alone is insufficient to characterize the structure of these polymers. This inference is confirmed for PC by plots of f_c versus V_{cl}. Evidently, different f_c values at the same V_{cl} indicate that one more order parameter besides V_{cl} is needed to describe the state of the loose-packed matrix.

Thermal ageing of cross-linked polymers (native EPAh and EPAh$_{ag}$ aged for 3 years) was investigated in Ref. [322]. It has been shown in a preceding paragraph that the modulus of elasticity E in the polymer glassy state is a function of the total contribution from clusters and loose-packed matrix (E_{lm}). In the case of matrix devitrification, $E_{lm} = 0$ (Fig. 18a). Therefore, the dependence $E(V_{cl})$ permits one to find E_{lm} by the extrapolation of the plots to $V_{cl} = 0$. The dependences of E and E_{lm} on K_{st} for EPAh and EPAh$_{ag}$ suggest that thermal ageing is accompanied by a significant decrease of the elasticity modulus, which is almost completely due to a decrease of E_{lm}. Because all effective relaxants are concentrated in the loose-packed matrix, the observed effects of ageing may be interpreted as being induced by stress relaxation in this matrix [322].

Analysis of the dependences $F(K_{st})$ for EPAh and EPAh$_{ag}$ has demonstrated that thermal ageing leads to a slight decrease of F. Taken together, this observation and patterns of $V_{cl}(K_{st})$ dependences suggest that ageing of cross-linked polymers is associated with a rise in the number of unstable clusters rather than segments in the existing clusters [322] (cf. data for PC). This explains the appearance of the 'yield tooth' on $\sigma - \varepsilon$ curves for aged epoxy polymers and its disappearance after yield is reached [279].

Thus, the interpretation of the thermal ageing process below T_g in amorphous glassy polymers in the framework of the cluster model provides a quantitative characteristic of the attending structural changes [171, 321, 322].

Plasticization. Plasticization is the incorporation of organic compounds with a polymer for imparting to it such properties as elasticity, freeze resistance, and lower processing temperature [323]. Different aspects of plasticization have been at the focus of many research works during the last 40 years because of the important practical implications of this process. These studies resulted in the discovery of so-called antiplasticization, i.e. enhanced polymer stiffness and strength achieved by a rise in the content of a plasticizer introduced into the specimen [323]. At present, the most rational explanation of the observed effects consists in that the addition of a small amount of a plasticizer leads to the appearance (or modification) of structural order and the resulting enhancement of polymer stiffness [324–326]. Continued enhancement of a plasticizer amount fails to further improve ordering; in fact, it decreases the polymer stiffness and impairs its durability. However, until recently these structural changes have been described only in qualitative terms. The concluding paragraphs below present a quantitative characteristic of these changes in PC doped with dibutyl phthalate (DBP) accounting for the well-known effects of plasticization and antiplasticization [171].

Figure 20a illustrates the effect of DBP content in PC on V_{cl} and the number of segments $F/2$ in one cluster. Of special interest is the different behavior of V_{cl} and $F/2$ depending on DBP levels. The former parameter monotonically grows with increasing C_{DBP}. In other words, the plasticizer causes a monotonic decrease in the degree of local ordering in PC. At the same time, a conspicuous rise in the number of segments in a cluster suggests cluster restructuring. Simultaneous examination of the dependences $V(C_{DBP})$ and $F/2(C_{DBP})$ shows that the admission of the plasticizer leads to the destruction of less stable (with smaller $F/2$) clusters and the concurrent formation of more stable (with larger $F/2$) structures.

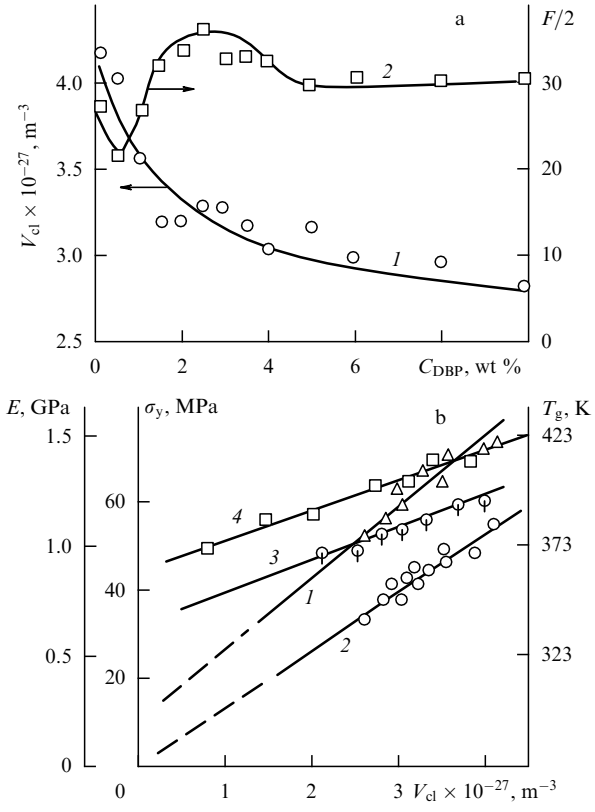

Figure 20. Plots of (a) cluster entanglement network density V_{cl} (*1*) and number of segments in a cluster $F/2$ (*2*) vs. dibutyl phthalate content C_{DBP}, and (b) glass transition temperature T_g (*1*), yield stress σ_y (*2*) and elastic modulus E (*3*, *4*) vs. cluster entanglement network density V_{cl} for PC plasticized with dibutyl phthalate [171]. Curve *3* — without DBP, curve *4* with 10% DBP.

The dependences of E, T_g, and σ_y on the plasticizer content C_{DBP} indicate that the two latter parameters decrease monotonically with growing C_{DBP}, whereas E has a maximum at $C_{DBP} \sim 2.5\%$ corresponding to the maximum $F/2$ in Fig. 20a [171].

If T_g and σ_y are assumed to be fully determined by V_{cl} (i.e. by the local order level), the relationship between E and the structural parameters is of a more complicated character. The former assumption is confirmed by plots $T_g(V_{cl})$ and $\sigma_y(V_{cl})$ presented in Fig. 20b. Both plots are linear. Moreover, extrapolation of the dependence $T_g(V_{cl})$ to $V_{cl} = 0$ shows that glass transition temperature of PC in the absence of local order is equivalent to the testing temperature (293 K). In other words, PC acquires rubber-like properties under these conditions. Thus, the breakdown of the local order forms a prerequisite for devitrification of amorphous polymers. Naturally, in this case $\sigma_y = 0$, as is shown by the extrapolation of the plot $\sigma_y(V_{cl})$ to $V_{cl} = 0$ (Fig. 20b). Unlike curves *1* and *2*, the dependences of the modulus of elasticity E on V_{cl} for unmodified PC and PC containing 2.5 or 10% of DBP (curves *3*, *4*) as $V_{cl} \to 0$ are extrapolated to nonzero E values. Comparison of curves presented in Fig. 20b (*3*, *4*) shows in the first place that antiplasticized PC has the lowest E_{lm} at $V_{cl} = 0$. This suggests that the antiplasticizing effect is due not only to the formation of more stable clusters but also to the disintegration of the loose-packed matrix, leading to a reduction in its stiffness. Secondly, antiplasticized PC is characterized by the steepest slope of the line $E(V_{cl})$, which in the end compensates for the impaired stiffness of the loose-packed matrix (i.e. the most stable clusters are also the stiffest ones). Thirdly, E_{lm} is higher for plasticized than for unmodified PC at a similar slope of the corresponding curves. It may be conjectured that an enhanced stiffness of the loose-packed matrix in plasticized PC is due to the filling of its free volume cavities with the plasticizer. This inference is supported by a monotonic decrease of gas permeability coefficient with growing C_{DBP}. The plots in Fig. 20 provide a highly descriptive quantitative estimation of structural changes in PC plasticized by DBP, in conformity with the reports of other authors.

6. Conclusions

The present work is concerned with the physical grounds of the cluster model of glassy polymers in the amorphous state. Analysis of experimental findings and theoretical studies has demonstrated the possibility of realization of local order conditions in amorphous polymers. The available data give evidence in support of the following inferences: (a) macromolecular entanglement network sites in noncrystalline regions of amorphous–crystalline polymers are the regions of local order (clusters), and (b) density changes in the cluster entanglement network have a marked effect on the polymer structure and properties. It is concluded that a crystallite analogue with prolate chains is the most likely type of ordered supersegmental structures in the amorphous state of polymers. With this in mind, consideration of the two principal models of the regions of local order in glassy polymers,

treating them either as folded ('bundles') or prolate (clusters) chains, leads to the conclusion that they must behave differently under mechanical strain. 'Bundles' appear to be able to unfold and adopt a fully stretched conformation under large strains, whereas clusters are not, and deformation of the polymer only occurs via straightening of the so-called penetrating chains. These assumptions and analogies with crystalline materials in which any violation of the long-range order presents a defect give reason to consider the regions of local order in glassy polymers as structural defects disturbing complete disorder. In this context, a segment participating in the cluster may be interpreted as a linear defect, viz. an analogue of dislocation in crystalline solids.

It is proposed that the experimental findings should be interpreted based on the description of the amorphous state of glassy polymers in terms of the cluster model, taking into account that it does not contradict a wealth of previously obtained data (when considering the Grüneisen parameter, the Poisson coefficient, the Mooney – Rivlin equation, the fluctuation free volume, percolation models, etc.) but offers a rational explanation of them and provides a sort of a standard model for structure characteristics. An obvious advantage of this approach consists in that the parameters of the cluster model can be obtained in independent tests and by different methods.

The application of the cluster model to the description of processes in amorphous polymers has demonstrated that the modulus of elasticity depends on the stiffness of the non-crystalline component. Also, this makes it possible to quantitatively evaluate the contribution of crystalline and amorphous entities to overall elasticity, flowing quality, and degradation. The process of devitrification is associated with the break of the 'frozen' local order (cluster decomposition) and therefore occurs over a wide temperature range. It should be noted that flow behavior depends on the loss of stability by clusters rather than on devitrification of the loose-packed matrix. Scaling analysis of molecular characteristics and structural relaxation showed that the mechanisms of these processes can be elucidated with the aid of the cluster model. In a vitrified loose-packed matrix relaxation is mediated through its conformational restructuring (mechanism I); after devitrification the same process occurs via mutual displacements of clusters (mechanism II). Investigation of crazing, physical ageing, and plasticization revealed the relationship between parameters of these processes and characteristics of the cluster model. Hence the possibility of quantitative evaluation of the attending structural changes.

Comparative analysis of a large store of available data gives no reason to doubt the existence of local order in the structure of amorphous glassy polymers. The only matter of controversy is the choice of the model. One of them, the cluster model, is superior to the others in that: (a) its parameters are determined by independent methods; (b) it provides a quantitative description of a large number of properties; (c) it is consistent with current physical concepts, and (d) it can be used to simulate the polymer structure in order to predict its characteristics.

The relationship between the local order and fractal nature of the polymer structure in the condensed state is underlain by the fact that both are manifestations of a fundamental property of this state, i.e. its departure from thermodynamic equilibrium. It has been shown in Ref. [327] that nonequilibrium processes give rise to fractal structures. The physical description of these structures in polymers in terms of the local order concept is feasible within the framework of the cluster model which allows for the quantitative identification of amorphous phase structural elements. Because the two models simulate different aspects of the polymer structure, they fairly well supplement each other.

Structures behaving like fractal ones on small distance scales and like homogeneous ones on large distance scales are known as self-similar fractals [191]. They are represented by percolation clusters at a percolation threshold. It has been shown above (see Section 4) that cluster systems are percolation systems and therefore should be regarded as self-similar fractals. Thus, the existence of local order in the condensed (glassy) amorphous state of polymers determines their structure. Glassy polymers and self-similar fractals are analogs so far as the structure of glassy polymers needs more than one order parameter to be described, since it does not obey the Prigogine – Defay criterion. Because Euclidean objects possess translational symmetry, a single parameter is needed to describe them, e.g., the Euclidean dimension d. Fractal objects exhibit dilational symmetry which makes it necessary to have at least three dimensions (Hausdorff dimension d_f, spectral d_s, and Euclidean d) to characterize them. Even if $d = 3$, at least two other dimensions are needed, viz. d_f and d_s.

Being a quantitative tool, the cluster model is designed for the analytical description of structure – property relationships in polymers. In connection with this, one promising line of further local order research is the examination of clusters as dissipative structures. Such an approach allows the mathematical apparatus of synergetics to be employed for the description of polymer structures. Its indisputable advantage consists in the possibility of investigating the interrelation of the initial and modified (by mechanical, thermal, and other factors) structures. Considering amorphous glassy polymers as a combination of structural elements (i.e. their certain distribution) opens prospects for the application of multifractal concepts to the parametrization of their structures.

References

1. Kargin V A, Kitaĭgorodskiĭ A I, Slonimskiĭ G L *Kolloidn. Zh.* **19** (2) 131 (1957)
2. Yoon D Y, Flory P J *Polymer* **18** 509 (1977)
3. Boyer R F *J. Macromol. Sci. Phys. B* **12** (2) 253 (1976)
4. Fischer E W et al., in *33rd IUPAC Int. Symp. Macromol.: Montreal, July 8 – 13, 1990: Book Abstr.* (1990) p. 335
5. Crist B, Tanzer J D, Graessley W W *J. Polymer Sci. B* **25** 545 (1987)
6. Callea K P et al. *J. Polymer Sci. B* **25** 651 (1987)
7. Ĭekh T S *Vysokomol. Soedin. A* **21** 2433 (1979)
8. Fischer E W *Z. Naturforsch. A* **12** 753 (1957)
9. Keller A *Philos. Mag.* **2** 1171 (1957)
10. Till P H *J. Polymer Sci.* **24** (106) 301 (1957)
11. Pechhold V W *Kolloid Z. Z. Polymere B* **228** (1 – 2) 1 (1968)
12. Kausch H H *Polymer Fracture* (Berlin: Springer-Verlag, 1978) [Translated into Russian (Moscow: Mir, 1981)]
13. Antipov E M et al. *Vysokomol. Soedin. B* **17** (3) 172 (1975)
14. Poddubnyĭ V I, Lavrent'ev V K *Vysokomol. Soedin. B* **32** (5) 354 (1990)
15. Ovchinnikov Yu K et al. *Vysokomol. Soedin. A* **20** 1742 (1978)
16. Antipov E M et al. *Vysokomol. Soedin. A* **20** 1727 (1978)
17. Kashaev R S et al. *Vysokomol. Soedin. B* **26** (2) 115 (1984)
18. Fedotov V D, Kadievskiĭ G M *Vysokomol. Soedin. A* **20** 1565 (1978)
19. Fedotov V D et al. *Vysokomol. Soedin. A* **19** 327 (1977)
20. Rashchupkin V P et al. *Vysokomol. Soedin. B* **14** 484 (1972)
21. Grubb D T, Yoon D Y *Polymer Commun.* (3) 84 (1986)
22. Jager E, Muller J, Jungnickel B Y *Prog. Colloid Polymer Sci.* **71** 145 (1985)

23. Ovchinnikov Yu K, Markova G S, Kargin V A *Vysokomol. Soedin. A* **11** 329 (1969)
24. Gervinska L, Fischer E W *J. Non-Cryst. Solids* **75** (1 – 3) 63 (1985)
25. Takeuchi Y,Yamamoto F, Shuto Y *Macromolecules* **19** 2059 (1986)
26. Muzeau E, Johari G P *Chem. Phys.* **149** (1 – 2) 173 (1990)
27. Bouda V *Polymer Degrad. Stab.* **24** (4) 319 (1989)
28. Kargin V A et al. *Dokl. Akad. Nauk SSSR* **167** 384 (1966)
29. Kargin V A, Berestneva Z Ya, Kalashnikov V T *Usp. Khim.* **36** (2) 203 (1967)
30. Nadezhin Yu S, Sidorevich A V, Asherov B A *Vysokomol. Soedin. A* **18** 2626 (1976)
31. Kitaĭgorodskiĭ A I *Smeshannye Kristally* (Mixed Crystals) (Moscow: Nauka, 1983) [Translated into English (Berlin: Springer-Verlag, 1984)]
32. Fischer E W, Dettenmaier M *J. Non-Cryst. Solids* **31** (1 – 2) 181 (1978)
33. Wendorff J H *Polymer* **23** 543 (1982)
34. Honeycombe R W K *The Plastic Deformation of Metals* (London: Edward Arnold, 1968) [Translated into Russian (Moscow: Mir, 1972)]
35. Argon A S *Philos. Mag.* **28** 839 (1973)
36. Argon A S *J. Macromol. Sci. Phys. B* **8** 573 (1973)
37. Bowden P B, Raha S *Philos. Mag.* **29** 149 (1974)
38. Escaig B *Ann. Phys.* (Paris) **3** 207 (1978)
39. Pechhold W R, Stoll B *Polymer Bull.* **7** (4) 413 (1982)
40. Sinani A B, Stepanov V A *Mekh. Kompozit. Mater.* (1) 109 (1981)
41. Aliguliev R M, Khiteeva D M, Oganyan V A *Vysokomol. Soedin. B* **30** (4) 268 (1988)
42. Aliguliev R M et al. *Dokl. Akad. Nauk AzSSR* **45** (5) 28 (1989)
43. Perepechko I I, Maksimov A V *Vysokomol. Soedin. B* **31** (1) 54 (1989)
44. Kozlov G V, Beloshenkov V A, Varyukhin V I *Prikl. Mekh. Tekh. Fiz.* **37** (3) 115 (1996) [*J. Appl. Mech. Tech. Phys.* **37** 396 (1996)]
45. Ivanova V S et al. *Sinergetika i Fraktaly v Materialovedenii* (Synergetics and Fractals in the Materials Science) (Moscow: Nauka, 1994)
46. Ivanova V S *Sinergetika*: *Prochnost' i Razrushenie Metallicheskikh Materialov* (Synergetics: Strength and Fracture of Metallic Materials) (Moscow: Nauka, 1992)
47. Kozlov G V, Sanditov D S *Angarmonicheskie Éffekty i Fiziko-Mekhanicheskie Svoĭstva Polimerov* (Anharmonic Effects and Physicomechanical Properties of Polymers) (Novosibirsk: Nauka, 1994)
48. Sanditov D S, Kozlov G V *Fiz. Khim. Stekla* **21** 547 (1995)
49. Haward R N *J. Polymer Sci. B* **33** 1481 (1995)
50. Haward R N *Polymer* **28** 1485 (1987)
51. Boyce M C, Parks D M, Argon A S *Mech. Mater.* **7** (1) 15 (1988)
52. Boyce M C, Parks D M, Argon A S *Mech. Mater.* **7** (1) 35 (1988)
53. Haward R N *Macromolecules* **26** 5860 (1993)
54. Bartenev G M, Frenkel' S Ya *Fizika Polimerov* (Physics of Polymers) (Leningrad: Khimiya, 1990)
55. Belousov V N et al. *Dokl. Akad. Nauk SSSR* **313** 630 (1990)
56. Flory P J *Polymer J.* **17** (1) 1 (1985)
57. Bershteĭn V A, Egorov V M *Differentsial'naya Skaniruyushchaya Kalorimetriya v Fizikokhimii Polimerov* (Differential Scanning Calorimetry in Physical Chemistry of Polymers) (Leningrad: Khimiya, 1990) [Translated into English: *Differential Scanning Calorimetry of Polymers*: *Physics, Chemistry, Analysis, Technology* (New York: Ellis Horwood, 1994)]
58. Graessley W W *Macromolecules* **13** 372 (1980)
59. Perepechko I I, Startsev O V *Vysokomol. Soedin. B* **15** (5) 321 (1973)
60. Belousov V N, Kotsev B Kh, Mikitaev A K *Dokl. Akad. Nauk SSSR* **270** (5) 1145 (1983)
61. Arzhakov S A, Bakeev N F, Kabanov V A *Vysokomol. Soedin. A* **15** 1154 (1973)
62. Narasawa I *Prochnost' Polimernykh Materialov* (Strength of Polymer Materials) (Moscow: Khimiya, 1987)
63. Kozlov G V, Sanditov D S *Vysokomol. Soedin. B* **35** 2067 (1993)
64. Gent A N, Madan S *J. Polymer Sci. B* **27** 1529 (1989)
65. Graesley W W, Edwards S F *Polymer* **22** 1329 (1981)
66. Wu S *J. Polymer Sci. B* **27** 723 (1989)
67. Budtov V P *Fizicheskaya Khimiya Rastvorov Polimerov* (Physical Chemistry of Polymer Solutions) (St. Petersburg: Khimiya, 1992)
68. Mashukov N I et al. *Lakokrasochn. Mater. Ikh Primenen.* (1) 16 (1992)
69. Barinov V Yu *Vysokomol. Soedin. B* **23** (1) 66 (1981)
70. Flory P J *Pure Appl. Chem.* **56** (3) 305 (1984)
71. Mashukov N I et al. *Dokl. Adyg. Akad. Nauk* (Cherkessk) **2** (3) 66 (1997)
72. Forsman W C *Macromolecules* **15** 1032 (1982)
73. Aharoni S M *Macromolecules* **16** 1722 (1983)
74. Gladyshev G P *Termodinamika i Makrokinetika Prirodnykh Ierarkhicheskikh Protsessov* (Thermodynamics and Macrokinetics of Natural Hierarchical Processes) (Moscow: Nauka, 1988)
75. Gladyshev G P *J. Theor. Biol.* **75** (4) 425 (1978)
76. Gladyshev G P, Gladyshev D P "O fiziko-khimicheskoĭ teorii evolyutsii" (On the physicochemical theory of evolution), Preprint (Moscow: Olimp, 1993)
77. Gladyshev G P *J. Biol. Systems* **1** (2) 115 (1993)
78. Gladyshev G P *Zh. Fiz. Khim.* **68** 790 (1994)
79. Gladyshev G P, Gladyshev D P *Izv. Ross. Akad. Nauk Ser. Biol.* (31) 5 (1995)
80. Baronin D V, Kozlov G V, Novikov V U, in *Simp.* "*Sinergetika 96*", Moscow, 12 – 14 Noyabrya 1996 (Proc. Symposium "Synergetics 96", Moscow, 12 – 14 November 1996) (1996) p. 221
81. Beloshenko V A, Kozlov G V, Lipatov Yu S *Fiz. Tverd. Tela* **36** 2903 (1994) [*Phys. Solid State* **36** 1543 (1994)]
82. Matsuoka S, Bair H E *J. Appl. Phys.* **48** 4058 (1977)
83. Wu S *J. Appl. Polymer Sci.* **46** 619 (1992)
84. Privalko V P, Lipatov Yu S *Vysokomol. Soedin. A* **13** 2733 (1971)
85. Gladyshev G P *J. Biol. Phys.* **20** (2) 213 (1994)
86. Kozlov G V, Belousov V N, Mikitaev A K *Fiz. Tekh. Vysokikh Davlen.* **8** (1) 64 (1998)
87. Fellers J F, Huang D C *J. Appl. Polymer Sci.* **23** 2315 (1979)
88. Lin Y-H *Macromolecules* **20** 3080 (1987)
89. Andrianova G P, Kargin V A *Vysokomol. Soedin. A* **12** (1) 3 (1970)
90. Kozlov G V, Beloshenko V A, Varyukhin V N *Ukr. Fiz. Zh.* **41** (2) 218 (1996)
91. Shogenov V N et al. *Vysokomol. Soedin. A* **33** (1) 155 (1991)
92. Thierry A, Oxborough R J, Bowden P B *Philos. Mag.* **30** 527 (1974)
93. Charlesby A, Jaroszkiewicz E M *Eur. Polymer J.* **21** (1) 55 (1985)
94. Beloshenko V A et al. *Fiz. Tekh. Vysokikh Davlen.* **4** (3 – 4) 113 (1994)
95. Beloshenko V A et al. *Fiz. Tekh. Vysokikh Davlen.* **5** (2) 75 (1995)
96. Kozlov G V et al. *Dokl. Nats. Akad. Nauk Ukrainy Ser. B* (12) 126 (1994)
97. Mashukov N I et al., in *Tez. Dokl. VI Vsesoyuzn. Koordin. Soveshchan. po Spektroskopii Polimerov* (Abs. VI All-Union Coordin. Workshop on Polymer Spectroscopy) (Minsk, 1989) p. 81
98. Mashukov N I et al. "Stabilizatsiya i modifikatsiya poliétilena aktseptorami kisloroda" (Polymer stabilization and modification by oxygen acceptors) Preprint Inst. Khim. Fiz. Akad. Nauk SSSR (Moscow: IKhF AN SSSR, 1990)
99. Mashukov N I et al. *Izv. Akad. Nauk SSSR Ser. Khim.* (8) 1915 (1990)
100. Mashukov N I et al. *Lakokrasochn. Mater. Ikh Primenen.* (5) 38 (1990)
101. Mashukov N I et al., in *Teoriya i Praktika Kataliticheskikh Reaktsiĭ i Khimii Polimerov* (Theory and Practice of Catalytic Reactions and Polymer Chemistry) (Cheboksary: Izd. ChGU, 1990)
102. Mashukov N I et al. *Plast. Massy* (5) 61 (1991)
103. Mashukov N I, Gladyshev G P, Kozlov G V *Vysokomol. Soedin. A* **33** 2538 (1991)
104. White R M, Geballe T H *Long-Range Order in Solids* (New York: Acad. Press, 1979) [Translated into Russian (Moscow: Mir, 1982)]
105. Boyer R F *Polymer Engng. Sci.* **8** (3) 161 (1968)
106. Belousov V N, Kozlov G V, Mashukov N I *Dokl. Adyg. Akad. Nauk* (Cherkessk) 2 (2) 74 (1996)
107. Kozlov G V, Mil'man L D, Mikitaev A K "Lokal'nyĭ poryadok v amorfno-kristallicheskom polimere" (Local order in amorphous – crystalline polymers) Dep. VINITI RAN No. 622-V97 (1997)
108. Curro J J, Roe R-J *Polymer* **10** 1424 (1984)
109. Rathje J, Ruland W *Colloid Polymer Sci.* **254** (3) 358 (1976)
110. Sanditov D S, Bartenev G M *Fizicheskie Svoĭstva Neuporyadochennykh Struktur* (Physical Properties of Disordered Structures) (Novosibirsk: Nauka, 1982)

111. Kozlov G V, Afaunov V V, Novikov V U *Materialovedenie* (9) 19 (2000)
112. Wunderlich B *Macromolecular Physics* in 3 volumes (New York: Acad. Press, 1973 – 1980) [Translated into Russian (Moscow: Mir, 1976 – 1983)]
113. Seguela R, Rietsch F *Polymer* **27** 703 (1986)
114. Wedgewood A R, Seferis J C *Pure Appl. Chem.* **55** 873 (1983)
115. Okada T, Mandelkern L *J. Polymer Sci. A-2* **5** (2) 239 (1967)
116. Jones T E et al. *J. Chem. Phys.* **88** 3338 (1988)
117. Yavorskiĭ B M, Detlaf A A *Spravochnik po Fizike* 2nd ed. (Handbook of Physics) (Moscow: Nauka, 1964) [Translated into English (Moscow: Mir, 1972)]
118. Kosobudskiĭ I D et al. *Vysokomol. Soedin. A* **27** 689 (1985)
119. Gladyshev G P et al. "Fiziko-khimicheskie svoĭstva poliétilena, stabilizirovannogo ingibitorami 'netsepnogo tipa'" (Physicochemical properties of polyethylene stabilized by 'nonchain type' inhibitors), Preprint OIKhF AN SSSR (Chernogolovka: OIKhF AN SSSR, 1985)
120. Piskorskiĭ V P, Lipanov A M, Balusov V A *Zh. Vses. Khim. Obshchestva* **32** (1) 47 (1987)
121. Belyĭ V A et al. *Dokl. Akad. Nauk SSSR* **302** (2) 355 (1988)
122. Privalko V P et al. *Vysokomol. Soedin. A* **20** 2777 (1978)
123. Kozlov G V et al. *Dokl. Nats. Akad. Nauk Ukrainy Ser. B* (11) 102 (1995)
124. Boyer R F, Miller R L *Macromolecules* **10** 1167 (1977)
125. Miller R L, Boyer R F *J. Polymer Sci. B* **22** 2043 (1984)
126. Miller R L, Boyer R F, Heijboer J *J. Polymer Sci. B* **22** 2021 (1984)
127. Balankin A S *Sinergetika Deformiruemogo Tela* Pt. 1 (Synergetics of Deformable Materials) (Moscow: MO SSSR, 1991)
128. Balankin A S et al. *Dokl. Ross. Akad. Nauk* **326** 463 (1992)
129. Kozlov G V et al. *Fiz. Tekh. Vysokikh Davlen.* **5** (3) 59 (1995)
130. Oleĭnik É F et al. *Dokl. Akad. Nauk SSSR* **286** 135 (1986)
131. Melot D et al. *J. Polymer Sci. B* **32** 1805 (1994)
132. Nikol'skiĭ V G et al. *Vysokomol. Soedin. A* **25** 2366 (1983)
133. Flory P J *Brit. Polymer J.* **8** (1) 1 (1976)
134. Lin C et al. *Phys. Rev. B* **29** 5060 (1984)
135. Kozlov G V, Beloshenko V A, Lipskaya V O *Ukr. Fiz. Zh.* **41** (2) 222 (1996)
136. Guinier A *Theorie et Technique de la Radiocristallographie* (Paris: Dunod, 1956) [Translated into Russian (Moscow: Fizmatgiz, 1961)]; see also *X-ray Diffraction in Crystals, Imperfect Crystals, and Amorphous Bodies* (San Francisco: W.H. Freeman, 1963)
137. Majid C A et al. *Radiat. Phys. Chem.* **16** (5) 379 (1980)
138. Petric S E B *J. Macromol. Sci. Phys. B* **12** (2) 225 (1976)
139. Ball R C *Physica D* **38** (1) 13 (1989)
140. Song H-H, Roe R-J *Macromolecules* **20** 2723 (1987)
141. Murthy N S et al. *Macromolecules* **26** 1712 (1993)
142. Kumar S, Adams W W *Polymer* **28** 1497 (1987)
143. Beloshenko V A, Kozlov G V *Mekh. Kompozit. Mater.* **30** (4) 451 (1994)
144. Kozlov G V, Shogenov V N, Mikitaev A K *Dokl. Akad. Nauk SSSR* **298** (1) 142 (1988)
145. Kozlov G V, Novikov V U *Materialoved.* (8 – 9) 3 (1997)
146. Liu R S, Li J Y *Mater. Sci. Engng. A* **114** (1) 127 (1989)
147. Aleksanyan G G et al. *Khim. Fiz.* **5** 1225 (1986)
148. McClintock F A, Argon A S *Mechanical Behavior of Materials* (Reading, Mass.: Addison-Wesley, 1966) [Translated into Russian (Moscow: Mir, 1970)]
149. Mil'man L D, Kozlov G V, in *Polikondensatsionnye Protsessy i Polimery* (Polycondensation Processes and Polymers) (Nal'chik: Izd. KBGU, 1986) p. 130
150. Shogenov V N, Kozlov G V, Mikitaev A K *Vysokomol. Soedin. A* **31** 1766 (1989)
151. Peschanskaya N N, Bershteĭn V A, Stepanov V A *Fiz. Tverd. Tela* **20** 3371 (1978) [*Sov. Phys. Solid State* **20** 1945 (1978)]
152. Sanditov D S, Kozlov G V *Fiz. Khim. Stekla* **19** 593 (1993)
153. Careri J *Ordine e Disordine nella Materia* (Roma: Laterza & Figli, 1982) [Translated into English: *Order and Disorder in Matter* (Reading, Mass.: Benjamin, 1984)] [Translated into Russian (Moscow: Mir, 1985)]
154. Ivanova V S et al. *Dokl. Ross. Akad. Nauk* **330** (1) 222 (1993) [*Phys. Dokl.* **38** (5) 35 (1993)]
155. Novikov V, Gazaev M, Kozlov G, in *Second Symposium "Advances in Structured and Heterogeneous Continua", Moscow, Russia, 14 – 16 Aug., 1995* Abstracts (1995) p. 45
156. Kozlov G V et al. "Povedenie dissipativnykh polimernykh matrits" (Behavior of dissipative polymeric matrices), Dep. VINITI RAN No. 2944-B95 (1995)
157. Boyer R F *Macromolecules* **25** 5326 (1992)
158. Kozlov G V, Belousov V N, Mikitaev A K *Izv. Vyssh. Uchebn. Zaved. Severo-Kavkaz. Region Ser. Estestv. Nauki* (1 – 2(86)) 71 (1994)
159. Belousov V N, Kozlov G V, Lipatov Yu S *Dokl. Akad. Nauk SSSR* **318** 615 (1991)
160. Mark J E, Sullivan J L *J. Chem. Phys.* **66** 1006 (1977)
161. Sanjuan J, Llorente M A *J. Polymer Sci. B* **26** 235 (1988)
162. Knopoff L, Shapiro J N *Phys. Rev. B* **1** 3893 (1970)
163. Sharma B K *Acoust. Lett.* **4** (2) 19 (1980)
164. Sharma B K *Acoust. Lett.* **4** (1) 11 (1980)
165. Olemskoĭ A I, Katsnel'son A A, Umrikhin V V *Fiz. Tverd. Tela* **27** 318 (1985) [*Sov. Phys. Solid State* **27** 195 (1985)]
166. Sanditov D S et al. *Ukrain. Polymer J.* **1** (3 – 4) 241 (1992)
167. Kozlov G V, Mikitaev A K *Vysokomol. Soedin. B* **29** (3) 214 (1987)
168. Kozlov G V, Shetov R A, Mikitaev A K *Dokl. Akad. Nauk SSSR* **290** 885 (1986)
169. Frenkel' Ya I *Kineticheskaya Teoriya Zhidkosteĭ* (Kinetic Theory of Liquids) (Moscow – Leningrad: Izd. AN SSSR, 1945) [Translated into English (Oxford: The Clarendon Press, 1946)]
170. Ferry J D *Viscoelastic Properties of Polymers* (New York: Wiley, 1961) [Translated into Russian (Moscow: IIL, 1963)]
171. Sanditov D S et al. *Fiz. Khim. Stekla* **20** (1) 3 (1994)
172. Belousov V N et al. *Ukr. Khim. Zh.* **62** (1) 1 (1996)
173. Lipatov Yu S *Usp. Khim.* **47** (2) 332 (1978)
174. Sanchez I C *J. Appl. Phys.* **45** 4204 (1974)
175. Beloshenko V A, Kozlov G V, Varyukhin V I *Fiz. Tekh. Vysokikh Davlen.* **4** (2) 70 (1994)
176. Averkin B A et al. *Vysokomol. Soedin. A* **31** 2173 (1989)
177. Yagfarov M Sh *Vysokomol. Soedin. A* **30** 79 (1988)
178. Yagpharov M *J. Therm. Anal.* **31** 1073 (1986)
179. Kozlov G V et al. *Vysokomol. Soedin. B* **31** 417 (1989)
180. Kozlov G V et al. *Izv. Vyssh. Uchebn. Zaved. Severo-Kavkaz. Region Ser. Estestv. Nauki* (1 – 2(86)) 54 (1994)
181. Balankin A S *Dokl. Akad. Nauk SSSR* **319** 1098 (1991)
182. Filyanov E M *Vysokomol. Soedin. A* **29** 975 (1987)
183. Hong S-D et al. *J. Polymer Sci. B* **21** 1647 (1983)
184. Lamarre L, Sung C S P *Macromolecules* **16** 1729 (1983)
185. Yu W-C, Sung S P *Macromolecules* **21** 365 (1988)
186. Robertson R E, Simha R, Curro J G *Macromolecules* **17** 911 (1984)
187. Kozlov G V et al. *Fiz. Khim. Stekla* **20** 519 (1994)
188. Jean Y C, Sandreczki T C, Ames D P *J. Polymer Sci. B* **24** 1247 (1986)
189. Deng Q, Zandiehnadem F, Jean Y C *Macromolecules* **25** 1090 (1992)
190. Bantle S et al. *Polymer* **23** 1889 (1982)
191. Sokolov I M *Usp. Fiz. Nauk* **150** 221 (1986) [*Sov. Phys. Usp.* **29** 924 (1986)]
192. Manevich L I et al. *Dokl. Akad. Nauk SSSR* **289** 128 (1986)
193. Maryolina A, Wu S *Polymer* **29** 2170 (1988)
194. Mashukov N I et al. "Fluktuatsionnaya setka molekulyarnykh zatsepleniĭ kak perkolyatsionnaya sistema" (Fluctuation molecular entanglement network as a percolation system) Dep. VINITI RAN No. 1537-V94 (1994)
195. Kozlov G V et al. *Inzh.-Fiz. Zh.* **71** (2) 241 (1998) [*J. Eng. Phys. Thermophys.* **71** 241 (1998)]
196. Kozlov G V et al. *Izv. Vyssh. Uchebn. Zaved. Severo-Kavkaz. Region Ser. Estestv. Nauki* (3 – 4(83 – 84)) 88 (1993)
197. Bucknall C B *Toughened Plastics* (Cambridge: Cambridge Univ. Press, 1977) [Translated into Russian (Leningrad: Khimiya, 1981)]
198. Kozlov G V, Belousov V N, Mikitaev A K *Dokl. Akad. Nauk SSSR* **274** (2) 338 (1984)
199. Jang B Z, Uhlmann D R, Van der Sande J B *J. Appl. Polymer Sci.* **29** 3409 (1984)
200. Kozlov G V, Shetov R A, Mikitaev A K *Vysokomol. Soedin. A* **28** 1848 (1986)
201. Donald A M, Kramer E J *J. Polymer Sci. B* **20** 899 (1982)
202. Donald A M, Kramer E J *J. Polymer Sci. B* **20** 1129 (1982)

203. Donald A M, Kramer E J *Polymer* **23** 461 (1982)
204. Kramer E J *Polymer Engng. Sci.* **24** 741 (1984)
205. Henkee C S, Kramer E J *J. Polymer Sci. B* **22** 721 (1984)
206. Yang A C-M et al. *Macromolecules* **19** 2010 (1986)
207. Donald A M *J. Mater. Sci.* **20** 2630 (1985)
208. Berger L L, Kramer E J *Macromolecules* **20** 1980 (1987)
209. Plummer C J G, Donald A M *J. Polymer Sci. B* **27** 325 (1989)
210. Plummer C J G, Donald A M *Macromolecules* **23** 3929 (1990)
211. Haward R N, Murphy B M, White E E T *J. Polymer Sci. A-2* **9** 801 (1971)
212. Hoare J, Hull D *J. Mater. Sci.* **10** 1861 (1975)
213. Serdyuk V D, Kosa P N, Kozlov G V *Fiz. Tekh. Vysokikh Davlen.* **5** (3) 37 (1995)
214. Jud K, Kausch H, Williams J G *J. Mater. Sci.* **16** (1) 204 (1981)
215. Kausch H *Pure Appl. Chem.* **55** 833 (1983)
216. Kozlov G V, Mikitaev A K *Izv. SKNTs VSh Ser. Estestv. Nauki* (3(59)) 66 (1987)
217. Ward I M *Mechanical Properties of Solid Polymers* (London: Wiley-Interscience, 1971) [Translated into Russian (Moscow: Khimiya, 1975)]
218. Kambour R P, Gruner C L *J. Polymer Sci. B* **16** 703 (1978)
219. Kambour R P *Polymer Commun.* **24** 292 (1983)
220. Kambour R P *Polymer Commun.* **25** 357 (1984)
221. Willbourn A H *Polymer* **17** 965 (1976)
222. Mikitaev A K, Kozlov G V, Shogenov V N *Plast. Massy* (2) 32 (1985)
223. Brown N *Mater. Sci. Engng.* **8** (1) 69 (1971)
224. Lee W A, Sewell J H *J. Appl. Polymer Sci.* **12** 1397 (1968)
225. Termonia Y, Smith P *Macromolecules* **21** 2184 (1988)
226. Donald A M, Kramer E J *J. Mater. Sci.* **16** 2967 (1981)
227. Baskes M I *Engng. Fract. Mech.* **6** (1) 11 (1974)
228. Termonia Y, Smith P *Macromolecules* **20** 835 (1987)
229. Kozlov G V et al. *Vysokomol. Soedin. B* **29** 311 (1987)
230. Aharoni S M *Macromolecules* **18** 2624 (1985)
231. Ciferri A, Ward I M (Eds) *Ultra-High Modulus Polymers* (London: Applied Science Publ., 1979) [Translated into Russian (Leningrad: Khimiya, 1983)]
232. Brown D J *Polymer Commun.* **26** (2) 42 (1985)
233. Botto P A, Duckett R A, Ward I M *Polymer* **28** (2) 257 (1987)
234. Raha S, Bowden P B *Polymer* **13** (4) 174 (1972)
235. Kahar N, Duckett R A, Ward I M *Polymer* **19** (2) 136 (1978)
236. Milagin M F, Shishkin N I *Vysokomol. Soedin. A* **14** 357 (1972)
237. Lomonosova N V *Vysokomol. Soedin. A* **20** 2270 (1978)
238. Milagin M F, Shishkin N I *Vysokomol. Soedin. A* **30** 2249 (1988)
239. Andrews E H *Pure Appl. Chem.* **39** (1–2) 179 (1974)
240. Krigbaum W R, Roe R-G, Smith K J *Polymer* **5** (3) 533 (1964)
241. Popli R, Mandelkern L *J. Polymer Sci. B* **25** 441 (1987)
242. Peacock A J, Mandelkern L *J. Polymer Sci. B* **28** 1917 (1990)
243. Pakhomov P M et al. *Vysokomol. Soedin. A* **26** 1288 (1984)
244. Kozlov G V et al., in *Mater. Nauchno-Tekh. Konf. po Estestv. Naukam* (Abs. Sci. Tech. Conf. on Nat. Sci.) (Nal'chik: Izd. KBGU, 1992) p. 34
245. Levene A, Pullen W J, Roberts J *J. Polymer Sci. A-2* **3** (2) 697 (1965)
246. Kozlov G V et al. *Dokl. Nats. Akad. Nauk Ukrainy Ser. B* (11) 79 (1996)
247. Kachanova I M, Roĭtburd A L *Fiz. Tverd. Tela* **31** (4) 1 (1989)
248. Hartman B, Lee G F, Cole R F *Polymer Engng. Sci.* **26** (8) 554 (1986)
249. Kozlov G V et al., in *Mater. Nauchno-Tekh. Konf. po Estestv. Naukam* (Abs. Sci. Tech. Conf. on Nat. Sci.) (Nal'chik: Izd. KBGU, 1992) p. 61
250. Kozlov G V et al. *Mekh. Kompozit. Mater.* **32** (2) 270 (1996)
251. Kartsovnik V I, Volkov V N, Rozenberg V A *Vysokomol. Soedin. B* **19** (4) 280 (1977)
252. Gazaev M A et al. *Fiz. Tekh. Vysokikh Davlen.* **6** (1) 7 (1996)
253. Bekichev V I *Vysokomol. Soedin. A* **16** 1479 (1974)
254. Bekichev V I *Vysokomol. Soedin. A* **16** 1745 (1974)
255. Panin V E, Likhachev V A, Grinyaev Yu V *Strukturnye Urovni Deformatsii Tverdykh Tel* (Structural Levels of Deformation in Solids) (Novosibirsk: Nauka, 1985)
256. Balankin A S *Pis'ma Zh. Tekh. Fiz.* **16** (7) 14 (1990) [*Sov. Tech. Phys. Lett.* **16** 248 (1990)]
257. Ivanova V S, Vstovskiĭ G V, in *Itogi Nauki i Tekhniki Ser. Metalloveden. i Termich. Obrabotka* Vol. 24 (Recent Progress in Sci. and Technol. Sciences. Ser. 1 of Metal Science and Thermal Processing) (Ed. L A Petrova) (Moscow: VINITI, 1990) p. 43
258. Mashukov N I et al. *Izv. Akad. Nauk SSSR Ser. Khim.* (9) 2143 (1990)
259. Belousov V N et al. *Dokl. Ross. Akad. Nauk* **328** 706 (1993)
260. Kargin V A, Sogolova T I *Zh. Fiz. Khim.* **27** 1039 (1953)
261. Bernshteĭn V A et al. *Vysokomol. Soedin. A* **31** 776 (1989)
262. Di Benedetto A T, Trachte K L *J. Appl. Polymer Sci.* **14** 2249 (1970)
263. Sanditov D S, Mantatov V V *Vysokomol. Soedin. B* **32** 869 (1990)
264. Beatty C L, Weaves J L *Polymer Engng. Sci.* **18** 1109 (1978)
265. Bersted B H *J. Appl. Polymer Sci.* **23** (1) 37 (1979)
266. Wool R P, Boyd R H *J. Appl. Phys.* **51** 5116 (1980)
267. Kozlov G V, Belousov V N, Lipatov Yu S *Dokl. Akad. Nauk Ukr. SSR Ser. B* (6) 50 (1990)
268. Mashukov N I et al. *Vopr. Oboron. Tekh. Ser. 15* (3(97)) 13 (1991)
269. Mikos A G, Peppas N A *J. Chem. Phys.* **88** 1337 (1988)
270. Kozlov G V et al. *Dokl. Nats. Akad. Nauk Ukr. Ser. B* (5) 100 (1995)
271. Schrager M *J. Appl. Polymer Sci.* **22** 2379 (1978)
272. Krysyuk B É, Sandakov G I *Vysokomol. Soedin. A* **37** 615 (1995)
273. Lobanov A M, Frenkel' S Ya *Vysokomol. Soedin. A* **22** 1045 (1980)
274. Enns J B, Boyer R F, in *Proc. 17th Int. Symp., Midland, Mich., Aug. 18–21, 1985* (New York, 1987) p. 221
275. Boyer R F *J. Macromol. Sci. Phys. B* **18** (2) 461 (1980)
276. Kalinchev É L, Sakovtseva M B *Svoĭstva i Pererabotka Termoplastov* (Properties and Processing of Thermoplastics) (Leningrad: Khimiya, 1983)
277. Irzhak V I, Rozenberg B A, Enikolopyan N S *Setchatye Polimery: Sintez, Struktura i Svoĭstva* (Cross-Linked Polymers: Synthesis, Structure and Properties) (Moscow: Nauka, 1979)
278. Timm D C, Ayorinde A J, Foral R F *Brit. Polymer J.* **17** (2) 227 (1985)
279. Chang T-D, Brittain J O *Polymer Engng. Sci.* **22** 1221 (1982)
280. Kozlov G V et al. *Dokl. Nats. Akad. Nauk Ukr. Ser. B* (10) 117 (1995)
281. Beloshenko V A et al. *Mekh. Kompozit. Mater.* **26** (2) 195 (1990) [*Mech. Composite Mater.* **26** (2) 149 (1990)]
282. Beloshenko V A et al. *Fiz. Tekh. Vysokikh Davlen.* **3** (4) 24 (1993)
283. Flory P J *J. Chem. Phys.* **66** 5720 (1977)
284. Stoyanov O V, Deberdeev R Ya *Vysokomol. Soedin. B* **29** (1) 22 (1987)
285. Boyd R H *Polymer* **26** 323 (1985)
286. Boyd R H *Polymer* **26** 1123 (1985)
287. Papkov S P *Vysokomol. Soedin. A* **19** (1) 3 (1977)
288. Zhurkov S N, Egorov E A *Dokl. Akad. Nauk SSSR* **152** 1155 (1963)
289. Bartenev G M, Shut N I, Kasperskiĭ A V *Vysokomol. Soedin. B* **30** (5) 328 (1988)
290. Aharoni S M *J. Appl. Polymer Sci.* **23** (1) 223 (1979)
291. Peterlin A *J. Macromol. Sci. Phys. B* **11** (1) 57 (1975)
292. Godovskiĭ Yu K *Teplofizika Polimerov* (Thermophysics of Polymers) (Moscow: Khimiya, 1982) [Translated into English: *Thermophysical Properties of Polymers* (Berlin: Springer-Verlag, 1992)]
293. Slutsker A I, Filippov V É *Vysokomol. Soedin. A* **30** 2386 (1988)
294. Vaĭnshteĭn B K *Difraktsiya Rentgenovykh Lucheĭ na Tsepnykh Molekulakh* (Diffraction of X-Rays by Chain Molecules) (Moscow: Izd. AN SSSR, 1963) [Translated into English (Amsterdam: Elsevier, 1966)]
295. Volynskaya A V, Godovskiĭ Yu K, Papkov V S *Vysokomol. Soedin. A* **21** 1059 (1979)
296. Lipatov Yu S et al. *Vysokomol. Soedin. A* **28** 573 (1986)
297. Wunderlich B *J. Chem. Phys.* **61** 1052 (1960)
298. Boyer R F *J. Macromol. Sci. Phys. B* **7** 487 (1973)
299. Nielsen L *Mechanical Properties of Polymers and Composites* (New York: M. Dekker, 1974) [Translated into Russian (Moscow: Khimiya, 1978)]
300. Mashukov N I et al. *Plast. Massy* (11) 21 (1990)
301. Popova G S et al. *Analiz Polimerizatsionnykh Plastmass* (Analysis of Polymerized Plastics) (Leningrad: Khimiya, 1988)
302. Kavassalus T A, Noolandi J *Macromolecules* **21** 2869 (1988)
303. Mills P J, Hay J N, Haward R N *J. Mater. Sci.* **20** 501 (1985)
304. Arzhakov S A, Kabanov V A *Vysokomol. Soedin. B* **13** (5) 318 (1971)
305. Askadskiĭ A A, Matveev Yu I *Khimicheskoe Stroenie i Fizicheskie Svoĭstva Polimerov* (Chemical Structure and Physical Properties of Polymers) (Moscow: Khimiya, 1983)

306. Kambour R P *J. Polymer Sci.: Macromol. Rev.* **7** 1 (1973)
307. Kramer E J *J. Polymer Sci. B* **13** 509 (1975)
308. Fraser R A W, Ward I M *J. Mater. Sci.* **12** 459 (1977)
309. Ishikawa M, Ogawa H *J. Macromol. Sci. Phys. B* **19** 421 (1981)
310. Kozlov G V, Shetov R A, Mikitaev A K *Vysokomol. Soedin. A* **29** 1109 (1987)
311. Michler G H *Macromol. Chem., Macromol. Symp.* **45** (1) 39 (1991)
312. Plati P E, Williams J G *Polymer Engng. Sci.* **15** (6) 470 (1975)
313. Kozlov G V, Shogenov V N, Mikitaev A K, in *Polikondensatsionnye Protsessy i Polimery* (Polycondensation Processes and Polymers) (Nal'chik: Izd. KBGU, 1984) p. 35
314. Li J C M, Wu J B C *J. Mater. Sci.* **11** 445 (1976)
315. Berens A R, Hodge I M *Macromolecules* **15** 756 (1982)
316. Chan A H, Paul D R *J. Appl. Polymer Sci.* **24** 1539 (1979)
317. Morgan R J, O'Neal J E *J. Polymer Sci. B* **14** 1053 (1976)
318. Wyzgoski M G *J. Appl. Polymer Sci.* **25** 1455 (1980)
319. Aoki Y, Brittain J O *J. Polymer Sci. B* **15** 199 (1977)
320. Bubeck R A, Yusar H Y *Polymer Commun.* **30** (1) 25 (1989)
321. Kozlov G V et al. *Materialoved.* (8) 21 (2000)
322. Kozlov G V et al. *Vysokomol. Soedin. B* **38** 1423 (1996)
323. Barshtein R S, Kirilovich V I, Nosovskiĭ Yu E *Plastifikatory dlya Polimerov* (Plasticizers for Polymers) (Moscow: Khimiya, 1982)
324. Perepechko I I, Yakovenko S S *Vysokomol. Soedin. A* **23** 1166 (1981)
325. Zvonkova E M et al. *Vysokomol. Soedin. A* **26** 1228 (1984)
326. Zvonkova E M, Zvonkov V V, Kerber M L *Vysokomol. Soedin. A* **27** 595 (1985)
327. Novikov V U, Kozlov G V *Usp. Khim.* **69** (6) 576 (2000)